TOWARDS FURTHERING THE APPLICATION OF ATTAINABLE REGION THEORY TO BATCH REACTORS

UNIVERSITY OF THE WITWATERSRAND,
JOHANNESBURG

Ryan Adam Mc Kelvey

A dissertation submitted to the Faculty of Engineering and the Built Environment, University of the Witwatersrand, in fulfilment of the requirements for the degree of Master of Science in Engineering.

Johannesburg, 2016

Declaration

I, Ryan Mc Kelvey, declare that this dissertation is my own unaided work. It is being submitted for the Degree of Master of Science by Research in Engineering to the University of the Witwatersrand, Johannesburg. It has not been submitted before for any degree or examination to any other university.

Signature .....

Date .....

Abstract

Traditional work in batch processes has focused mainly on the optimisation of batch reactors and the scheduling of batch processes. Recent development in the application of attainable region (AR) theory has allowed for its entry into this landscape. As time is a crucial consideration in the study of these systems, furthering the application of AR theory to batch reactors required the incorporation of time into the ARs. This was previously done in terms of residence time for continuous systems. With its use in batch systems this work sought to investigate how the time component differs within ARs between batch and continuous systems. It demonstrated that while residence time could be undergo linear mixing, the time in batch systems could not due to its nature. Therefore the ARs generated in concentration-residence time and concentration-time space would differ slightly. A way to circumnavigate this was proposed in that the AR be plotted in terms of concentration and residence time following which the continuous reactor structure is obtained. From this the batch structure can be determined by substituting the equivalent reactor types. Production rates were also introduced as a method of interpreting an AR plotted in concentration-residence time space. By minimising the time taken to reach a particular point in the AR, one may effectively increase the rate at which the desired product can be produced. The developed concepts were applied to two example systems with the aim of obtaining the batch reactor structure for the most productive point that satisfied a given objective. Success was achieved for 2D single reaction system as well as a more complex 3D two biological reaction system. The more complex system led to the development of non-conventional attainable regions in terms of another process variable; in this case pH was used to demonstrate the concept although other variables such as temperature and pressure may be used in a similar fashion. Such plots may be used to further optimise the reaction system or identify a particular region in which to operate. Further development of AR theory to batch reactors has indeed allowed its use in conjunction with optimisation and scheduling of batch processes. Most notably, scheduling may utilise the obtained batch structure as part of the process to be scheduled or use the indicated reaction time.

Acknowledgements

My heartfelt thanks go to my supervisors, Dr David Ming and Ms Michelle Low, who supported me throughout this work.

National Research Foundation (NRF), Thuthuka funding instrument for student stipend: The NRF has financially supported the author. The views are those of the author and not of the NRF. This work is based on the research supported in part by the NRF of South Africa for the grant, 84344. Any opinion, finding and conclusion or recommendation expressed in this material is that of the author(s) and the NRF does not accept any liability in this regard.

Contents

List of Figures

List of Tables

Nomenclature

α	Scalar value that determines the distribution quantity of material along the length of DSR
$\beta(S_{inj})$	Coefficient of variable term of processing time of state s, s being an element of S_{inj}
$\tau(S_{inj})$	Coefficient of constant term of processing time of state s, s being an element of S_{inj}
$c_{i,t}$	Concentration of component *i* at time t (mol/volume)
$\mathbf{z}^*$	Mass fractions after mixing
$\mathbf{C_o}$	DSR side-stream concentration ($mol/length^3$)
$\mathbf{C}$	Concentration vector containing the concentrations of all components in a system ($mol/length^3$)
c_{if}	Concentration of component *i* in feed (mol/volume)
$\mathbf{C_f}$	Feed concentration vector containing the feed concentrations of all components in a system ($mol/length^3$)
c_i	Concentration of component *i* ($mol/length^3$)
$\mathbf{C}^*$	Concentration after mixing ($mol/length^3$)
$dr(C)$	Jacobian of rate vector
$Null$	Null space of stoichiometric matrix, A
d	Number of independent reactions
ρ	Density (mass/volume)
$K_{s,aceto}$	Half-velocity constant for acetogenesis reaction (mol/L)
$K_{s,meth}$	Half-velocity constant for methanogenesis reaction (mol/L)
k_{hyd}	Hydrogen inhibition constant (mol/L)
$\mu_{max,aceto}$	Maximum specific growth of the acetogenesis reaction (hr^{-1})
$\mu_{max,meth}$	Maximum specific growth of the methanogenesis reaction (hr^{-1})
$\mathbb{H}$	Set of points in concentration space or concentration-residence time space
$[H^+]$	Hydrogen ion concentration (mol/L)

t_o	Reference time or time at initiation of reactor structure - feed time (mol/volume)
m_i	Mass flow rate for component i (mass/time)
G	Total mass flow rate for stream (mass/time)
z_i	Mass fraction for component i
$\mathbf{z}$	Mass fraction vector
λ_m	Mixing fraction for mass concentrations/fractions
λ	Mixing fraction
pH	pH of a solution
P_{im}	Mass production rate for component i (mass/time)
P_i	Molar production rate of component i (mol/time)
$F(t)$	Rate of material addition in to the reactor (varies with time) (volume/time)
$\mathbf{r}(\mathbf{C})$	Rate vector as a function of the concentration vector ($mol/length^3.time$)
τ^*	Resultant residence from mixing (time)
τ	Residence time (time)
A	Stoichiometric matrix
t	Time/reaction time (units of time)
Q	Volumetric flow rate ($length^3/time$)
$V(t)$	Volume of the reactor as it changes with time (volume)
V	Reactor volume ($length^3$)

Acronyms

DSR	Differential side-stream reactor
PFR	Plug flow reactor
CSTR	Continuously-stirred tank reactor
ODE	Ordinary differential equation
$C-\tau$	Concentration-residence time
$C-t$	Concentration-time
2D	Two dimensional
3D	Three dimensional
AR	Attainable region
SSN	State-sequence network
STN	State-task network
RTN	Resource-task network

Chapter 1

Introduction

1.1 Backround

Attainable regions were first proposed by Horn (1964) as the total set of outcomes that could be achieved through the summed utilisation of all possible reactor structure designs for a given system and feed. This concept was developed by Glasser et al. (1987); Hildebrandt et al. (1990); Feinberg and Hildebrandt (1997); Glasser and Hildebrandt (1997); Feinberg (1999) as a geometric approach to determining an optimal reactor network for a given system. Most work has focused on the application of attainable regions to continuous reactor systems. Until 2013 Davis et al. (2008) was the only work that attempted application to batch reactors but an automated attainable region generation technique was utilised.

Ming et al. (2013) took the concepts as applicable to continuous systems and showed that one could apply them almost in its entirety to batch reactors as well. Hence attainable regions could be used as a technique to determine the optimal batch reactor structure to achieve a desired output. This made attainable regions applicable to industries that relied on batch reactors rather than continuous ones such as the pharmaceutical and biological industries (Oktem et al., 2008; Cheong et al., 2007). An element that was not considered in Ming et al. (2013) was the treatment of reaction time. More specifically whether the reaction time used in batch reactors had the same properties as residence time used in continuous reactors and hence whether it could be used in the same fashion. Such a distinction becomes more evident when time is used as a component of the attainable region and hence would need to be investigated before using such constructions.

Much of the work done on optimising batch processes has focused on the scheduling of these processes such as that shown in Méndez et al. (2006). Scheduling is largely performed on an existing or proposed structure of processes and the generation of the structure is not necessarily included in the problem to be addressed. The advances of attainable region theory as a method to determine an optimal reactor structure, and the recent application of this theory to batch reactors in Ming et al. (2013), puts it in a position to be used in conjunction with batch scheduling. This is especially true in the early design stages of a plant where no reactor structure has yet been determined. Attainable region theory could not previously be used in conjunction with batch scheduling as it was applied to continuous systems and the incorporation of time had not yet been investigated. Only one barrier now exists which is the incorporation and understanding of time in batch attainable regions. The use of attainable regions with time as a component has potential appeal to be used as a tool for reactor structure design within batch scheduling. Visualisation of the reaction time as it progresses throughout the reactor structure or system could provide additional insight when scheduling and assigning a reaction time to the reaction process.

1.2 Problem Statement and Research Questions

1.2.1 Problem Statement

Furthering the application of attainable region (AR) theory to batch reactors requires understanding the use of reaction time as a component in the AR. Specifically when time is included as a dimension of the AR for a batch reactor system, it needs to be determined how it is treated compared to the use of residence time in continuous reactor systems. Furthermore it needs to be determined whether the same mixing and reaction processes apply.

Production rate will be introduced as a method of interpreting the optimal batch reactor structure from an AR constructed in concentration-time space. The use of production rates and the conditions surrounding its use need to be investigated.

With these new developments, the positioning of AR theory within batch processes and optimisation will need to be discussed.

1.2.2 Research Questions

Answers to the following questions were sought in this work.

1. What differences exist between residence time in continuous systems and reaction time in batch systems?
2. Would differences in the representation of time affect the construction of attainable regions with time as a variable? Are these differences present only when constructing in concentration-time space?
3. Does the linear mixing law apply to reaction time as it does with residence time?
4. What does it mean to mix residence time?
5. Can production rates be used as a tool for interpreting ARs constructed for batch systems?
   (a) Can an increase in production rate be obtained through manipulation of the reactor structure?
   (b) Can production rates also be applied to continuous systems?
6. How does the application of AR theory to batch reactors fit within the traditional batch landscape?

1.3 Aims and Objectives

The aim of this work is to evaluate the use of reaction time as a variable in the attainable region for batch systems. This should include a comparison of residence time and reaction time and understanding the similarities and difference between them. A secondary aim is to assess whether batch systems can be designed using AR theory so as to increase the production output of the system. Following achievement of the above aims the resultant concepts should be able to be applied to selected case studies or examples.

A number of objectives exist to investigate the research questions posed in Section 1.2.2. The objectives are numbered to correspond to the research questions and are given as follows:

1. Investigate the concepts of residence time and reaction time. Note differences and similarities and contrast how they are applied in continuous systems and batch systems respectively.

2. As a variable in ARs investigate how the differences between residence time and reaction time materialise in AR construction for continuous and batch systems respectively. If the construction method differs then a new construction algorithm should be proposed. The proposed algorithm should be applied to constructions where differences exist such as when ARs are plotted in concentration-time space. The need to use such a plot and the possibility of using a single plot for continuous and batch systems needs to be evaluated.

3. Based on the definition of reaction time determine whether a linear mixing law applies to it. This objective is closely linked to objectives 1 and 2 and may be included in them.

4. Evaluate what it means to mix residence time in terms of physical interpretation and how this relates to an AR constructed in $C - \tau$ space.

5. Introduce production rates as a method of assessing batch reactor system output. Investigate its application to batch ARs and list its properties.

   (a) Through investigating its application, determine whether production rate may be increased for a given system by manipulation of the reactor structure or sequence used.

   (b) Determine whether production rates can be applied to continuous systems and investigate the correlation between production rates in continuous and batch systems.

6. Identify the role AR theory can play in the batch landscape and how it may be used in conjunction with batch scheduling and optimisation.

This work is organised into 5 chapters, the first of which offers an introduction and is concluded here. The second chapter provides introductory theory to attainable regions as well as a brief literature review applicable to the scope of this work. Development and evolution of the theory is contained in Chapter 3. This includes the investigation of residence time and reaction time, the introduction of production rates and the application of AR plots with time as a component to continuous and batch systems. Chapter 4 contains two examples in which the concepts developed are applied as well as developments that arose as a consequence of the second example. A brief discussion of the positioning of AR theory in relation to batch scheduling and optimisation is also included. Conclusions and recommendations are given in the final chapter.

Chapter 2

Introductory Theory and Literature Review

2.1 Introductory Attainable Region Theory

Attainable region (AR) theory is largely carried out in a geometric space and hence many of the properties that lay the foundation for the theory are geometric in nature (Feinberg and Hildebrandt, 1997). This section provides some introductory theory and concepts that will later be utilised in constructing or investigating attainable regions.

Only two processes are allowable while constructing the attainable region namely reaction and mixing (Hildebrandt et al., 1990). Therefore the theory develops the mathematical framework for the use of these two processes in constructing the AR.

2.1.1 Concentration Vector

The attainable region represents all possible outputs of a given system and feed after utilising the sum of all possible design structures (Horn, 1964; Feinberg and Hildebrandt, 1997). A given point within that region should therefore represent a unique output achievable through one (or more) of the possible reactor structures. Since work in AR is generally geometric in nature that output should be represented in a multidimensional format. A vector representation of concentration is used to accomplish this. If N components or chemical species are present in the system then the concentration vector is defined by Equation 2.1.1 where c_i is the concentration of component i (Feinberg, 2000b).

$$\mathbf{C} = [c_1, c_2, c_3, ..., c_N]^T \in \mathbb{R}^{\mathbb{N}} \tag{2.1.1}$$

The molar concentration of component i is given by Equation 2.1.2. An assumption of constant density is used in conjunction with the use of this equation. This follows directly from a mass balance performed over a reactor where the volumetric flow rate into the reactor is equal to the exiting flow rate.

$$c_i = \frac{n_i}{V} \tag{2.1.2}$$

2.1.2 Mixing

Mixing is described by the linear combination of two or more distinct concentrations as shown in Equation 2.1.3 (Hildebrandt et al., 1990). Hence mixing is a linear process facilitated by varying the mixing fraction λ. The geometric interpretation for mixing would be that $\mathbf{C}_1$ and $\mathbf{C}_2$ both lie on the same line i.e. $\mathbf{C}_1$ and $\mathbf{C}_2$ may be joined by a straight line.

$$\mathbf{C}^* = \lambda \mathbf{C}_1 + (1-\lambda)\mathbf{C}_2 \tag{2.1.3}$$

$$where \quad \lambda = \frac{V_1}{V_{total}} \quad and \quad 0 < \lambda < 1$$

In fact, mixing is a linear process even if the assumption of constant density is not adhered to. If molar concentration is replaced by the mass concentration/fraction of the species in the system, then the linearity of the mixing law still applies in a system that does not conform to the constant density assumption (Hildebrandt et al., 1990). The mass fraction expression for species i is given in Equation 2.1.4 and the relevant mixing law given in Equation 2.1.5. Note that the concentration vector described in Equation 2.1.1 would then simply contain the mass fractions and would be denoted $\mathbf{z}$.

$$z_i = \frac{m_i}{G} \tag{2.1.4}$$

$$\mathbf{z}^* = \lambda_m \mathbf{z}_1 + (1-\lambda_m)\mathbf{z}_2 \tag{2.1.5}$$

$$where \quad \lambda_m = \frac{G_1}{G_{total}} \quad and \quad 0 < \lambda < 1$$

2.1.3 Rate Vector and Rate Field

A system is generally described by the kinetics that dictate the reaction rate within the reactors. These kinetic expressions are treated similarly to concentrations in that they are placed in vector form. For a system with N species or components the rate vector is given by Equation 2.1.6 (Hildebrandt et al., 1990). Note that the rate of reaction for a given component has the same position or index in the rate vector as the concentration of that component in the concentration vector.

$$\mathbf{r}(\mathbf{C}) = [r_1, r_2, r_3, ..., r_N]^T \in R^N \tag{2.1.6}$$

The rate vector is a function of the concentration vector and hence a vector can be determined for each unique concentration. If this is done across the whole concentration space then a vector field is generated which is known as the rate field (Ming et al., 2013). A rate field is shown in Figure 2.1.1 for the following rate vector where the rate constants are unity:

$$\mathbf{r}(\mathbf{C}) = \begin{bmatrix} r_A \\ r_B \end{bmatrix} = \begin{bmatrix} -c_A \\ c_A - c_B \end{bmatrix}$$

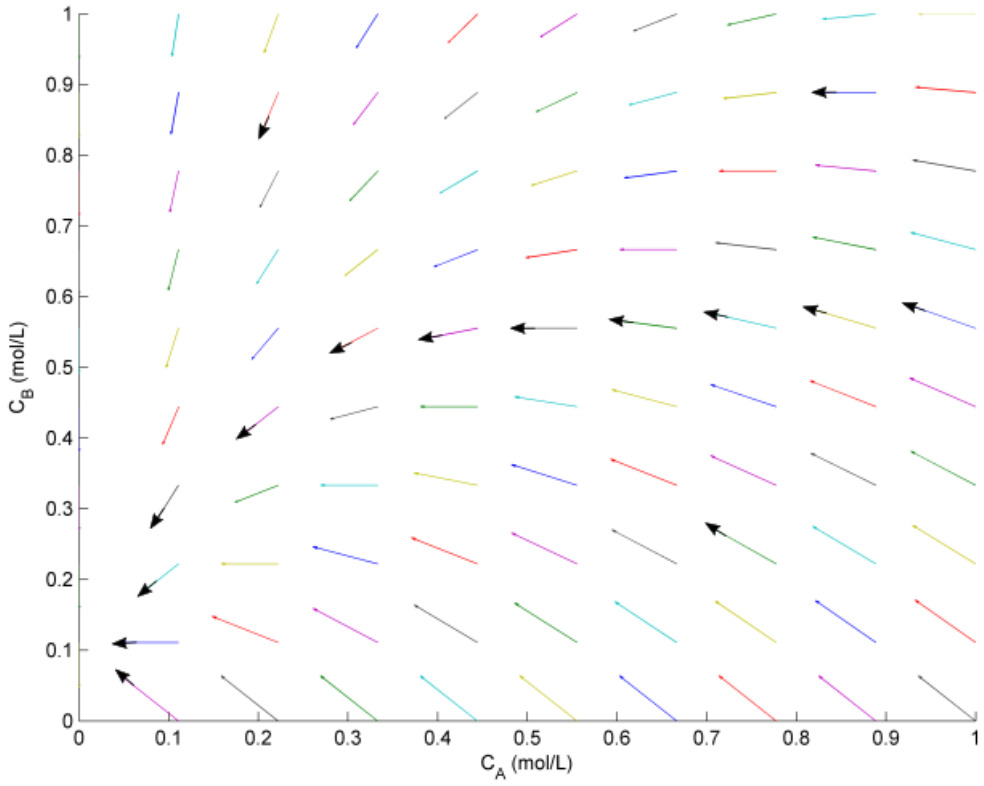

Figure 2.1.1: Graphical demonstration of a rate field for the given kinetics.

2.1.4 Reactor Types

Three reactor types are used in the construction of attainable regions namely the Plug Flow Reactor (PFR), Continuously-stirred Tank Reactor (CSTR) and the Differential Side-stream Reactor (DSR). This is a result of the fact that all possible outcomes of a given system and feed are achievable through the combination of these three reactor types alone (Feinberg and Hildebrandt, 1997). Each reactor is discussed giving both the mathematical description and the assumptions associated with each reactor.

2.1.4.1 Continuously-stirred Tank Reactor (CSTR)

CSTRs are assumed to be perfectly mixed such that all of the reactor contents has the same composition (Fogler, 2010). Consequently the effluent stream from a CSTR has the same concentration as the contents of the reactor. Equation 2.1.7 gives the mathematical expression for a CSTR derived under this assumption as well as that of constant density (Ming et al., 2013).

$$\mathbf{C} = \mathbf{C}_f + \tau \mathbf{r}(\mathbf{C}) \tag{2.1.7}$$

where

$$\tau = \frac{V}{Q} \tag{2.1.8}$$

Equation 2.1.7 has been rearranged to express it in terms of the reactor residence time and the concentration vector. Since the concentration vector is used, Equation 1 in fact represents a system of equations, one for each component in a given system.

It is clear from Equation 2.1.7 that for a given residence time and feed a single effluent concentration is possible. Therefore the CSTR is represented in concentration space as a point given by the effluent concentration vector. If the residence time is altered then the effluent concentration would differ. Therefore multiple points would be formed in concentration space if many potential residence times were substituted in the equation. This collection of points is known as the CSTR locus (Glasser and Hildebrandt, 1997). There is however the potential that multiple solutions (or multiple steady states) exist for the CSTR equation and hence multiple loci are possible (Glasser and Hildebrandt, 1997). This must be kept in mind when constructing the AR and all solutions should ideally be found.

If Equation 2.1.7 were manipulated to give

$$\mathbf{C} - \mathbf{C}_f = \tau \mathbf{r}(\mathbf{C})$$

once could recognise that the vector on the left hand side is a scalar multiple of the rate vector. Hence the line joining the feed point to the effluent point is collinear to the rate vector (Glasser and Hildebrandt, 1997). Figure 2.1.2 gives loci drawn for different feed points for the kinetics given in Section 2.1.3. Each loci consists of CSTRs at different residence times with each cross being a CSTR at a unique residence time. These loci are plotted on the rate field to demonstrate that the rate vectors are collinear to the lines joining the feed point and effluent of each CSTR.

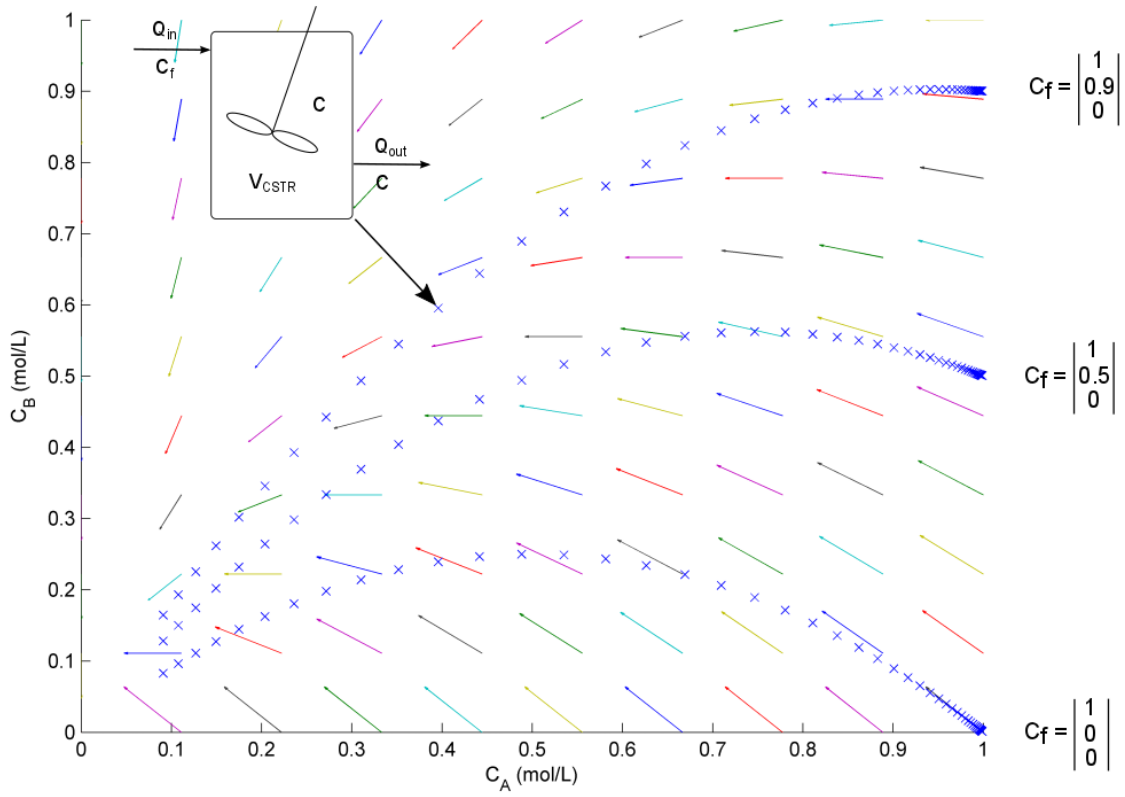

Figure 2.1.2: Geometric representation of CSTRs for given kinetics overlaid on the corresponding rate field. Each loci corresponds to a different feed point as indicated.

2.1.4.2 Plug Flow Reactor (PFR)

In contrast to the CSTR, a PFR is assumed to exhibit no axial mixing along the length of the reactor (Fogler, 2010). Instead the contents moves within the reactor as a "plug" reacting as it progresses down the reactor's length. Each cross sectional slice of the contents does not interact with material ahead of or behind it. Equation 2.1.9 gives the mathematical expression for the PFR which is again expressed in terms of the concentration vector and residence time (Ming et al., 2013). This equation therefore represents a system of Ordinary Differential Equations (ODEs). Each equation in the set of ODEs is with reference to one of the components of the respective reactor system.

$$\frac{d\mathbf{C}}{d\tau} = \mathbf{r}(\mathbf{C}) \tag{2.1.9}$$

Based on Equation 2.1.9, PFRs form a trajectory from the starting concentration to an effluent concentration (Glasser and Hildebrandt, 1997). Since the derivative of the concentration vector with respect to residence time is equal to the rate vector, the rate vector at a given point on the trajectory is tangent to the trajectory (Glasser and Hildebrandt, 1997). This is demonstrated in Figure 2.1.3 where the PFR trajectories from three different feed points are drawn for the kinetics given in Section 2.1.3.

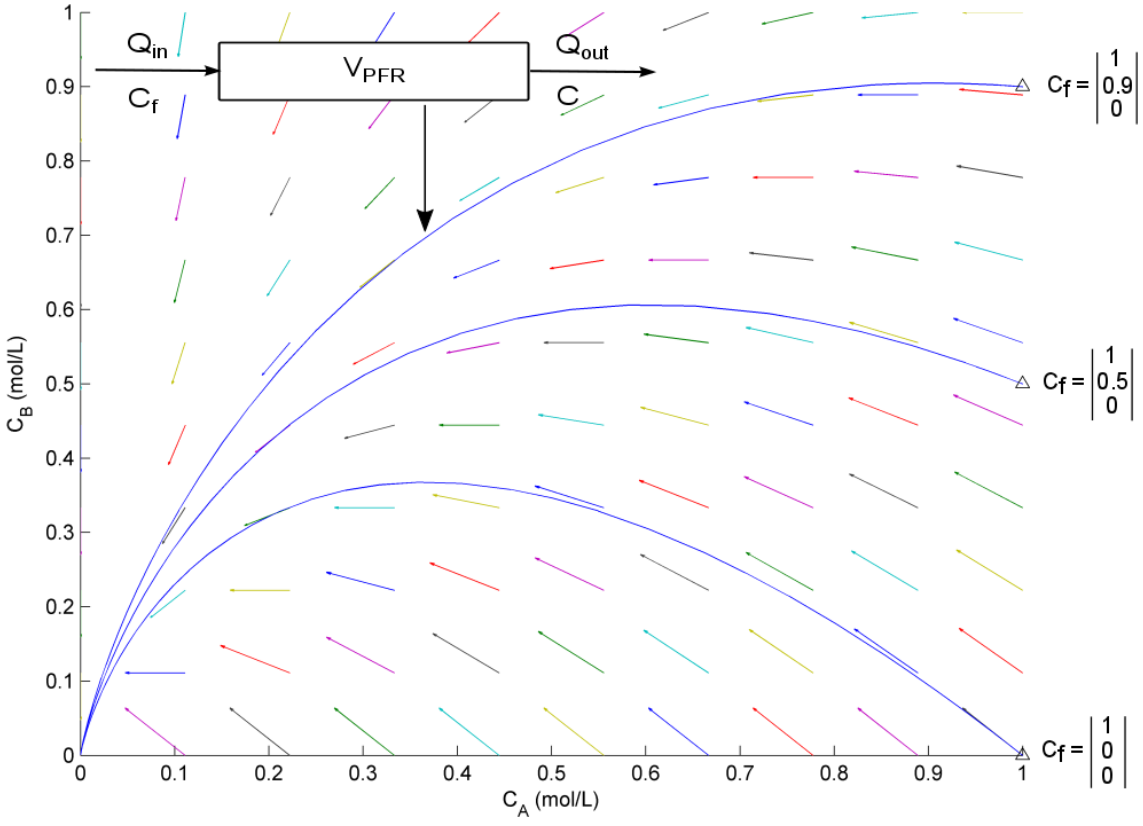

Figure 2.1.3: Geometric representation of PFRs for given kinetics overlaid on the corresponding rate field. Each trajectory corresponds to a different feed point as indicated.

2.1.4.3 Differential Side-stream Reactor (DSR)

A DSR is similar to a PFR with the exception that it has a side-stream being fed to it along its length. The amount of material added to the reactor with concentration $\mathbf{C_o}$ in the side-stream is governed by the α value shown in Equation 2.1.10 (Ming et al., 2013). As can be seen Equation 2.1.10 is different to Equation 2.1.9 only through the addition of a second term on the right hand side of the expression. DSRs are only required for problems that have three or higher dimensions (Glasser and Hildebrandt, 1997). Different policies or expressions of α may be used. Figure 2.1.4 demonstrates three different α values or expressions for a DSR for the kinetics given in Section 2.1.3 with the same feed point for each. Note that when α is equal to zero Equation 2.1.10 reduces to the PFR equation and hence the PFR trajectory is obtained.

$$\frac{d\mathbf{C}}{d\tau} = \mathbf{r}(\mathbf{C}) + \alpha(\mathbf{C_o} - \mathbf{C}) \tag{2.1.10}$$

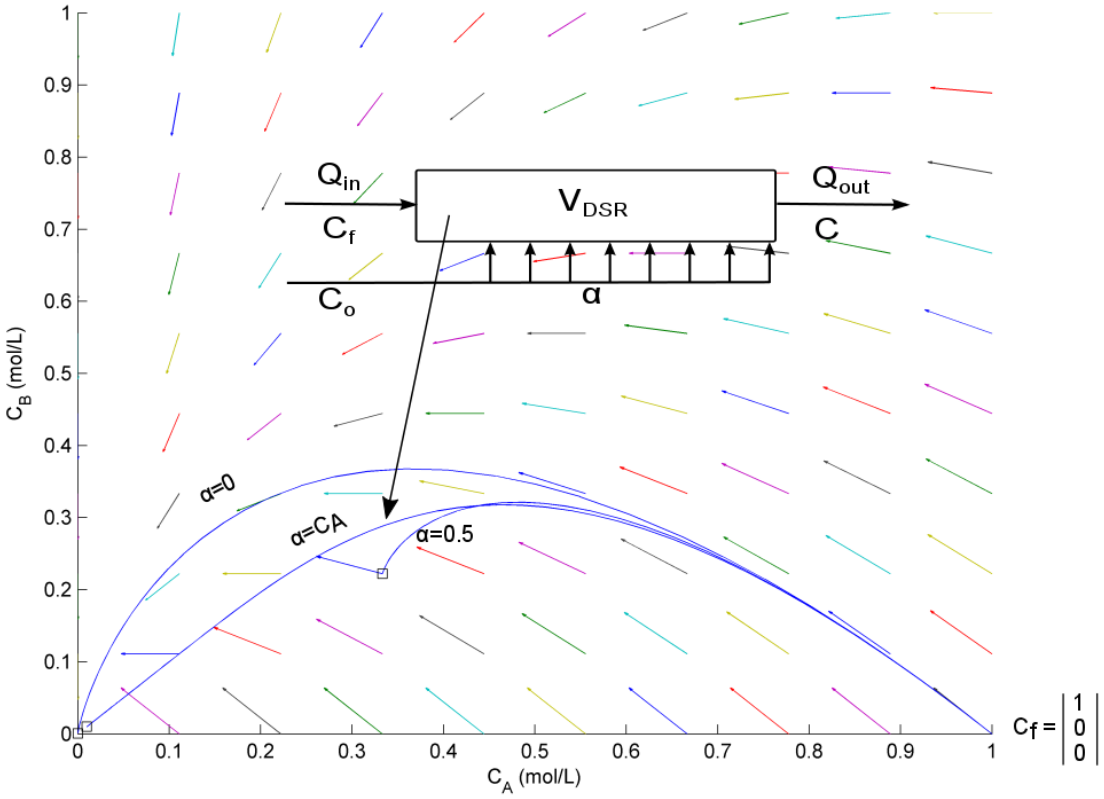

Figure 2.1.4: Geometric representation of DSRs for given kinetics overlaid on the corresponding rate field. Each trajectory corresponds to a different alpha policy as indicated.

When a DSR lies on the boundary of the AR then the DSR is said to be a critical DSR (Feinberg, 2000b). The α value has to follow the critical alpha policy for this to occur which can be determined through Equations 2.1.11 and 2.1.12 (Glasser and Hildebrandt, 1997). $\mathbf{J}(\mathbf{C})$ is the Jacobian matrix of $\mathbf{r}(\mathbf{C})$. Note that this method of determining α is restricted to three dimensional problems.

$$\varphi(\mathbf{C}) = [\mathbf{J}(\mathbf{C}).(\mathbf{C}_o - \mathbf{C})]^T [(\mathbf{C}_o - \mathbf{C}) \times \mathbf{r}(\mathbf{C})] \tag{2.1.11}$$

$$\alpha(\mathbf{C}) = -\frac{[\nabla\varphi(\mathbf{C})]^T \mathbf{r}(\mathbf{C})}{[\nabla\varphi(\mathbf{C})]^T (\mathbf{C}_o - \mathbf{C})} \tag{2.1.12}$$

Another type of critical reactor that exists is the critical CSTR. A critical CSTR is a CSTR that lies on the boundary of the AR and hence often take the role of a connector on the AR boundary, as does the DSR (Feinberg, 2000a). Feinberg (2000a) have proven that for a CSTR to lie on the boundary of the AR, the following condition must be satisfied:

$$Det\left[\left(\mathbf{C}-\mathbf{C}_f\right), dr(\mathbf{C})\left(\mathbf{C}-\mathbf{C}f\right), \left(dr(\mathbf{C})\right)^2\left(\mathbf{C}-\mathbf{C}_f\right), ..., \left(dr(\mathbf{C})\right)^{d-1}\left(\mathbf{C}-\mathbf{C}_f\right), Null\right] = 0 \tag{2.1.13}$$

The matrix formed in Equation 2.1.13 has to be square in order for the determinant of the matrix to be calculated and has size $n \times n$. *Null* is the null space of A^T (Equation 2.1.14) where A is the stoichiometric matrix of the system. The stoichiometric matrix (Equation 2.1.15) consists of the stoichiometric coefficients in the reactions of the system and has size $n \times d$, n being the number of components and d the number of independent reactions. This results in *Null* having a size of $n \times n - d$.

$$Null = null(A^T) \tag{2.1.14}$$

$$A = \begin{bmatrix} A_{1,1} & \cdots & A_{1,d} \\ \vdots & \ddots & \vdots \\ A_{n,1} & \cdots & A_{n,d} \end{bmatrix} \tag{2.1.15}$$

2.1.5 Construction of the Attainable Region

Using the concepts and principles discussed thus far one can construct the AR for a system given the kinetics and feed concentrations. The construction is started at the feed point and the region is then extended using the allowable processes of reaction and mixing (Hildebrandt et al., 1990). This region must still satisfy the mass balance and is hence constrained by the stoichiometry of the reactions. The region that is attainable by stoichiometry alone is known as the stoichiometric subspace and serves as an upper bound to the AR (Ming et al., 2013). The dimension of the AR is given as the number of independent reactions taking place in the system (Ming et al., 2013).

2.1.5.1 Convex Hull

The mixing process is not explicitly included in the construction of the AR. Instead, it is applied to the most extreme points achieved by reaction so as to obtain the final region. Any point that lies in this final region may be achieved through a combination of reaction and mixing although each point is not determined explicitly in its construction. The method used to apply mixing and fill in concavities is known as finding the convex hull. The convex hull is defined as the smallest set, of a set $\mathbb{H}$, that is convex and contains all of $\mathbb{H}$ (Ming et al., 2013). In other words if set $\mathbb{H}$ was a collection of concentration vectors then the convex hull of $\mathbb{H}$ would be the smallest number of vectors in $\mathbb{H}$ that would define the region containing $\mathbb{H}$ if only straight line or flat surfaces were used to connect the points of the convex hull.

By finding the the points that are attainable through reaction a set ($\mathbb{H}$) is found. Mixing has not yet been applied at this stage. The convex hull of $\mathbb{H}$ is then found and the region it encompasses is filled in to determine the final AR. Figure 2.1.5 provides a graphical illustration of the concept in 2D form. In this case points 1-8 form the set $\mathbb{H}$ in $c_A - c_B$ space. Points 1-6 form the convex hull of $\mathbb{H}$ as these points define the entire region that contains all the points. These points are joined with straight lines as mixing of concentrations is a linear process. Any point within the bounds is now achievable through mixing even though not every achievable point has been explicitly considered. For example, points 1 and 3 can be mixed to obtain any point between them but these intermediate points were not considered in the construction of the region and are instead inherently attainable by being within the bounds of the region.

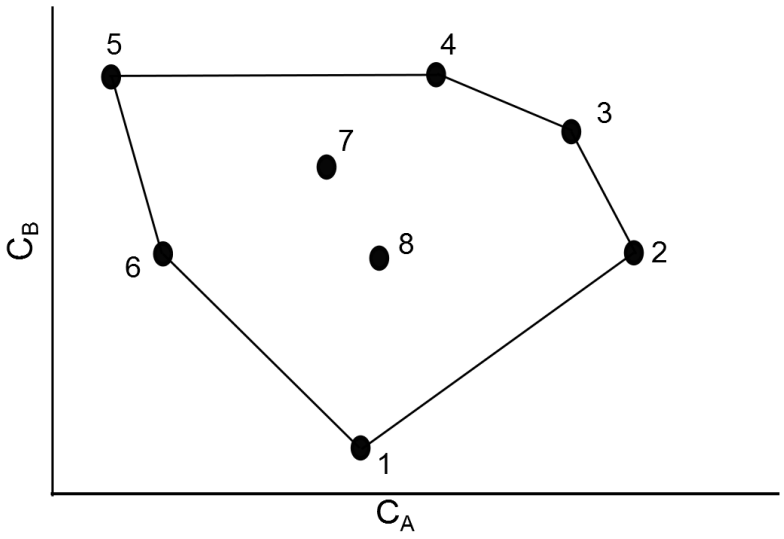

Figure 2.1.5: Example set of points that illustrates the concept of convex hulls. Each point is a defined point in concentration space with a subset or convex hull of the points forming the outer boundary of the region.

2.1.5.2 Properties of the Attainable Region

Based on the geometric properties of the tools used to construct the AR, the resultant AR must conform to certain conditions. These conditions are given by Glasser et al. (1987); Glasser and Hildebrandt (1997) with some listed below:

- The resultant AR has to contain the feed. This is the starting point before any processes have been applied and hence is attainable by default.
- The resultant AR has to be convex. Any concavities present within the region can be filled by mixing hence ensuring the region is convex.
- If a rate vector is on the boundary of the AR then it must have a direction that points into the region or be tangent to the boundary of the AR. Due the properties of the PFR a rate vector that points out of the region can be used to extend the region.
- All rate vectors that are located outside of the AR (otherwise known as the complement region) cannot intersect the boundary of the AR if extended backwards. This is due to the collinearity property of the CSTR. Hence the region could be extended further if this were the case.

These conditions do not constitute a sufficiency condition for the AR. Such a sufficiency condition does not yet exist (Ming et al., 2013).

2.1.6 Application to Batch Systems

In Section 2.1.4 the reactor types used in the construction of an AR were presented. These reactors are continuous reactors and are assumed to operate under steady-state conditions. Recently AR theory has also been applied to batch reactors in Ming et al. (2013). Previous to this automated AR construction methods had been used such as in Davis et al. (2008) but the essential AR theory had not been transcribed over to batch systems. It was shown in Ming et al. (2013) that the same equations used in continuous reactors were able to be applied to batch systems. This means that the AR for a continuous reactor system in concentration space was the same AR for the batch system (Ming et al., 2013). It is merely the interpretation of the AR as a continuous or batch system that changes and not the AR itself.

Discussed here are the three reactor types used for batch systems, namely, the standard batch reactor and two fed-batch reactors each with a different policy for material addition.

2.1.6.1 Standard Batch Reactor

This reactor type consists of no flow in to or out of the reactor while the reaction takes place (Fogler, 2010). It is assumed that the reactor contents is well mixed such that the reaction rate is constant throughout the reactor. The standard batch reactor equation is analogous to that of the PFR expression given in Equation 2.1.9 (Ming et al., 2013). Hence the batch reactor has the same trajectory through concentration space as the equivalent plug flow reactor. If one replaces the residence time, τ, in Equation 2.1.9 with reaction time, t, we get the equation for the standard batch reactor:

$$\frac{d\mathbf{C}}{dt} = \mathbf{r}(\mathbf{C}) \tag{2.1.16}$$

The same geometric properties exist for the batch reactor as for the PFR namely that the rate vector is always tangent to the solution trajectory when evaluated at points on the trajectory. It must be noted that $\tau = t$ and therefore a reaction carried out in a PFR for a residence time of τ can be achieved in a batch reactor by allowing it to react for the same length of time (Ming et al., 2013).

2.1.6.2 Fed-batch Reactors

Fed-batch (or semi-batch) reactors are most often used in the attempt to enhance the selectivity of a certain component within a set of reactions (Fogler, 2010). This is facilitated through the addition of fresh feed throughout the batch cycle. Ming et al. (2013) gives the general form of the fed-batch expression to be

$$\frac{d\mathbf{C}}{dt} = \mathbf{r}(\mathbf{C}) + \left[\frac{F(t)}{V(t)}\right](\mathbf{C}' - \mathbf{C}) \quad \textit{where} \quad \left[\frac{F(t)}{V(t)}\right] = \alpha \tag{2.1.17}$$

The change in volume of the reactor is equal to the feed rate into the reactor. As both change with time and from the expression for α above:

$$\frac{dV}{dt} = F(t) = \alpha V$$

Rearranging:

$$\int_{V_o}^{V} \frac{dV}{V} = \int_{t_o}^{t} \alpha dt \tag{2.1.18}$$

Equation 2.1.18 may be further developed and used to express the volume of the reactor and the feed rate as a function of α and time

Note that Equation 2.1.17 is similar to that for a DSR. Each fed batch reactor is described using Equation 2.1.17 but with a different expression for α. In fact three different cases exist for what α may be (Ming et al., 2013).

1. The first is when $\alpha = 0$ and Equation 2.1.17 reduces to Equation 2.1.16 hence obtaining standard batch operation. This is intuitive since no material is added to the vessel. The other two cases result in different fed-batch operations.

2. The second case is that of a standard DSR in that $\alpha = f(C(t))$. The value for α thus varies along the length of the DSR as a function of the concentration within the reactor. Interpreting this for a fed-batch reactor, the feed rate into the reactor varies with respect to the reactor volume both of which can vary with time. Hence when using a DSR with a variable α to construct the AR, one can determine the necessary rate of material addition to obtain a fed-batch reactor that acts as the DSR equivalent. This is done by integrating the α with respect to time and using it in conjunction with the differential volume expression to obtain $F(t)$ and $V(t)$ (Ming et al., 2013).

3. The third case is when α is equal to a constant value throughout the reaction period (Ming et al., 2013). Therefore the rate of material addition with respect to the reactor volume is kept constant. When a sufficient reaction time is allowed the contents may approach equilibrium at which change in concentration no longer occurs. Equation 2.1.17 then reduces to

$$0 = \mathbf{r}(\mathbf{C}) + \alpha\left(\mathbf{C}' - \mathbf{C}\right) \tag{2.1.19}$$

It is easy to see that with $\frac{d\mathbf{C}}{dt} = 0$ and $\alpha = 1/\tau$ Equation 2.1.19 is equivalent to Equation 2.1.7. Therefore a constant α DSR operated at equilibrium has an effluent concentration equivalent to a CSTR with the same residence time. Hence when equilibrium is reached in a fed-batch reactor the concentrations obtained are equivalent to that of CSTR concentrations (Ming et al., 2013). CSTR equivalence in a fed-batch reactor is thus only obtainable at equilibrium. Recall Figure 2.1.4 where the trajectory resulting from an α of 0.5 terminated at a point within the concentration space. This would be the effluent point of the corresponding CSTR.

Ming et al. (2013) states that in order to achieve equilibrium in a fed-batch reactor the reactor has to be initiated at or near the equilibrium point. In other words the initial reactor contents must have the same concentration as the equilibrium concentration. This could be achieved by either using the effluent of the equivalent CSTR to seed the reactor or by allowing the reactor to reach equilibrium before assuming fed-batch operation (Ming et al., 2013).

2.1.7 Time in Continuous Reactor Systems

Residence time, τ, is used as the time component of Equations 2.1.7, 2.1.9 and 2.1.10. τ is expressed as Equation 2.1.8 (Fogler, 2010) and is simply the amount of time a reacting substance is present in a reactor as determined by the reactor volume and flow rate of the feed stream. This does in fact equate to the amount of time allowed for the reactants to undergo reaction and hence why an equivalence is drawn to reaction time in batch reactors in Ming et al. (2013).

Residence time serves as a useful measure of the volume of a continuous reactor network but as yet the connection between residence time, τ, and reaction time, t, in batch systems has not been fully investigated within the context of ARs. This work serves to fill this gap in understanding.

2.1.7.1 Attainable Regions in Concentration-residence Time Space

Using residence time as a component in the concentration vector one may construct an attainable region in concentration-residence time ($C-\tau$) space (Glasser et al., 1992a). This is allowable as a result of residence time following the linear mixing law shown in Equation 2.1.20 (Hildebrandt et al., 1990). Mixing may therefore be applied between any points achievable within the attainable region resulting in a convex region. The properties of an AR are therefore satisfied.

$$\tau^* = \lambda\,\tau_1 + (1-\lambda)\,\tau_2 \quad 0 < \lambda < 1 \tag{2.1.20}$$

The rate vector used in conjunction with the concentration vector is (Glasser et al., 1992a):

$$\mathbf{r}(\mathbf{C}) = [r_1, r_2, r_3, ..., r_N, 1] \tag{2.1.21}$$

where the residence time component of $\mathbf{r}$ is one since the derivative of r_τ with respect to τ is one.

When such an attainable region is plotted, an unbounded region is essentially obtained. The concentrations are still bound by the mass balance but residence time does not possess an upper bound and hence can tend towards infinity (Hildebrandt et al., 1990). This means that a concentration achievable at a given residence time is available from that residence time to an infinite residence time.

2.2 Literature Review

The aim of this work is to further investigate the application of AR theory in batch reactors as initiated by Ming et al. (2013). Therefore the literature review presented here focuses on the current batch landscape and the approaches generally followed when optimising and designing batch systems. It may be said that there are two general areas on which to focus namely batch scheduling and batch reactor optimisation (optimisation of operating conditions). The former concerns itself with determining the optimal schedule for a batch process including both reactive and non-reactive processes such as mixing, heat transfer and distillation. Optimisation of batch reactors on the other hand attempts to optimise an existing reactor or reactor structure in terms of process conditions and variables. It is intended to provide a brief overview of these areas so that the positioning of AR theory in the batch landscape may be better understood.

2.2.1 Batch Process Scheduling

The time inherent nature of batch systems where every participating process has a certain duration makes scheduling of batch processes crucial in operation of a batch plant (Seid and Majozi, 2012). A resultant schedule provides the order of operations and defines certain times at which processes are run (Seid and Majozi, 2012). Naturally the schedule would then take the form of a Gantt chart. This is confirmed by a quick review of the literature with a basic adaptation of such a Gantt chart shown in Figure 2.2.1 (Méndez et al., 2006; Ferrer-Nadal et al., 2007; Liu and Karimi, 2007; Pan et al., 2009; Seid and Majozi, 2012; Moniz et al., 2014).

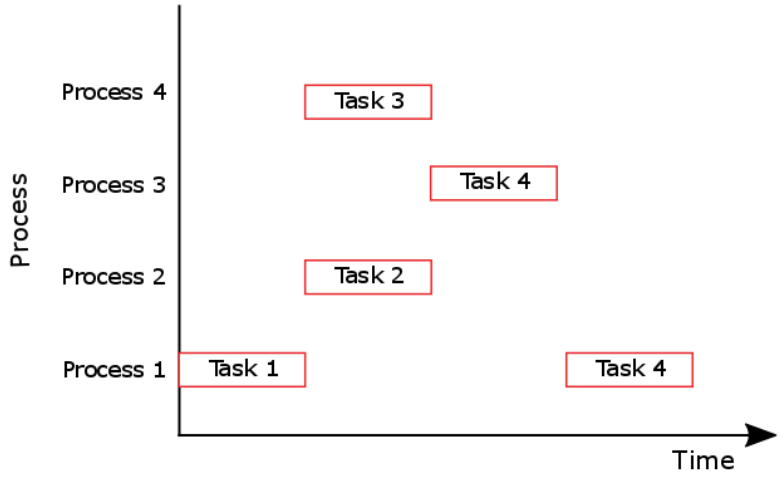

Figure 2.2.1: Basic adaptation of a Gantt chart used to define the schedule of a batch process.

If we were to review the same literature we would find that while various different techniques and models are used to derive the schedules for the batch plants, they all arrive at a similar representation of the schedule in the form of the Gantt chart in Figure 2.2.1. We will not delve into the various techniques used for scheduling here as a greater focus will be placed on the reactor element of the processes being scheduled.

In the papers consulted the input information for the process case studies followed the form found in Seid and Majozi (2012) which is given in Figure 2.2.2 and Table 2.2.1. In all cases the reaction processes were considered to be black boxes with the length of reaction predefined in the table of parameters. In Méndez et al. (2006) the representation of the process considered the length of reaction to be a function of the reactor size (Figure 2.2.3) but the reactions and reaction process itself were still viewed as a black box. The possibility of a reactor network or further optimisation of the reaction to reduce the reaction time was not considered in any of the cases reviewed. This is to be expected as the main aim of these works was to provide a scheduling of the full batch process. However, the case may be put forward for reducing the length of the batch process by reducing the reaction time of the reaction portion.

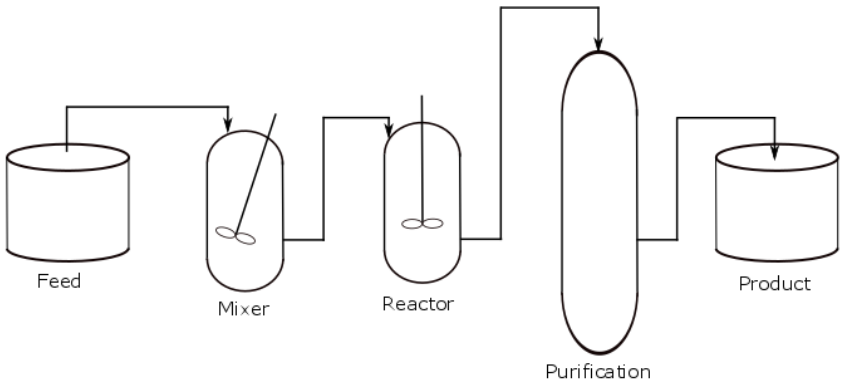

(a)

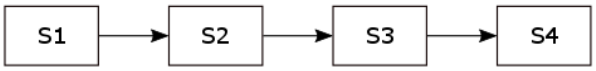

(b)

(c)

Figure 2.2.2: Adapted process representation of case study in Seid and Majozi (2012) with the process (a), the state-sequence network (SSN) (b) and state-task network (STN) (c).

Table 2.2.1: Table providing parameters for each of the processes in Figure 2.2.2 (Seid and Majozi, 2012).

Unit	Capacity	Suitability	$\tau\left(s_{in,j}\right)$	$\beta\left(s_{in,j}\right)$
Heater	100	Mixing	3 for batch dependent 4.5 for fixed duration	0.03
Reactor	75	Reaction	2 for batch dependent 3 for fixed duration	0.0266
Separator	50	Purification	1 for batch dependent 1.5 for fixed duration	0.02
Storage capacity	Initial amount	Price		
Unlimited	Unlimited	0		
0	0	0		
0	0	0		
Unlimited	0	1		

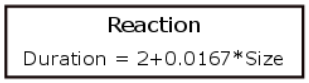

Figure 2.2.3: Adaptation of extract from the Resource Task Network (RTN) representation of a process in Méndez et al. (2006).

2.2.2 Batch Reactor and Process Optimisation

A separate focus in the batch process landscape is the optimisation of batch processes or reactors excluding the scheduling consideration. Dietz et al. (2006) offers a solution to batch plant design and optimisation using a multiobjective genetic algorithm with a Pareto optimal ranking system. The result of the proposed method is a set of optimal designs optimised in various extents considering both cost and environmental impact. A designer would then select the appropriate design weighing up the benefits of each solution provided as some solutions would provide greater cost benefit versus environmental benefit and vice versa. In the case of Dietz et al. (2006), the process variables that were varied for optimisation purposes were the size of the different equipment pieces and the operating conditions. The process itself however in terms of the structure remained unchanged and a single fermenter reactor was used as the reactor portion of the process. Optimisation of reactor network itself did not form part of the optimisation in this case.

Review of the available literature reveals that it is not a popular approach for batch optimisation to consider the reactor network. Instead traditional batch optimisation follows an approach similar to that of Aziz and Mujtaba (2002); Macku and Novosad (2015) . These works focus on optimisation of the operating conditions of a single batch reactor. Macku and Novosad (2015) for example optimised the reactor dimensions to produce more chemicals in the same or shorter amount of time. Aziz and Mujtaba (2002) on the other hand focuses on the standard practice on optimising the conversion or minimising the production time. Of course other objectives may be proposed and solved. Again in both instances it seems as if consideration towards an alternate arrangement of the reactors or an extended reactor structure was not considered. This definitely hints towards the positioning of AR theory within the batch landscape.

2.2.3 Evolution of Attainable Region Theory to Batch Reactors

Introductory theory to attainable regions was provided in Section 2.1. As mentioned previously the only two works that have moved to apply AR theory to batch reactors are that of Davis et al. (2008) and Ming et al. (2013). Ming et al. (2013) provided a translation of AR theory to batch reactors and showed that we may determine an optimal batch reactor structure from the same AR applied to a continuous system. This puts AR theory in a position to expand the batch landscape to include more consideration towards the batch reactor structure. Doing so may only improve the overall optimisation of batch processes.

We must emphasise at this point that AR theory does not impose on the current works on batch systems but approaches the problem from a different angle. By viewing the problem from additional angles we may improve the design and optimisation on batch processes. For example, suppose we are given a scenario in which we have the reaction kinetics for a system and are tasked with providing an initial design and scheduling of the batch process. All of the above-mentioned approaches may be used in conjunction to solve the problem. Firstly AR theory may be applied to obtain the most optimal batch reactor structure for the reaction portion of the process. These reactors may be further optimised in terms of desired process variables and then the process schedule may be determined. This work aims to investigate the use of attainable regions within this role. As batch systems are heavily defined in terms of time, the obvious space in which to work would be within an AR that includes time as a component. Therefore the use of time as a component in an attainable region as it relates to batch systems will have to be further investigated.

Chapter 3

Development of Theory

3.1 Investigation of Time in Batch Attainable Regions

As outlined in Section 1.2, this work concerns itself with the application of time in attainable regions applied to batch systems especially when time is used as a variable of the attainable region (AR). Naturally one must also consider the use of residence time as a component of an AR and how reaction time and residence time differ in their interpretation within the context of AR theory and how they may differ in application.

3.1.1 Reaction Time and Residence Time

Residence time is used as the time component of continuous systems with reaction time being used for batch systems. Ming et al. (2013) found that the ARs plotted in concentration space were the same for both continuous and batch systems and it was the interpretation that differed between the two systems. Interpretation is said to differ as there are reactor types in the two different systems that are equivalent in mathematical and geometrical representation and one would simply select the continuous or batch type based on the application at hand. What was not considered in Ming et al. (2013) was ARs plotted with time being one of the variables. Differences must surely exist between reaction time and residence time due to their definitions alone. This section concerns itself with defining both residence time and reaction time and evaluates their application as a variable in ARs. This includes differences that arise between the two as well as physical interpretations of such plots.

3.1.1.1 Residence Time

Residence time was defined in Section 2.1.7 as the amount of time a reacting substance was present in a continuous reactor as determined by the reactor volume and inlet flow rate. A mathematical representation of this was given by Equation 2.1.8 and is included here for convenience sake with an evaluation of the units.

$$\tau = \frac{V}{Q} \quad \left(\frac{volume}{volume/time} = time \right)$$

It is clear that residence time does not behave like time and that it merely has the units of time. In other words an action, passing a fluid through a reactor volume, has to occur in order for

the residence time of that fluid to increase. It is this nature of residence time that allows for residence time of two fluids to be mixed. For an illustration of this consider the schematic in Figure 3.1.1 which shows two PFRs of differing volume. Each has a different flow rate that passes through it resulting in different residence times at the outlet of each reactor. These two streams are then mixed to form one stream with the total flow rate being the sum of the two contributing flow rates. In this instance constant density has been assumed but this does not have to be the case.

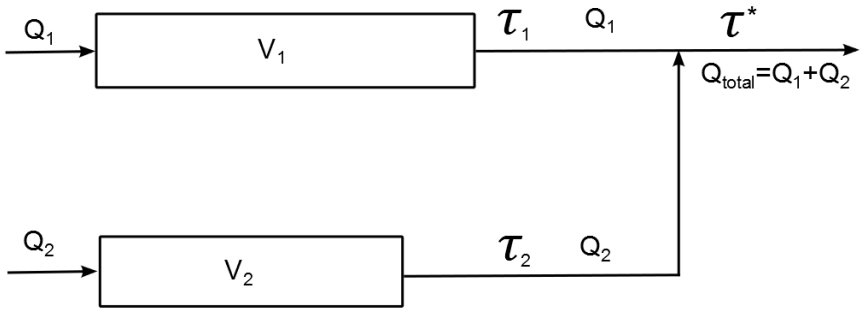

Figure 3.1.1: Schematic of two PFRs with different volumes. The exit streams mix downstream. Constant density is assumed in this example.

The total residence time of the system is given by the total volume divided by the total flow rate:

$$\tau^* = \frac{V_{total}}{Q_{total}} = \frac{V_1 + V_2}{Q_{total}}$$

The volume of each reactor can be expressed as the multiplication of the residence time by the associated flow rate:

$$\tau^* = \frac{\tau_1 Q_1 + \tau_2 Q_2}{Q_{total}}$$

Letting $\frac{Q_1}{Q_{total}} = \lambda$, where λ is the mixing fraction, Equation 2.1.20 is obtained:

$$\tau^* = \lambda\,\tau_1 + (1-\lambda)\,\tau_2 \quad 0 < \lambda < 1$$

By varying λ between 0 and 1 one can achieve a residence time, τ^*, that lies between τ_1 and τ_2. This was not purely a demonstration on how to arrive at Equation 2.1.20 but also as to the nature of why residence time can be mixed. The time itself is not being mixed but rather the volumes through which the fluid passes. This is also intuitive from the definition of residence time. The result is a mixture of fluids that have passed through two different volumes and hence spent different periods of time in each reactor.

Figure 3.1.2 provides an illustration of the mixing process that occurs in continuous systems. Points A and B are concentrations achieved at different residence times. When mixed, any point on the line is achievable by varying λ and mixing occurs in both concentration and residence time space.

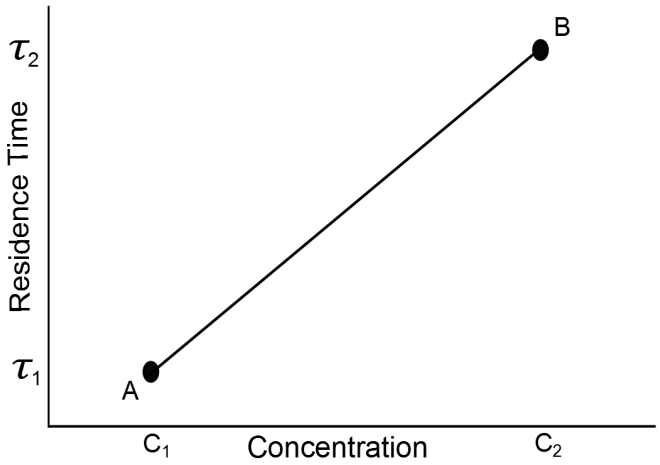

Figure 3.1.2: Mixing line in concentration-residence time space for continuous systems.

Similar procedures are followed when multiple points are present. Figure 3.1.3 includes points A-H in concentration-residence time space. An achievable region can be found by taking the convex hull of the points. The convex hull is the set of outermost points that define the region that contains all the points. The region can be formed by joining the outermost points with straight lines (mixing lines). This region is shaded in Figure 3.1.3. Any concentration-residence time point within this shaded area can be found through mixing just the initial points. Hence this is the attainable region in concentration-residence time space if only these points are available. This can be extended to three or more dimensions although in greater than than three dimensions it is difficult to visualise the result. This illustration does not consider the unbounded nature of residence time which will be discussed in Section 3.1.1.3.

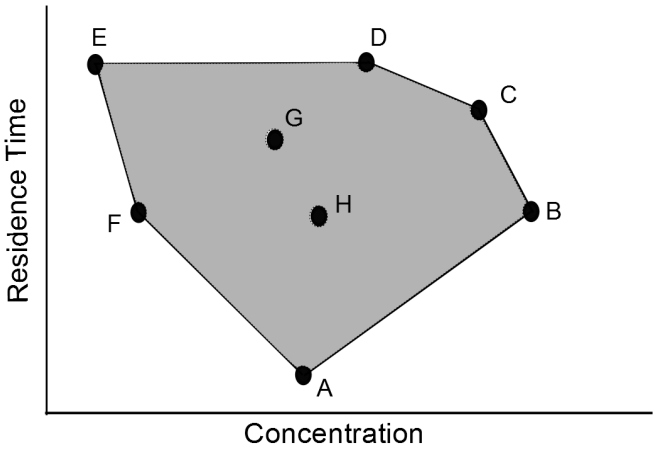

Figure 3.1.3: Forming a region from multiple points in concentration-residence time space.

Note how the region obtained in Figure 3.1.3 is convex. This is one of the properties of the attainable region given in Section 2.1.5 and is purely a consequence of the linear nature of mixing. Any concavity can be made convex through mixing (Glasser and Hildebrandt, 1997; Glasser et al., 1987).

3.1.1.2 Reaction Time

Reaction time has no mathematical expression in terms of other variables. It is not intended to investigate the philosophical nature or investigation of time by other disciplines but rather present the definition and understanding of time in a batch reactor context.

Reaction time can be defined as the amount of time a substance is allowed to react within a reactor. This definition is similar to that of residence time hence the equivalence drawn in Ming et al. (2013). A key contrast to residence time is that no action has to take place in order for time in batch systems to increase. Time will naturally increase even if no reaction occurs and hence the time in a batch system increases relative to the reference time whether the substance is in a reactor or not. Therefore it can be said that there are two "types" of time in batch reactor systems; reaction time, which is the time in which a reaction occurs, and the inherent time present in mass-time space. This distinction may seem pointless but it is key in understanding the similarities and differences between residence time and time in batch systems. Inherent time would naturally be included as part of batch scheduling and actions such as mixing, storing and other non-reactive processes would take part within this “type” of time.

Figure 3.1.4 represents these concepts graphically in the context of batch processes. Two batches A and B are initiated at the same time, t_o. Only batch A undergoes any form of reaction and the time in which this reaction takes place is indicated as reaction time. Note that even though batch B has no reaction taking place, the time allocated to it still increases due to the inherent nature of time. Once the time reaches t_1 both batches have no reactions taking place and the time increases for both A and B while the concentrations remain constant. The reaction time in batch A is the same residence time required in an equivalent PFR to achieve a concentration of C_1 from an inlet concentration of C_0. This is the equivalence drawn in Ming et al. (2013). However what is absent in the continuous equivalent is that residence time cannot escalate beyond t_1 without passing through a vessel with a specified volume. Nor could the case of B occur without any action. In a batch system the time component of B increases while the concentration remains constant simply by leaving the container alone. The manner in which residence time in continuous systems is escalated without reaction is discussed in Section 3.1.1.3.

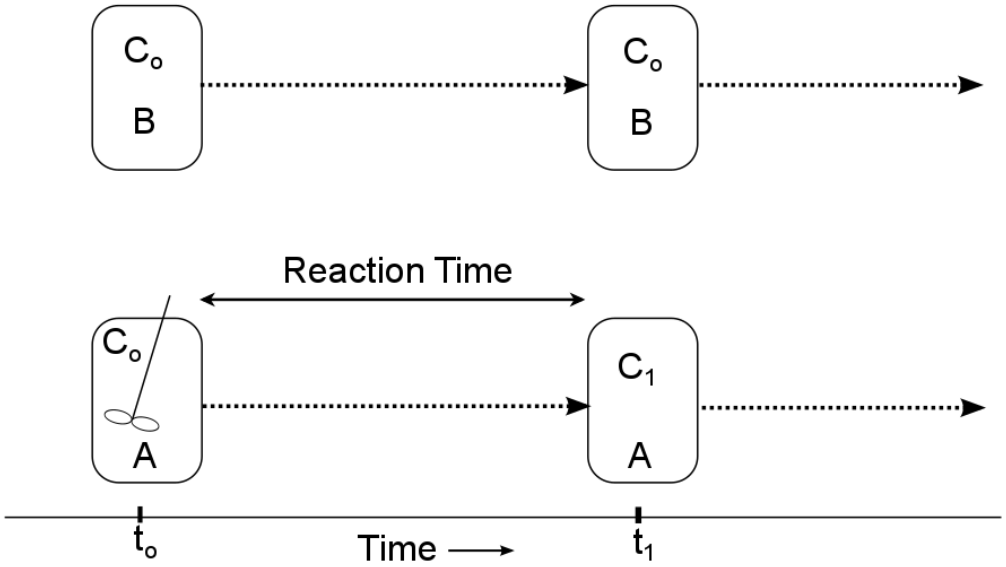

Figure 3.1.4: Two batch containers A and B placed on a time line and initiated at time t_o. Container B has no reaction taking place and the concentration remains the same throughout while A has reactions taking place between t_o and t_1. After the reaction time, t_1, A is allowed to rest with no reactions taking place.

From this point forward "residence time" refers to the time component used in continuous reactor systems while "time" shall refer to the time component of batch reactor systems. The latter is inclusive of both reaction time and time that naturally passes since reaction time is simply a portion of time itself.

From the definition of time in batch systems it is an intuitive consequence that time cannot be mixed in the same fashion as residence time is. Time in fact cannot be "mixed" at all. It takes a simple thought experiment to prove this. If one were to take any two days on the calendar at noon, with a desire to obtain a time and date between these, could such a mixture be achieved? No. When one is at the earlier calendar date the future date is inaccessible and when one is at the future calendar date the past date is inaccessible. In a given instant only one instance of time exists and hence one cannot mix two different times to achieve a point of time between them.

Mixing in concentration-time space in batch systems is therefore different from that in continuous systems. Figure 3.1.5 is the batch reactor version of Figure 3.1.2. It is clear from Figure 3.1.5 that mixing occurs only in concentration space in batch systems. The time component of point A increases until t_2 (to form point C) which is the time at which point B is formed. Only then can these two points be mixed to achieve a different concentration which follows the linear mixing law given in Equation 2.1.3. It is assumed in this case that the mixing process is instant and no delay in time is experienced.

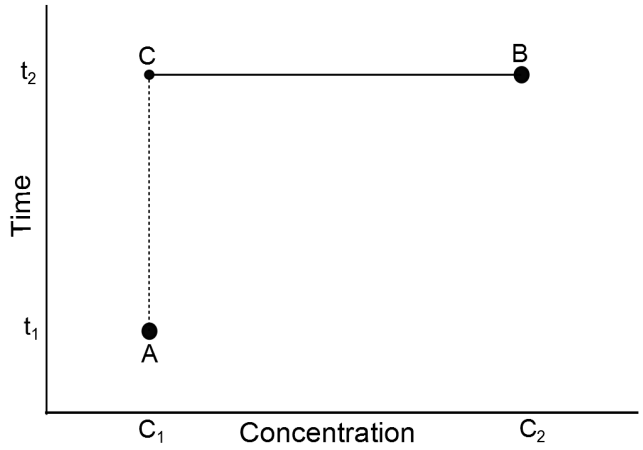

Figure 3.1.5: Mixing line in concentration-time space for batch systems.

Multiple points being present is treated in the same fashion where mixing is only allowed in the concentration space and not between times. For this reason the convex hull of points cannot be found when the points are in concentration-time space as it was for continuous systems. Figure 3.1.6 presents the same points as given in Figure 3.1.3 except the mixing is now executed in concentration space alone. Mixing lines are thus horizontal with vertical lines representing an increase in time. The full region found in Figure 3.1.3 is no longer available. Instead the time component of each point is raised until it reaches a point at which other points are available to mix concentrations with. For instance point A is raised until it reaches the F-H-B line where it can be used to mix with these concentrations. Points y and z are formed by increasing the time of points F and B respectively and can be mixed in concentration space to form point C. Likewise x can be formed through mixing points F and H after which it can be left to form point G.

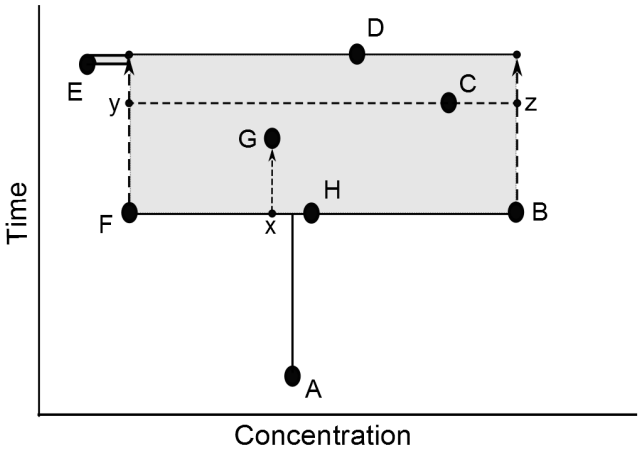

Figure 3.1.6: Forming a region from multiple points in concentration-time space.

The region formed in Figure 3.1.6 is no longer a convex region but rather a region formed through horizontal and vertical lines. Figure 3.1.6 closely resembles a Gantt chart which are often used to represent the results of batch scheduling. A vertical line forms part of the region and concavities are unable to be made convex. It is clear that the convex property of attainable regions plotted in concentration-time space no longer holds. Either the region plotted in Figure

3.1.6 is not referred to as the attainable region or this property can be ignored when plotting the attainable region in such a space for batch systems. The property of the region being convex only holds when the construction algorithm contains a linear mixing law. Since the convex property is solely a result of the linear mixing law, this "region" may still be called the attainable region but will not have a convex boundary as one of its properties. A new construction algorithm for ARs constructed in concentration-time space would have to be formulated in this case which is a slight departure from standard AR theory. Whether such a method could or should be applied and used in conjunction with AR theory will have to be seen and is discussed later in the current work.

3.1.1.3 Unbounded Nature of Residence Time - Relevant Reactor Structures

Concentration in a reactor system is bound by the law of conservation of mass. The stoichiometric subspace represents the region of concentrations achievable through mass balance alone and not taking into account reaction kinetics. This subspace is the upper bound of the attainable region which cannot extend beyond this space. As mentioned in Section 2.1.7.1, residence time does not have such an upper bound and consequently when used as a variable in an AR, the AR becomes unbounded with reference to this variable (Hildebrandt et al., 1990).

It was stated in Section 3.1.1.1 that residence time does not increase without the action of passing through a vessel of specified volume due to its definition. The question that naturally arises in response is how the residence time of a point, such as the feed point, increases such that an unbounded region with respect to residence time is obtained. The feed point into a reactor network has a residence time of zero. From the definition of residence time

$$\tau \to \infty \quad as \quad V \to \infty$$

Therefore a portion of the feed point must be redirected to pass through a vessel such that no reaction occurs and that the exit flow rate of the vessel is equal to that of the entering flow rate. This vessel may be termed a dynamic holding tank which operates as a CSTR without the mixing and reaction. The stream exiting the holding tank therefore has a residence time as determined by the volume of the tank and the flow rate of the stream. If the volume of the tank tends to infinity then so to does the residence time. This offers an explanation as to how the residence time of any point may increase without reaction. These dynamic holding tanks become part of the potential reactor structure when an AR is plotted with these variables from a theoretical perspective at least. The practicality of forming such a reactor structure in an actual design remains in question.

A graphical illustration of various reactor structures required to achieve different points in $C-\tau$ space is provided in Figure 3.1.7. Point A is the feed point with a zero residence time. In order to achieve point B a portion of the feed must be redirected through a dynamic holding tank of sufficient volume such that the fluid resides in the tank for time equivalent to τ_2. Point C is achieved by first passing the fluid through a PFR with a volume that will achieve τ_1. Reaction occurs along the length of the PFR and hence the concentration changes as it moves along the PFR trajectory. The effluent of the PFR is then passed through a holding tank with a volume sufficient to achieve a residence time equal to the difference between τ_2 and τ_1. No reaction occurs in the holding tank so the concentration remains constant. Finally point D is achieved through a PFR alone. The PFR has a volume to achieve a residence time of τ_2 and reaction causes a change in concentration along the length of the PFR.

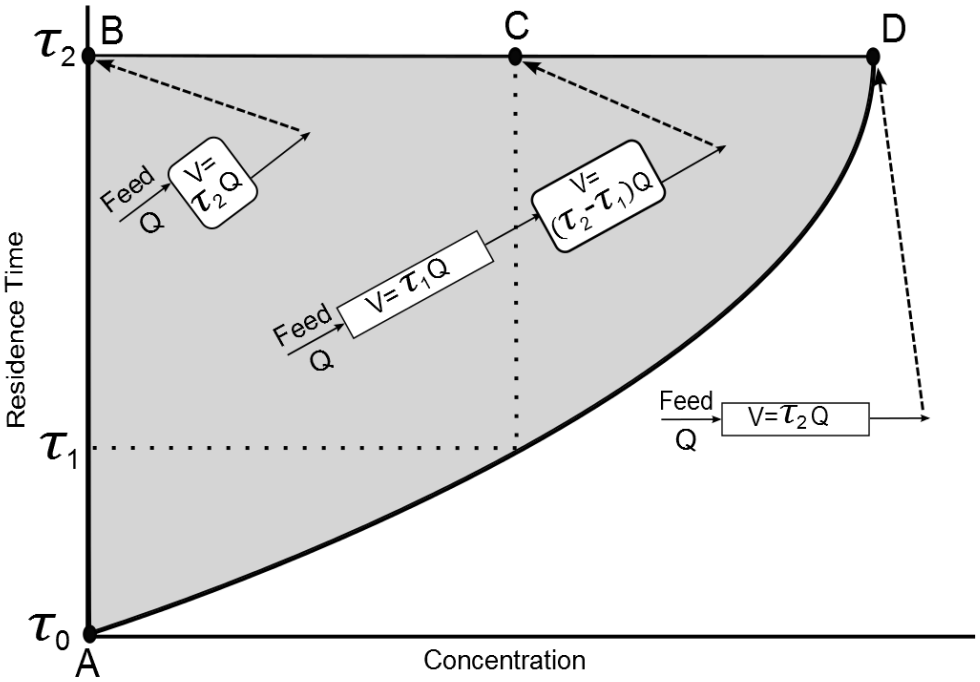

Figure 3.1.7: Reactor structures required to reach various points on a $C-\tau$ plot. Only a PFR and a dynamic holding tank are considered in this case but the concept extends to other reactor types.

3.1.1.4 Unbounded Nature of Time - Relevant Reactor Structures

Time is unbounded by its very nature. No action can be performed such that time is stopped or accelerated. Therefore simply leaving the products of a reactor or the feed solution to stand while other processes occur elevates their time component relative to the initial time, t_0. This may also incorporate the use of holding tanks where the substance/fluid is contained while the reactors are in use or other processes are in operation. However these holding tanks are much like batch reactors and do not have an inlet and outlet flow rate except no reaction occurs. They are charged with contents and left to stand before retrieving the contents at another time.

The batch equivalent of Figure 3.1.7 is given in Figure 3.1.8. In Figure 3.1.8 the batch reactor structures required to reach points B, C and D are provided. The arrows in each of the reactor structures do not represent continuous flow in this case, but rather an action at the given time point. As can be seen the structures are similar to those of the continuous system except the PFRs are replaced with standard batch reactors and the holding tanks do not have a inlet and outlet flow (non-dynamic holding tanks). It must be noted that when a fluid is placed in a holding tank it does not pass through it but merely resides in the tank for the specified time period. This is the key difference between how residence time and time are unbounded. Time merely passes in the batch system whereas the fluid has to pass through a volume in a continuous system.

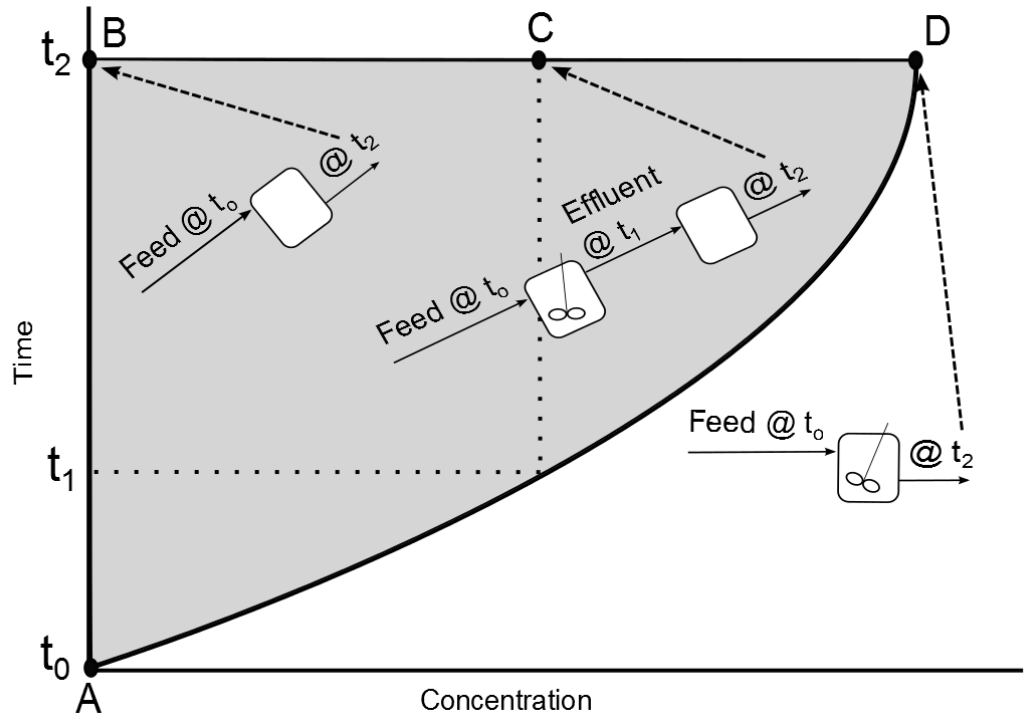

Figure 3.1.8: Reactor structures required to reach various points on a $C-t$ plot. Only a batch reactor (the batch equivalent of a PFR) and holding tank are considered in this case but the concept extends to other reactor types.

Key result of Section 3.1.1: Convex hulls represent the mixing process in AR theory and construction. Since mixing does not make sense in $C-t$ space (batch system), convex hulls may not be applied in this space as it can be in $C-\tau$ space (continuous system).

3.1.2 Attainable Regions in Concentration-time Space

Discussion in Section 3.1.1 led to the conclusion that residence time and time in batch systems have differences that result in alternate graphical approaches being followed in the mixing process. Mixing is only linear in concentration space but not in time space or concentration-time space. This means that an alternate AR construction algorithm may need to be followed when an AR is desired in $C-t$ space. The major difference between the two algorithms would be that the convex hull could not be found for the batch case as this would employ linear mixing in $C-t$ space. Both algorithms are presented here.

The algorithms presented here are for AR constructions based on AR theory and not automated construction methods such as those presented in Abraham and Feinberg (2004); Manousiouthakis et al. (2004); McGregor (1998); Rooney et al. (2000); Seodigeng et al. (2009). Automated AR construction methods can be found in the literature. All algorithms were executed in a suitable programming language.

3.1.2.1 Standard Theoretical AR Construction Algorithm

Presented here is the theoretical AR construction method that will be used in this work. This method will initiate at the feed point and build or outwardly "grow" the AR through reaction

and mixing processes. It is not claimed that this is the sole construction algorithm and various other approaches may be possible. The algorithm is presented in point form for a system with N components and d independent reactions. The algorithm is intended to apply to the general case for up to three reactions, isothermal and constant density systems. The latter two constraints may be relaxed by including an energy balance and plotting in mass fraction space respectively.

1. Obtain kinetic information and data for the system to be studied. This includes the applicable rate equations for each component in the system and the necessary kinetic parameters. A rate vector is formulated based on this information and put in the form of Equation 2.1.6. If the time component is to be included in the concentration vector then the rate vector takes the form of Equation 2.1.21.

2. The first reactor to be plotted is the PFR from the feed point. A single feed point may be specified according the problem at hand or multiple feeds may be available. If multiple feeds are available it is recognised that they themselves form an attainable region and the AR generated from them must consider each point in the feed region as a potential feed point. The PFR trajectory is generated by integrating Equation 2.1.9 over a sufficiently long period of time (at designers discretion). This trajectory is plotted in concentration space. R independent components are selected to represent the system with at least each one component selected from each reaction. The remaining components' concentrations in each reaction may be calculated through mass balance and the extent of reaction and hence only one component from each reaction is required to adequately represent the system.

3. CSTRs are then considered by solving the set of equations formulated by Equation 2.1.7 for a range of residence times from zero to the maximum residence time used for the PFR. Each solution provides a point in concentration space that represents the effluent of a single CSTR. These points are then plotted in the same space as the PFR. The potential presence of multiple solutions must be considered. Additional solutions may be sought by executing a search for points that satisfy the collinearity property of CSTRs.

4. PFRs are initiated at each of the CSTR points by integrating Equation 2.1.9 with the CSTR effluent concentrations as feed points.

5. The location of critical CSTRs must then be found. Critical CSTRs lie on the AR boundary and generally provide the starting or end points for critical DSRs. Methods for doing so can be found in Feinberg (1999, 2000a).

6. DSR trajectories can then be plotted by initiating them at the location of the critical CSTRs and the feed point. To ensure that these DSRs lie on the boundary of the AR, the critical alpha policy needs to be determined. Equations 2.1.11 and 2.1.12 can be used to determine this policy. This method is restricted to use in three dimensional concentration space.

7. PFRs can be initiated along the length of the DSR trajectory. These PFRs are ensured of being on the AR boundary.

8. The points from all reactor trajectories and points are gathered in a single matrix. The convex hull of these points are then found and the region these points enclose is then filled in. Graphically this produces a shaded area or filled in volume. Hence the attainable region of the system is obtained.

It must be noted that for a system with two reactions (d=2) steps 5-7 are omitted as the region may be constructed from PFRs and CSTRs alone (Feinberg and Hildebrandt, 1997). If the AR is to be plotted in concentration-residence time space then residence time is simply included as one of the variables above and beyond the concentration variables selected. For instance a system with two reactions will then have a 3D AR in $C-\tau$ space. Likewise a system with three reactions has a 4D AR in $C-\tau$ space. It is noted that the addition of residence time as a variable of the AR would still require steps 5-7 to be performed if in a three dimensional space. The associated mathematical operations may be simpler however, since the τ component of the rate vector is unity.

3.1.2.2 Proposed Adaptation for Application to Concentration-time Space

Ming et al. (2013) showed that this algorithm or approach (presented in Section 3.1.2.1) may be applied in the exact same manner to construct the AR for a batch system in concentration space. The interpretation of the equations and resulting reactor structure is different. Due to the fact that time cannot be mixed as discussed in Section 3.1.1, the convex hull cannot be found and connected with linear lines when applying the algorithm to batch systems with the intention of constructing the AR in concentration-time space.

If an AR is to be plotted in concentration-time space (in either 2D or 3D) then the algorithm presented in Section 3.1.2.1 is followed for steps 1-4. Steps 5-7 would need to be performed for constructions in 3D space. This is discussed later on in Section 4.2. Step 8, which consists of finding the convex hull of the points, is not followed but instead replaced by the method presented below. In the method horizontal lines refer to mixing lines where the concentration is mixed and the time remains constant. Vertical lines indicate the increasing of time ("time elevation") while the concentration remains constant. Lines which represent a change in both concentration and time along the length of the line are not permissible.

Proposed amendment to finding convex hull and connecting the points linearly:

- A maximum time is set. While the time variable of an AR is unbounded, for graphical purposes it is convenient to set a maximum time that the AR will reach. The user must keep in mind that this variable may, in fact, tend to infinity.
- The time of the feed point is elevated and mixed, using horizontal lines, with points of the plotted batch reactor and fed-batch reactors that have the same time value as the elevated feed point. This can be performed with a loop in the program that elevates the feed point to equal the time of a point on the batch reactor trajectory and then plots the line connecting the two. A second loop is used to do the same with all the fed-batch reactor points. Batch reactor trajectories that are initiated at fed-batch reactor points may also be mixed with time-elevated feed points where necessary.
- Vertical lines are then plotted from each fed-batch reactor and points along batch reactor trajectories until the set maximum time is reached. This effectively raises the time component of these concentrations and will be termed "time elevation".

This amendment to the AR construction algorithm essentially tries to achieve the same result of finding the convex hull and filling in the encompassed region but without filling in concavities naturally present in $C-t$ space. This is achieved by permitting only the graphical plotting of vertical and horizontal lines. The points provided merely indicate possible actions and it is at the designers discretion as to which actions are performed. For 2D constructions in $C-t$ space all actions may be performed, if desired, to fill in the region as much as possible. In 3D space

however, the designer may wish simply to obtain the boundary of the AR which requires less computational power and memory than filling in the entire region with vertical and horizontal lines. Sections A.1-A.3 in Appendix A provide examples of ARs plotted using this method in 2D and 3D $C-t$ space and the exact procedure followed for each.

An obvious shortcoming is that this construction method is meant to provide a visual representation of an AR in $C-t$ space and hence is limited to application in 2D and 3D construction.

3.1.2.3 Noticeable Results from Example Constructions

Sections A.1-A.3 in Appendix A provide example AR constructions in $C-t$ space for batch reactor systems. In each example the continuous reactor AR was also shown for comparison purposes. These examples were done so as to display the proposed construction method for plotting batch ARs in $C-t$ space. They do also, however, provide insight into ARs constructed in this manner as well as differences between the batch and continuous ARs. Insights in to the determination of critical reactors were not sought in this instance and therefore these steps were not completed for these examples.

When comparing the ARs for batch and continuous systems, the regions generated are extremely similar. This is expected as the same shape or volume would develop if the same kinetics were used. The only differences between the two were the presence of concavities in the batch reactor AR. The concavities in the example systems were slight however. It is possible that more noticeable concavities may be present in other systems which would be determined when other systems are constructed in this manner.

From these differences one is able to make a prediction concerning the comparable area or volume between batch and continuous system ARs constructed in this manner. Since the batch system contains potential concavities it is expected that the generated AR be of a lower area or volume (for 2D and 3D constructions respectively) than the equivalent continuous reactor AR. At this point it cannot be said that this is true of all possible cases and hence

$$AR\,Area_{continuous} \geq AR\,Area_{batch} \quad (2D\,constructions)$$

$$AR\,Volume_{continuous} \geq AR\,Volume_{batch} \quad (3D\,constructions)$$

Whether the regions generated for both batch and continuous systems can indeed be equivalent in area or volume is a valid question to be asked. A potential answer can be found in the concavities focused upon in the example constructions. All three examples had concavities that involved the feed point. In other words the concavities could be filled with a line connecting the feed point to a point associated with a reactor if mixing of time were allowed. The effluent of the reactor must have a time component greater than zero and a concentration different from that of the feed. There is therefore potential for a concavity to exist provided the batch reactor trajectories do not form a convex lower boundary.

This leads to the impression that every AR generated for a batch system will have at least one concavity and that this concavity will be associated with the feed point. The reason one can *potentially* make this general statement is a result of the nature of reactors. In order for a change in concentration to occur a reaction has to take place. This reaction occurs over a period of time. This means that when plotted in $C-t$ space, the point plotted for the reactor used will have a noticeable change in both concentration and time. Since the feed point to the reactor cannot simply be mixed with the reactor outlet due to the different value of the time components of the points, a concavity will form between the two points. There is a simple argument

against making such a general statement however and it was mentioned above. Systems may be naturally convex and when plotted in 2D $C-t$ space this would result in no concavities being formed. The addition of a third variable in 3D constructions however seems to increase the likelihood that concavities will arise. The example construction presented in Section A.2 illustrates this point. When plotted in $c_A - c_B$ space the AR generated is entirely convex. So to is the individual reactions of the system when plotted in $C-t$ space as shown in Figure 3.1.9. The addition of time as a variable and the fact that reactor outlets have different time components than the feed resulted in a concavity. Therefore it is *possible* that all or most 3D batch reactor ARs constructed in this manner contain concavities.

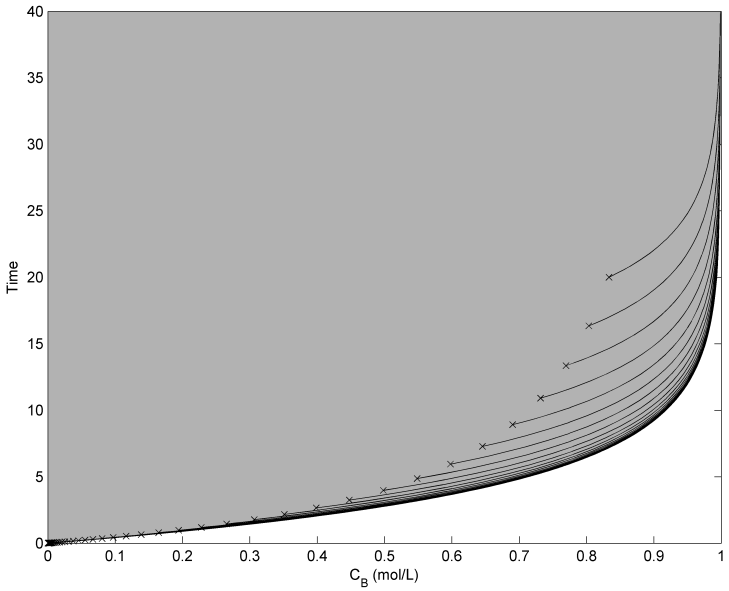

Figure 3.1.9: AR in $C-t$ space for reaction $A \rightarrow B$ which is entirely convex.

Key result of Section 3.1.2: Concavities will most likely exist in an AR constructed in $C-t$ space unless the reaction kinetics used are entirely convex. This is due to mixing only taking place in concentration space and not in concentration-time space. The associated representation of a batch structure in $C-t$ space therefore differs from that of a continuous structure in $C-\tau$ space.

3.2 Production Rates

The definition of residence time in Section 3.1.1.1 provides a potential way to optimise a reactor network. Since residence time is a function of reactor volume and they are directly proportional, reducing the residence time reduces the associated reactor network volume. Reduction in residence time can be obtained through mixing as will be demonstrated. As time in batch systems is not related to reactor volume and cannot be mixed, this same approach cannot be adopted for ARs in batch systems. It is intuitive to assume that minimising the time taken to reach a desired product concentration allows one to produce more of the product in a given time frame. This concept will be developed in this section as maximising the production rate of a reactor network.

3.2.1 Interpretation of Plots in $C-\tau$ Space - Reducing Residence Time through Mixing

Before the concept of production rates can be explored for batch reactor structures, understanding regarding production rates in continuous reactor systems is first required. Most theory related to attainable regions translated well between continuous and batch systems so it is natural to assume that the same would apply to production rates. This is investigated by providing interpretation of AR plots in $C-\tau$ space and how these plots could be interpreted in terms of production rates. Production rates will be defined for continuous reactors in this section and later redefined for batch reactors, noting similarities between the two.

In Section 3.1, residence time and time in batch reactors were discussed with regards to the difference between them and how this relates to the plots in $C-\tau$ and $C-t$ space respectively. Further interpretation of these plots were not provided which is the aim of this section. As given in Equation 2.1.8, residence time is defined as $\tau = \frac{V}{Q}$.

Mixing of residence time is permissible as it follows the linear mixing law that is also applicable to concentration. Therefore any residence time between two points in residence time space is achievable with the correct mixing proportions. This is shown in Figure 3.2.1 which displays a PFR trajectory A-B with linear mixing applied between points A and D. Any residence time on line A-D between τ_o and τ_2 is achievable using the correct mixing fraction. Hence while concentration c_1 is achieved at only τ_1 through reaction, it could be achieved at the lower residence time τ^* by reacting to point D and then mixing with point A (feed point) to achieve point E.

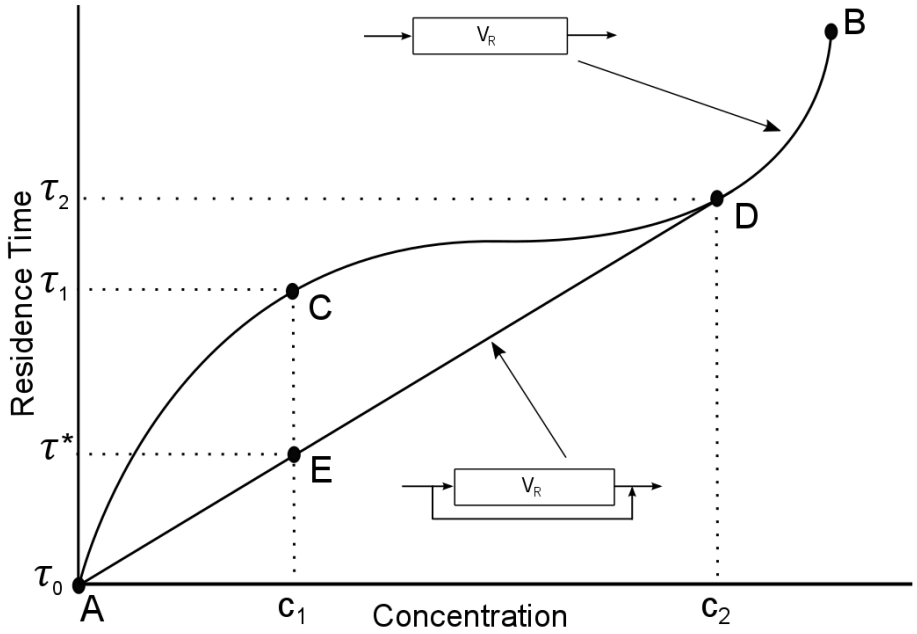

Figure 3.2.1: PFR trajectory with linear mixing applied to fill in concavities. Mixing of residence times allows a lower residence time to be used to obtain the same concentration as shown by points C and E.

An obvious question to ask is what it actually means to reduce the residence time. When mixing is applied to reduce the residence time of the system, this can be interpreted in two ways as residence time is defined in terms of two variables.

1. Residence time decreases due to a decrease in the volume of the system (if the flow rate remains constant) or the volume decreased by a larger amount than what the flow rate decreased by. In other words a lower volume is used to achieve the same amount of product.

2. Residence time decreases due to an increase in the volumetric flow rate exiting the reactor structure (if the volumes remains constant) or the volumetric flow rate increased by a larger amount than what the volume increased by. In other words a greater amount of product is produced using the same volume.

Reducing the volume of the system is advantageous as it reduces the capital, and potentially the operating, costs of the system. Increasing the flow rate exiting the system essentially means more mass is being produced and hence the number of mols being produced from the system is higher. The rate at which the product is being produced is therefore higher. This is the first instance in which production rate is encountered and it must be noted that it is linked to an increase in system throughput. In order to confirm this and investigate it further, each of these scenarios was considered in Sections 3.2.1.1 and 3.2.1.2 respectively. The reactor structures required to achieve points C and D at concentrations c_1 and c_2 respectively in Figure 3.2.1 are shown in Figure 3.2.2. Both these points are achieved through reaction in a PFR alone.

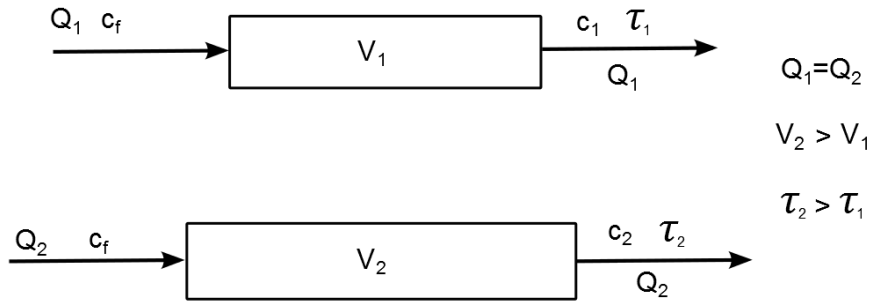

Figure 3.2.2: PFRs required to achieve points C and D in Figure 3.2.1. The flow rates through each PFR are equal and it is the volume that increases from V_1 to V_2 to effect an increase in residence time to reach point D.

Before these scenarios are discussed, production rates can be generally defined as the amount of mols or mass of product that are produced over a given time period. As continuous reactor systems have continuous flow rates by definition, the production rate can be defined as the product of the flow rate and the concentration of the desired product in the effluent of the reactor structure. In terms of mols this is given as Equation 3.2.1 which determines the number of mols of component i exiting the reactor structure per unit of time.

$$P_i = Q_{effluent}\left(c_i - c_{i,f}\right) \tag{3.2.1}$$

3.2.1.1 Scenario 1 - Decrease Reactor Volume to Decrease Residence Time

The discussion presented herein refers to the situation outlined in Figures 3.2.1 and 3.2.2.

The first scenario entails maintaining the total flow rate at Q_2 which is split between a portion being fed to the reactor and a portion bypassing the reactor to later be combined with the reactor effluent. A schematic of this arrangement is provided in Figure 3.2.3. Q_R is the flow rate passed

through the reactor while $Q_{B,1}$ is the flow rate that bypasses the reactor. As $Q_R < Q_2$, the required volume of the reactor is less than V_2 to maintain the residence time of the reactor at τ_2. The residence time has to be equal to τ_2 as the reactor achieves a concentration of c_2 at point D. Hence the resultant residence time of the reactor effluent is τ_R, which is equal to τ_2.

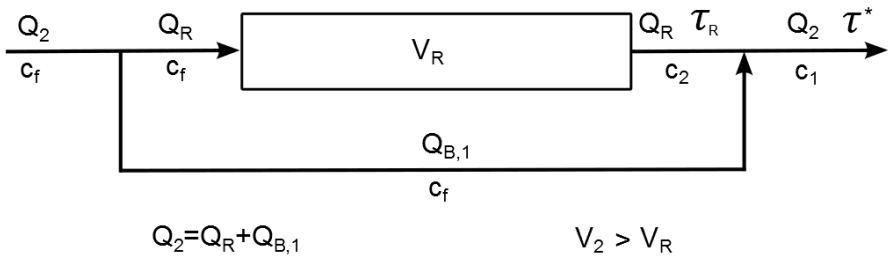

Figure 3.2.3: Schematic diagram of the first scenario which results in a decrease in the reactor volume as the flow rate fed to the reactor is lower.

The volume V_R can be related to V_2 using the linear mixing law. The reduced residence time, τ^*, that is obtained after mixing can be expressed as the linear combination of τ_o and τ_2 using Equation 2.1.20. As τ_o is zero this provides a simple relationship between the two residence times.

$$\tau^* = \lambda\,\tau_2 + (1-\lambda)\,\tau_o = \lambda\,\tau_2 \quad \lambda = \frac{Q_R}{Q_2}$$

Since $\tau_2 = \tau_R$, the relationship between the reactor volumes can be determined as follows

$$\tau_2 = \tau_R$$

$$\frac{V_2}{Q_2} = \frac{V_R}{Q_R}$$

$$V_R = \frac{Q_R}{Q_2} V_2 = \lambda V_2$$

Hence the reduced reactor volume is a scalar multiple of V_2. A reduced reactor volume signifies a reduced capital cost for the system. Therefore reducing the residence time through mixing has provided a benefit in terms of saving capital outlay.

Consider now the production rate that would be achieved for the given scenario. In order to reach c_1 through reaction alone, a PFR of volume V_1 is used through which a flow rate of Q_1 is passed. Using Equation 3.2.1 the production rate for point C is found to be

$$P_{point\,C} = Q_1\left(c_1 - c_f\right)$$

Likewise the production rate for point E when a reduced reactor volume is obtained is determined as

$$P_{point\,E} = Q_2\left(c_1 - c_f\right)$$

From Figure 3.2.2 $Q_1 = Q_2$ and hence if the ratio of the production rates is taken:

$$\frac{P_{point\,E}}{P_{point\,C}} = 1$$

The production rate achieved after mixing is therefore identical when the total flow rate is maintained at the same value. The benefit to this scenario is a reduced reactor volume, which reduces capital costs, but no increase in the rate of production is achieved.

3.2.1.2 Scenario 2 - Increase Flow Rate to Decrease Residence Time

The discussion presented herein refers to the situation outlined in Figures 3.2.1 and 3.2.2.

The second scenario is different from the first in that the reactor volume is maintained at V_2 and that the flow rate passing through the PFR is kept at Q_2. The schematic diagram depicting this is provided in Figure 3.2.4. As the flow rate to the PFR is kept constant at Q_2, the total flow rate to the system is greater than that of the first scenario. As the reactor volume remains constant, it is this increase in the total flow rate that facilitates the decrease in residence time to τ^*.

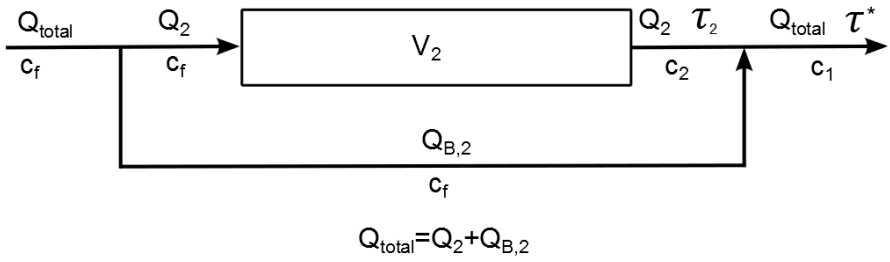

Figure 3.2.4: Schematic diagram of the second scenario in which results in which the volume of the reactor and the flow rate to the reactor remain at V_2 and Q_2 respectively.

Consider the production rates for points C and E in this scenario. The production rate remains unchanged from that presented in Section 3.2.1.1 for point C:

$$P_{point\,C} = Q_1 \left(c_1 - c_f\right)$$

In the case of point E, the flow rate is $Q_{total} = Q_2 + Q_{B,1}$ and hence the production rate for point E is given as

$$P_{point\,E} = Q_{total} \left(c_1 - c_f\right)$$

Taking the ratio of the production rates

$$\frac{P_{point\,E}}{P_{point\,C}} = \frac{Q_{total}}{Q_1} = \frac{Q_2 + Q_{B,1}}{Q1}$$

The linear mixing law for residence time in this case has a mixing fraction of $\lambda = \frac{Q_2}{Q_{total}}$. As $Q_1 = Q_2$, the ratio of production rates reduces to

$$\frac{P_{point\,E}}{P_{point\,C}} = \frac{1}{\lambda}$$

Since $\lambda \in [0\ 1]$, the production rate increases provided the mixing fraction is not equal to one. λ is clearly not equal to one in this scenario. When this does occur the production rates would be equal and the system would reduce to the case where the total flow rate is Q_2 as was the case in the first scenario.

In this scenario no capital is saved due to a smaller PFR volume being required. However, an increase in production rate was achieved which would potentially result in greater revenue. When comparing the two scenarios one must consider the pay-off period for the reactor. In scenario 2, even though a larger reactor was used which would cost more initially, the increase in revenue may pay off the reactor cost in equal or less time than that of the first scenario. In other words the second scenario is in fact most likely the better option in most cases as the benefit is provided over an extended period of time rather than an initial once-off cost. This would be assessed on a case to case basis.

Key result: Production rate is closely linked to the throughput of the system as earlier suspected. This fact must be remembered when applying these concepts to batch reactors as it may aid in the interpretation of such systems.

3.2.1.3 Scenarios Considering Convex Kinetics

The scenarios considered in Sections 3.2.1.1 and 3.2.1.2 were based on the use of a concave PFR trajectory where mixing could be applied to reduce the residence time at a given concentration. A convex trajectory, shown in Figure 3.2.5, is now considered. c_1 is still the target concentration with point C reaching c_1 through reaction alone and point D reaching c_1 through reaction and mixing.

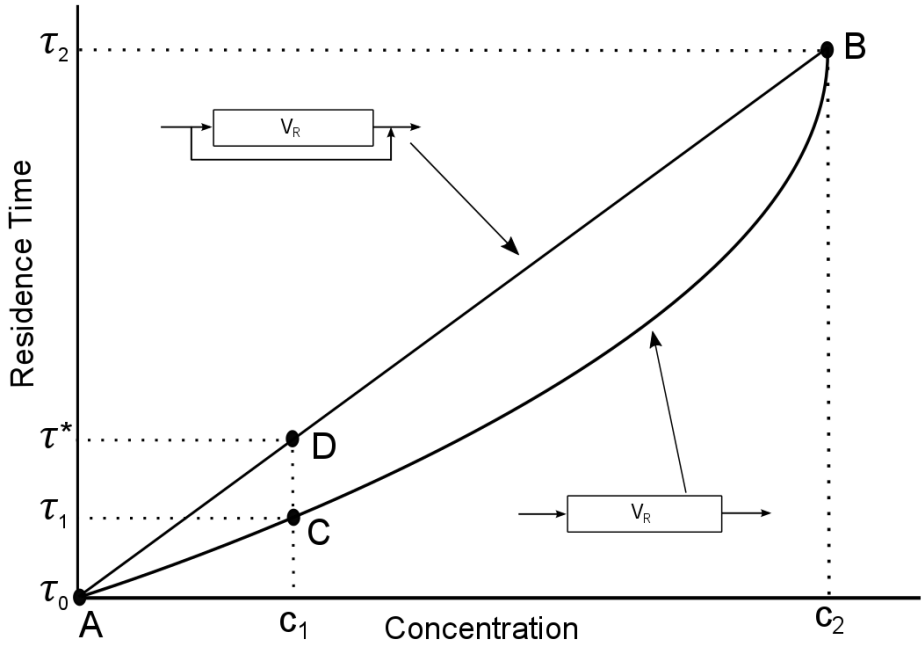

Figure 3.2.5: Convex PFR trajectory with linear mixing used to obtain c_1 at a higher residence time.

In Figure 3.2.5 it is clear that $\tau^* > \tau_1$ and hence the residence time has been *increased* by the process of mixing. As explained in Sections 3.2.1.1 and 3.2.1.2, this increase in residence time would be achieved by an increase in reactor volume or a decrease in flow rate. In Section 3.2.1.2 it was concluded that an increase in production rate is linked to an increased flow rate or throughput of the system. Since only a decrease in the flow rate is achievable for the current system, it follows that the production rate cannot be increased by mixing for the current case. Hence the highest production rate for producing a product at c_1 exists at point C.

The same analysis as used in Section 3.2.1.2 can be used to show this in a similar fashion. As residence time is defined as a function of two variables, two cases exist for why the residence time increases between points C and D after mixing is applied. Consider Figure 3.2.6 which may be used to develop the ratio of production rates as before except now applicable to the convex trajectory in Figure 3.2.5. This develops the case whereby the increase in residence time between points C and D is due to an increase in reactor volume. As before, point C is obtained by passing a flow rate of Q_1 through a PFR of volume V_1 such that the resultant residence time is τ_1 and the exiting concentration is c_1. To achieve point D in a single reactor *without* mixing, you would need to react the feed until point C and then pass the effluent through a non-reactive volume to raise the residence time to point D. This is equivalent to halting reaction and waiting to reach the time of point D in a batch system.

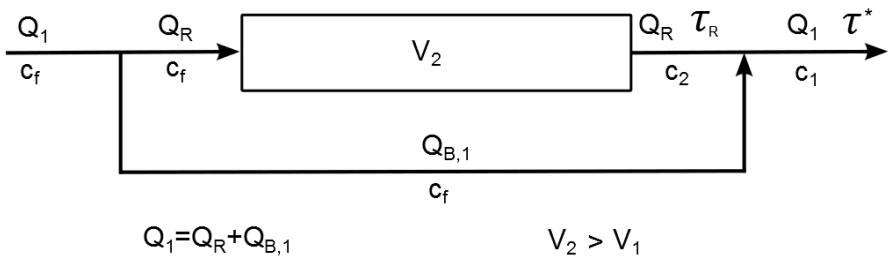

Figure 3.2.6: Schematic diagram of the continuous reactor structure for convex kinetics that results in an increase in the required reactor volume.

In obtaining point B, the same flow rate is passed though a larger PFR of volume V_2 such that the final residence time is τ_2. This increase in residence time is due to an increase in reactor volume. Figure 3.2.6 is the structure for when the total flow rate remains constant at Q_1. Therefore the flow rate to the reactor is reduced to $Q_{R,1}$, resulting in a residence time escalation. It was previously stated that to reach point B a larger reactor is used. Therefore the increase in residence time between τ_1 and τ_2 is due to both a reduction in flow rate and an increase in reactor volume. When the reactor effluent is mixed with the bypass however, the resultant residence time is caused by an increased reactor volume alone and is given by

$$\tau^* = \frac{V_2}{Q_1}$$

It is clear that $V_2 > V_1$ and hence $\tau^* > \tau_1$. The production rates of points C and D are given by

$$P_{point\,C} = Q_1 \left(c_1 - c_f\right)$$

$$P_{point\,D} = Q_1 \left(c_1 - c_f\right)$$

As the same final concentration is reached with the same total flow rate exiting the relevant structures, the ratio of production rates is

$$\frac{P_{point\,D}}{P_{point\,C}} = 1$$

Therefore no improvement is production rate is achieved. Point D however has been achieved with a higher reactor volume thus elevating the capital costs of the reactor structure. The costs have been increased with no beneficial return on the investment. Contrast this with the case in Section 3.2.1.1 which also did not have an increased production rate but did experience a reduction in reactor volume. Clearly the likelihood of mixing being beneficial in terms of reducing the reactor volume is dependent on the kinetics or shape of the system.

The alternate case presented in Section 3.2.1.2 is now considered for the kinetics given in Figure 3.2.5. In Section 3.2.1.2 the same reactor volume was maintained while increasing the total flow rate to achieve an increase in production rate. It is sensible to assume therefore that for the current kinetics the total flow rate would be reduced to achieve an increase in residence time. Figure 3.2.7 presents the reactor structure that applies to this scenario and it can be seen that the volume is maintained at V_1.

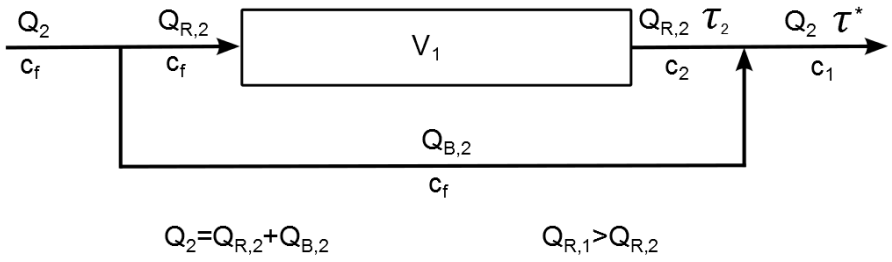

Figure 3.2.7: Schematic diagram of the continuous reactor structure for convex kinetics that results in a decrease in the flow rate.

The residence time at the reactor exit is the same residence time achieved at the same point in the previous scenario, τ_2. τ_2 can be expressed in terms of the variables of each scenario as follows:

$$\tau_{2,volume\ increase} = \tau_{2,volume\ maintained}$$

$$\frac{V_2}{Q_{R,1}} = \frac{V_1}{Q_{R,2}}$$

$V_2 > V_1$ and therefore in order to achieve the same value for τ_2, the flow rate for this case must be less than the previous case. Hence

$$Q_{R,2} < Q_{R,1}$$

As Figure 3.2.5 is used for both cases and the same residence time, τ^*, is achieved in both, the mixing fraction used for both cases are equal.

$$\lambda_{volume\ increase} = \lambda_{volume\ maintained}$$

If the mixing fractions are equivalent, then the ratios of flow rate to the reactor to the flow rate bypassed are also equivalent:

$$\frac{Q_{R,1}}{Q_{B,1}} = \frac{Q_{R,2}}{Q_{B,2}}$$

Since $Q_{R,2} < Q_{R,1}$ and the ratios are equivalent, it must be that $Q_{B,2} < Q_{B,1}$. As the contributing flow rates to Q_2 are both less than that of Q_1, it follows that $Q_2 < Q_1$.

Using this result, the ratio of production rates of points C and D can be found. First the production rates for each point are expressed as follows:

$$P_{point\ C} = Q_1 \left(c_1 - c_f\right)$$

$$P_{point\ D} = Q_2 \left(c_1 - c_f\right)$$

The ratio of the production rate of point D to C is therefore

$$\frac{P_{point\ D}}{P_{point\ C}} = \frac{Q_2}{Q_1}$$

As $Q_2 < Q_1$ a reduced production rate is achieved. Consequentially, for the case where the residence time is increased via mixing, no increase in the production rate can be achieved.

3.2.1.4 Conclusions for Production Rates in Continuous Systems

In Sections 3.2.1.1-3.2.1.3, two different sets of kinetics were evaluated to determine whether an increase in production rate could be achieved via mixing.

It was found that if no opportunity, such as a concavity in the kinetics, exists to enable the *reduction* of the residence time through mixing, then an increase in production rate through mixing cannot be achieved. The results of this section also serve to emphasise that the minimum residence time achievable should be the goal for the designer of the system. If a certain point can be achieved at the minimum residence time via reaction alone, then no additional mixing in the reactor structure should be added. Plots in $C - \tau$ space are crucial in determining what the minimum residence time is for a given concentration. Using a reactor structure that obtains the minimum residence time essentially guarantees that the highest production rate is being achieved aside from the case in which a reduced volume was obtained. This case provided its own benefit in reduced capital costs and therefore the minimum residence time was still the ideal outcome. A link between the residence time and production rate clearly exists and is a direct consequence of the definitions of production rate and residence time.

Simply from assessing a plot in $C - \tau$ space one can determine the point at which the maximum production rate for a given concentration may be achieved. This work has thus far placed emphasis on the differences between τ and t in batch systems. It is then only natural to assess the concept of production rate in batch systems and note the differences between them and continuous systems. The aim of this would be to correlate the ideas used in both types of

systems and arrive at an interpretation of $C-\tau$ plots that can be used to determine the most productive reactor structures for both continuous and batch systems.

Key result: The point in an AR at which a given concentration is achieved at the lowest residence time is associated with the highest production rate achievable for that concentration in a continuous system.

3.2.2 Definition of Production Rate in Batch Reactor Structures

The production rate of a reactor network/structure is defined to be the amount of a substance produced in a reactor or reactor network per unit of time. This is the rate associated only with the reactor network. In reality, the total production rate would include consideration of time to transfer product, clean the reactors and other processes. These are not considered here as maximising the production rate of the reactor portion of a batch process would still increase the overall production rate as the other processes would remain constant in terms of time. The amount of the substance can be expressed in either moles or mass. If expressed in moles then the amount of moles produced of component i in a given time period ending at time t within a reactor is given as

$$n_{produced} = V(c_{i,t} - c_{i,f})$$

This is simply the difference of the final and initial concentration of i multiplied by the volume of the reactor. In order to determine how much of i is produced per unit of time both sides are divided by the time interval to give Equation 3.2.2. A similar process may be followed to obtain the expression for production rates in terms of mass given in Equation 3.2.3.

$$P_i = \frac{n_{produced}}{t - t_o} = \frac{V(c_{i,t} - c_{i,f})}{t - t_o} \tag{3.2.2}$$

$$P_{im} = \frac{m_{produced}}{t - t_o} = \frac{\rho V(z_{i,t} - z_{i,f})}{t - t_o} \tag{3.2.3}$$

The time associated with the feed point is generally taken as zero and hence the t_o term in the denominator would not be shown. If this expression was used between two points that did not include the feed then the t_o term may have to be shown and used to define the applicable time interval.

Note the similarities between Equations 3.2.1 and 3.2.2 which are the production rate expressions for continuous and batch systems respectively. The flow rate, Q, in Equation 3.2.1 can be defined as the volume of fluid that flows through the exit of the reactor structure over a given time period and hence is equivalent to the $\frac{V}{t}$ in Equation 3.2.2. Knowing this, the insight gained regarding production rates in continuous systems may be applied to some extent for batch reactor systems and vice versa.

3.2.2.1 Production Rate Vector

Since production rate is with reference to a specific component, production rates can be determined individually for each of the components in a studied system. It is here that one may see some similarities with reaction rate. Reaction rate is also determined for each component and is usually dependent on the concentrations of components in the system. Production rate is only

dependent on the concentration of the component it is associated with but since production rates can be determined for each component, it is natural to conclude that these production rates may be expressed in vector form similar to that of reaction rates. Therefore, for a system with N components, the production rate vector can be expressed as Equation 3.2.4.

$$\mathbf{P}(\mathbf{C}) = [P_1, P_2, P_3, ..., P_N]^T \tag{3.2.4}$$

It is clear that the production rate vector has the same length as the concentration and reaction rate vectors if time is not included in either. When time is included as one of the components in the concentration and reaction rate vectors then the production rate vector takes the form of Equation 3.2.5. The production rate of the time component is simply one as the substitution of it into Equation 3.2.2 leads to time being divided by itself.

$$\mathbf{P}(\mathbf{C}) = [P_1, P_2, P_3, ..., P_N, 1]^T \tag{3.2.5}$$

3.2.2.2 Properties of Production Rates

From the expressions of production rate given in Equations 3.2.2 and 3.2.3 several properties of production rates can be deduced.

Property 1 The first property is the mathematical relationship between production rate and time. It is clear from Equations 3.2.2 and 3.2.3 that production rate and time are inversely proportional ($P \propto \frac{1}{t}$). Hence it follows that

$$P \to \infty \quad as \quad t \to 0$$

$$P \to 0 \quad as \quad t \to \infty$$

The former states that as time tends toward zero the production rate tends toward infinity. One immediately realises that the feed point is initiated at a time equal to zero but at this stage, no reaction has taken place and reactants are at their initial state. Since production rate can be expressed in vector form including the rates for all components, the reactants present at the feed point would have productions rates of infinity and the products would have undefined or indeterminate production rates. This leads to the conclusion that no meaningful information can be determined from evaluating the production rate at the feed point and hence at this point production rate is undefined.

The latter states that as time tends towards infinity the production rate tends towards zero. This highlights that as time increases the amount of substance produced per unit of time decreases. Hence a desired concentration should be obtained at the lowest time possible in order to maximise the production rate.

Property 2 The second property is the sign of production rates. The sign of the production rate of a chemical species is dependent on two factors, namely whether the species is formed or reacts and the point at which the production rate is evaluated.

1. A chemical species that is strictly formed in the reaction is expected to be ≥ 0 at all defined points. This is because the concentrations for these species will only increase or remain the same as the structure develops.

2. A chemical species that strictly reacts in the reaction is expected to be ≤ 0 at all defined points. This is because the concentrations for these species will only decrease or remain the same as the structure develops.

3. A chemical species that both reacts and forms during the course of reaction can be both ≤ 0 and ≥ 0 but not when evaluated at the same point. If this is a result of a single auto-catalytic reaction then it is expected that the sign of the production rate of the auto-catalytic component be positive or remain the same at all defined points. If multiple independent reactions are present where the species is a product of one and the reactant of another then the production rate could potentially be negative or positive depending on where the rate is evaluated. This is wholly dependent on the system at hand. For the simple case where a component is initially zero, produced and then reacted, it is expected that the production rate relative to the feed point is ≥ 0 as the amount of the component never decreases below its initial value of zero.

Property 3 The third property is that the production rate per unit volume for a single component at a point in concentration-time space is not unique to that point. This is apparent from Equation 3.2.2 which can be expressed with time as the subject of the formula as shown in Equation 3.2.6. If P is divided by V giving $\hat{P}$, which is the production rate per unit of reactor volume, then Equation 3.2.7 is obtained.

$$t = \frac{V}{P}(c_{i,t} - c_{i,f}) + t_o \tag{3.2.6}$$

$$t = \frac{1}{\hat{P}}(c_{i,t} - c_{i,f}) + t_o \tag{3.2.7}$$

Equation 3.2.7 is a straight line with $\frac{1}{\hat{P}}$ as the gradient in $c_i - t$ space. When extended to $C - t$ space with multiple components a plane in $C - t$ space would be formed. A given production rate per unit reactor volume is therefore not unique for a given point but applicable to all the points that satisfy Equation 3.2.7; all the points that lie on the line formed by Equation 3.2.7 have the same production rate per unit reactor volume. This property is specific to the production rate for a single component as only one component is considered at a time when using Equation 3.2.7. It is expected that since every point in concentration-time space is unique the production rate vector will be unique to each point it is evaluated at.

3.2.3 Investigating the Application of Production Rate in Batch Systems

In Section 3.2.1 further interpretation of plots in $C - \tau$ space was provided and production rates were introduced for continuous systems. It was found that when residence time could be reduced via mixing, the production rate could be increased provided the total flow rate was increased. Production rate in batch reactor systems was defined in Section 3.2.2 and can now be investigated with relation to batch systems in a similar fashion to Section 3.2.1.

Consider the same PFR trajectory used in Section 3.2.1 except now when applied to a batch reactor system the trajectory represents a standard batch reactor. The trajectory and mixing line as applied to a batch reactor is shown in Figure 3.2.8. Note the differences compared to Figure 3.2.1. The mixing line is no longer A-D (shown by the dashed line) but rather G-D due to the fact that only concentration can be mixed. This results in the fact that point E can not be achieved and concentration c_1 can not be obtained at a lower time than that specified by the

trajectory. Instead point F is now the point achieved via mixing and lies at t_2 which is the time reached through reaction to point D. As the mixing line is at t_2 the implicit assumption is that mixing takes no time to perform.

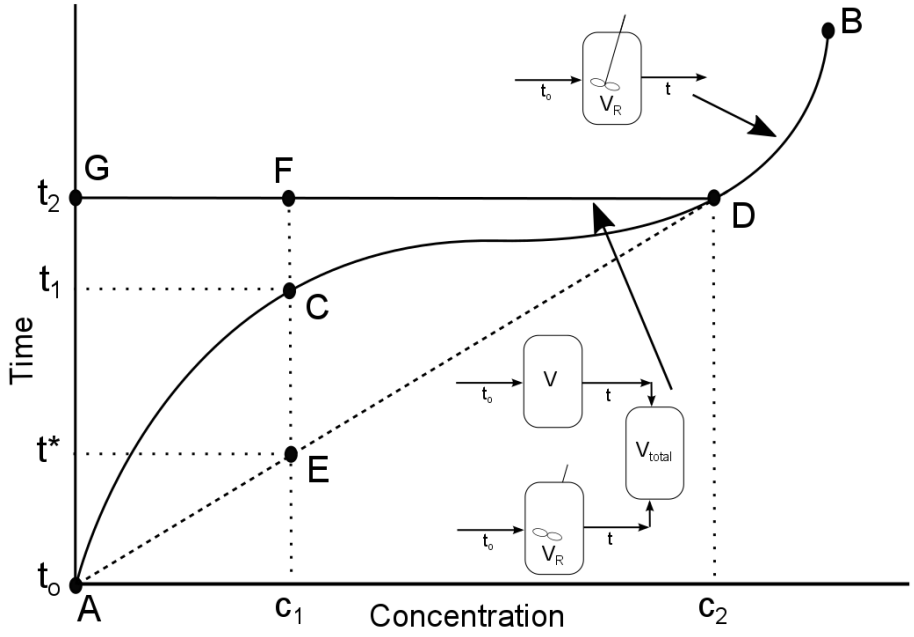

Figure 3.2.8: Standard batch reactor trajectory with a concavity present. Mixing of time is not allowed and hence c_1 cannot be obtained at a lower time. Mixing instead occurs in concentration space alone and is represented by a horizontal line at t_2. A dashed line between A and D indicates where the mixing line was for the continuous system.

In Section 3.2.1 it was found that the production rate of a reactor structure could be increased by increasing the flow rate, Q, to reduce the residence time rather than reducing the required reactor volume. In batch systems Q may be interpreted as the final volume obtained at the completion of a batch reactor structure divided by the time it took to reach that point. With reference to a single reactor it is the volume of the reactor divided by the time allowed for reaction to take place. In order to increase Q in a batch system either V must be increased or t must be reduced. As time cannot be reduced in this case the only option available is to increase the total volume of the system.

Volume is not tied to time as it is with residence time. Therefore the interpretation of the $C-t$ plot for a batch system differs slightly from that for a continuous system. Consider point C in Figure 3.2.8. In order to achieve point C a batch reactor of any volume is allowed to carry out its reaction for time t_1. Let this volume be V_1 for the purposes of this example. Unlike in continuous systems, this volume does not increase if the reaction is allowed to progress to point D at t_2. If $c_2 - c_1 > t_2 - t_1$ (which it is for concave kinetics such as these) then point D has a higher production rate per unit volume ($\hat{P}$) than point C. As the reactor volumes used for both points would be identical, point D has a higher production rate than point C. The question to ask is if the production rate at point F could be greater than that at point C if a concentration of c_1 was targeted. The outcomes of an analysis of a continuous system gave some indication that it could be increased but point E was obtained and not point F as in the batch system.

It is intended to do a similar analysis on a batch system shown in Figure 3.2.8. Consider the same scenarios done in Sections 3.2.1.1 and 3.2.1.2 for the continuous system. These are adapted in Sections 3.2.3.1 and 3.2.3.2 respectively to apply them to the case for batch reactors.

3.2.3.1 Scenario 1 - Reduced Reactor Volume to Maintain Total System Volume at V_1

The first scenario maintains the same total 'Q' value as if the system was allowed to react to point D in a reactor of volume V_1. As mixing occurs with point G, this results in a reduced required reactor volume, V_R. The schematic of the batch reactor structure for this scenario is provided in Figure 3.2.9. A standard batch reactor of volume V_R is allowed to react until t_2 at which point it is mixed with the storage tank of volume $V_{B,1}$ to obtain a total volume of V_1 and concentration c_1. In Figure 3.2.9 t_2 is *not* shown to span a period of time but in fact is represented as such to show that mixing occurs *at* t_2. A similar representation is used throughout this work.

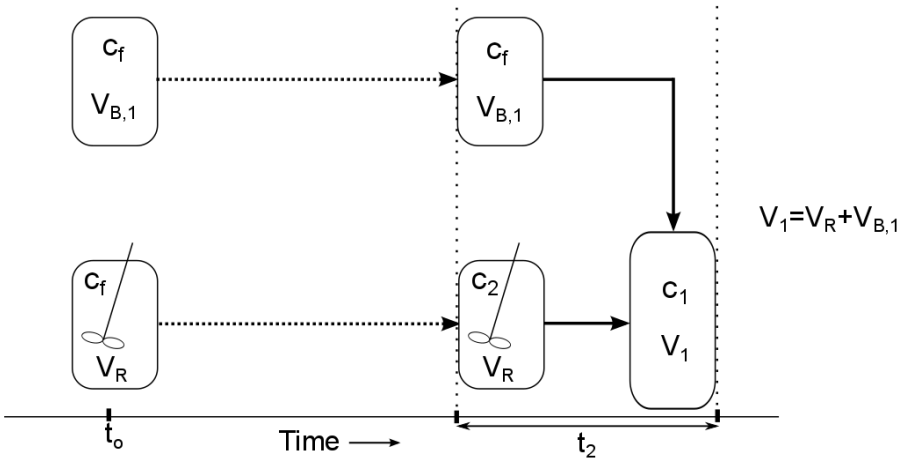

Figure 3.2.9: Schematic diagram of the first scenario which results in a decrease in the required reactor volume as the total volume of the system after mixing is kept at V_1.

The mixing law and mixing fraction is

$$c_1 = \lambda c_2 + (1-\lambda)c_f\,, \quad \lambda = \frac{V_R}{V_1}$$

The mixing fraction may also be expressed in terms of the concentrations by rearranging the mixing law:

$$\lambda = \frac{c_1 - c_f}{c_2 - c_f}$$

Now consider the production rate for points C and F. The same total volumes were used to achieve both points but the times taken to achieve each were different. For point C the production rate is

$$P_{point\,C} = \frac{V_1(c_1 - c_f)}{t_1}$$

while the production rate for point F is

$$P_{point\,F} = \frac{V_1(c_1 - c_f)}{t_2}$$

If the ratio of production rates is taken then

$$\frac{P_{point\,F}}{P_{point\,C}} = \frac{t_1}{t_2}$$

As $t_2 > t_1$, a decrease in production rate is experienced. This scenario differs from the continuous reactor version as in that case the production rates remained equal. The difference is solely a result of time not being able to be reduced via mixing in batch systems. Hence even though a smaller reactor volume was required which would lower capital costs, in terms of material produced it is more efficient to react the full volume V_1 to point C to obtain a concentration of c_1.

3.2.3.2 Scenario 2 - Increased System Volume to Maintain Reactor Volume at V_1

The second scenario increases the total 'Q' value and uses a batch reactor of volume V_1 to reach point D. The schematic diagram of the batch reactor structure for this scenario is provided in Figure 3.2.10. A volume $V_{B,2}$ is mixed with the reactor effluent to achieve a concentration of c_1 and a total system volume of V_{total}.

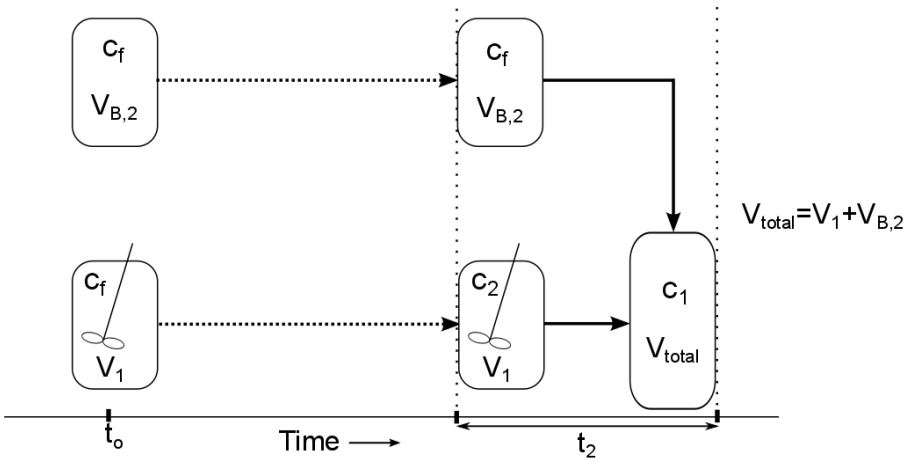

Figure 3.2.10: Schematic diagram of the second scenario which results in an increase in the total volume of the system with a reactor volume of V_1.

The mixing law is the same as for the first scenario but the mixing fraction changes accordingly:

$$c_1 = \lambda c_2 + (1-\lambda)c_f\,, \quad \lambda = \frac{V_1}{V_{total}}$$

The mixing fraction may still be expressed in terms of the same concentrations however:

$$\lambda = \frac{c_1 - c_f}{c_2 - c_f}$$

The production rates for points C and F are given as

$$P_{point\,C} = \frac{V_1(c_1 - c_f)}{t_1}$$

$$P_{point\,F} = \frac{V_{total}(c_1 - c_f)}{t_2}$$

If the ratio is taken of the production rates it is found that the volumes do not cancel as occurred in the first scenario:

$$\frac{P_{point\,F}}{P_{point\,C}} = \frac{V_{total}}{t_2}\frac{t_1}{V_1} = \frac{1}{\lambda}\frac{t_1}{t_2}$$

In order for an increase in production rate to be achieved over point C, the ratio of production rates should be greater than one. This can be used to determine the conditions under which an increase in production rates can be achieved.

$$\frac{P_{point\,F}}{P_{point\,C}} > 1$$

$$\frac{1}{\lambda}\frac{t_1}{t_2} > 1$$

$$t_1 > \lambda t_2$$

Therefore in order to achieve a higher production rate at the same concentration via mixing, the time reached via reaction alone must be greater than the product of the mixing fraction and the time reached after mixing. Even though the time taken to produce the concentration c_1 was increased, an increase in production rate is still possible for the case of concave kinetics provided the above condition is met.

It was assumed for these examples that mixing does not take time to perform. Given that the times play a crucial role in whether production rate may be increased, this assumption may cause disparity between theoretical and practically obtained production rates. Mixing times should therefore be considered in future work and may themselves be a key process considered in batch scheduling of processes.

3.2.3.3 Scenarios Considering Convex Kinetics

In Section 3.2.1.3, convex kinetics were considered for the same scenarios discussed in Sections 3.2.1.1 and 3.2.1.2. For continuous systems the results differed between concave and convex kinetics with regards to the production rate ratios obtained. This was to be expected as the the variables of volume and flow rate increase or decrease differently between the types of kinetics to effect an increase or decrease in the residence time. As a result, different points in $C - \tau$ space were obtained for convex and concave kinetics. The same cannot be said of time in batch systems. Figure 3.2.11 provides a convex batch trajectory from which it is apparent that the final point achieved (point E) is identical to that obtained when the concave kinetics were used. This is due to mixing occurring at the time achieved by reaction. Since the same point is achieved analysis of the system is expected to achieve the same results obtained from Sections 3.2.3.1 and 3.2.3.2.

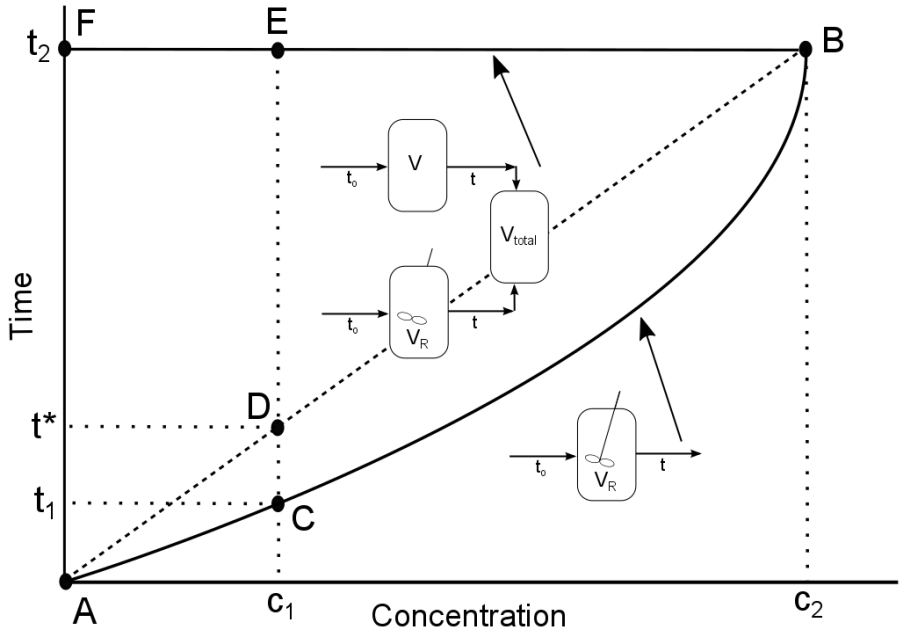

Figure 3.2.11: Convex batch trajectory with linear mixing in concentration space used to obtain c_1 at a higher point in time.

Section 3.2.3.1 discussed the scenario where the volume of the reactor was reduced in order to maintain the total production volume after mixing at the same value V_1. There is no difference in the steps taken to derive the ratio of production rates for the case of convex kinetics. Points C and E were obtained using the same total volume and the same concentration is reached but at different points in time. As such the production rates for these points are

$$P_{point\,C} = \frac{V_1(c_1 - c_f)}{t_1}$$

$$P_{point\,E} = \frac{V_1(c_1 - c_f)}{t_2}$$

Taking the ratio of the productions rates it can be seen that the same result of Section 3.2.3.1 is indeed obtained:

$$\frac{P_{point\,E}}{P_{point\,C}} = \frac{t_1}{t_2}$$

As $t_1 < t_2$, the production rate at point E is lower than that at point C. It is clear however that t_1 for this convex system is lower than that of the concave system and hence the reduction in production rate from point C to E is greater in the case of the convex system. It is even less beneficial to mix in this case as the desired concentration, c_1, is reached at a quicker time by reaction alone.

Section 3.2.3.2 discussed the scenario where the volume of the reactor used, V_1, was kept the same and the total production volume was increased to V_{total}. For the current case of convex kinetics the development of the production rate ratio does not change as the same final point in $C-t$ space is reached. Therefore the production rate ratio is

$$\frac{P_{point\,F}}{P_{point\,C}} = \frac{1}{\lambda}\frac{t_1}{t_2}$$

As in Section 3.2.3.2 this can be developed to obtain a condition for when the production rate is increased by mixing which is

$$t_1 > \lambda t_2$$

Comparing the concave and convex kinetics, t_1 was lower in the latter and thus less likely to result in an increase in the production rate. It must be emphasised that only through an increase in the total production volume was an increase in production rate possible and the condition above must be met in order for it to occur. Depending on the contributing values of t_1, t_2 and λ, the condition suggests that an increase in production is perhaps possible even in a case of convex kinetics. From Figures 3.2.8 and 3.2.11 however, it is simply more likely that the condition is satisfied with concave kinetics in the case of a single PFR or batch reactor being used. If more reactor types are considered this would be where mixing may be used to obtain lower residences times than obtainable through reaction alone.

3.3 Applying Batch and Continuous Interpretations to $C-\tau$ Plots

In Section 2.1.7.1 it was stated that attainable regions can be plotted in $C-\tau$ space due to the linear mixing law that applies to residence time. Hence these plots may be used to determine the reactor structure necessary to minimise the residence time, something that could not be done using plots in C space alone. The purpose of this work was to expand the application of $C-\tau$ plots to batch reactor systems as the time component had not yet been investigated in these systems.

Upon investigation in Section 3.1, it was ascertained that differences exist between the nature of residence time and time used in batch systems. While the reaction time was the same between equivalent reactors, the fact that time cannot be mixed meant that plots in $C-t$ space differ slightly from those in $C-\tau$ space. Example constructions were performed in Sections A.1, A.2 and A.3 to highlight the fact that concavities may exist when ARs are plotted in $C-t$ space and hence these concavities are not an accessible part of the region as they are in continuous systems.

Production rates have been introduced thus far in Section 3.2 as a method of interpreting the AR to achieve the highest output of desired product. This has been accomplished using plots in $C-\tau$ space and $C-t$ space for continuous and batch systems respectively. It would be more prudent to utilise a single plot to achieve reactor structures in both types of systems rather than constructing two different plots. $C-\tau$ plots are already utilised and arguably easier to construct. Therefore plots in $C-\tau$ space should be retained rather than introduce the utilisation of plots in $C-t$ space. In order to do so correlations between the two system types with regards to production rate need to be assessed. Doing so would aid the use of one plot to achieve the most productive structure for both systems.

Equation 3.2.1 gave the production rate for a continuous system as

$$P_i = Q\left(c_i - c_{i,f}\right)$$

As was apparent from Section 3.2.1, the production rate was dependent on the flow rate, Q. If the total flow rate was increased to decrease the residence time, then an increase in production rate could be achieved. From the definition of residence time the expression for production rate in a continuous system can be expressed as

$$P_i = \frac{V\left(c_i - c_{i,f}\right)}{\tau} \tag{3.3.1}$$

This is similar to the definition of production rate in batch systems given by Equation 3.2.2. From Equation 3.3.1, $P \propto \frac{1}{\tau}$ which indicates why plots in $C-\tau$ space can be used to give an indication of production rate. The maximum production rate is obtained by striving to achieve the lowest τ for a desired output.

All of the production rate expressions used thus far have referred to the use of two points to determine the production rate, namely the feed and effluent points. A line could be constructed between the two points with the gradient being obtained from Equation 3.3.1 and Figure 3.3.1. The difference between the starting concentration and effluent concentration represents the change in the x-coordinate while the residence time change represents the change in the y-coordinate. Making these substitutions in Equation 3.3.1

$$P_i = V\frac{\Delta x}{\Delta y}$$

is obtained which can further be expressed in terms of the line's gradient as

$$P_i = \frac{V}{m}$$

From this, the production rate is increased with a lower gradient and decreased with a higher gradient ($P_i \propto \frac{1}{m}$). Therefore the most shallow gradient would most likely afford the best opportunity to obtain the highest production rate in a given scenario.

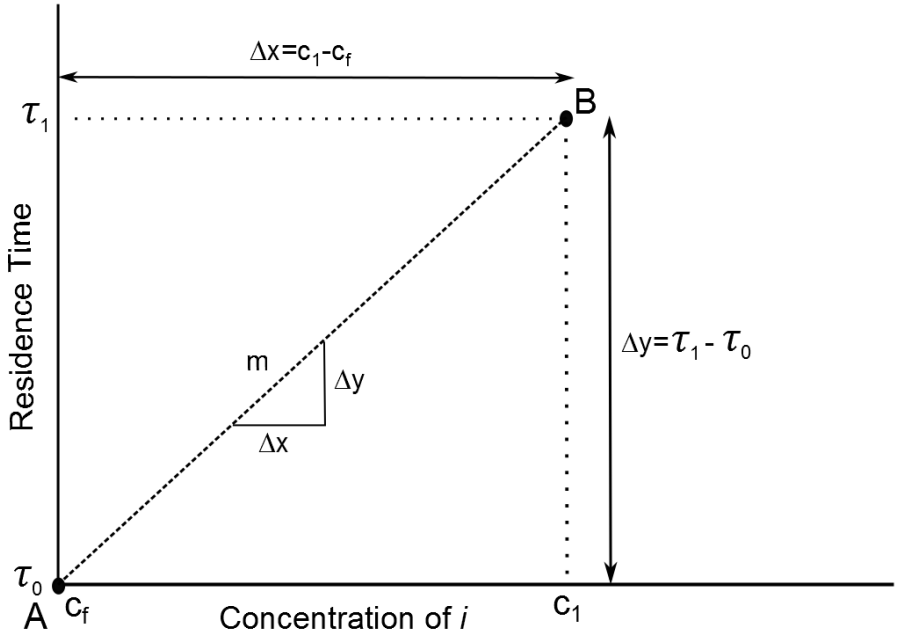

Figure 3.3.1: Arbitrary effluent point demonstrating the components of Equation 3.3.1 that form the gradient of the line between the feed and effluent points.

It is clear from Equation 3.3.1 that the line between the feed and effluent points for component i is in 2D concentration-residence time space. If Figure 3.3.1 was extended to multiple dimensions, with concentrations of N components, then the production rate at the effluent point could be represented by the production rate vector given in Equation 3.2.5:

$$\mathbf{P}(\mathbf{C}) = [P_1, P_2, P_3, ..., P_N, 1]^T$$

The production rate of residence time has been included as the last entry in the vector and is unity. This expression can be expanded and expressed in terms of gradient as before:

$$\mathbf{P}(\mathbf{C}) = \left[V\frac{\Delta x_1}{\Delta y}, V\frac{\Delta x_2}{\Delta y}, V\frac{\Delta x_3}{\Delta y}, ..., V\frac{\Delta x_N}{\Delta y}, V\frac{\Delta y}{\Delta y}\right]^T$$

The volume and change in residence time is common to all components, including residence time, and hence may be factored out of the bracket to obtain

$$\mathbf{P}(\mathbf{C}) = \frac{V}{\Delta y}[\Delta x_1, \Delta x_2, \Delta x_3, ..., \Delta x_N, \Delta y]^T$$

The production rate vector divided through by the volume hence represents all the lines connecting the feed and effluent points for all components. The volume in the expression acts as a scalar multiplier and would increase the vector's magnitude. Each line is located in 2D space with the dimensions of the space made up by the concentration of that specific component and residence time. This is merely a 2D projection of the line that exists in the multidimensional AR. Combining the 2D projections one may arrive at the multidimensional production rate line.

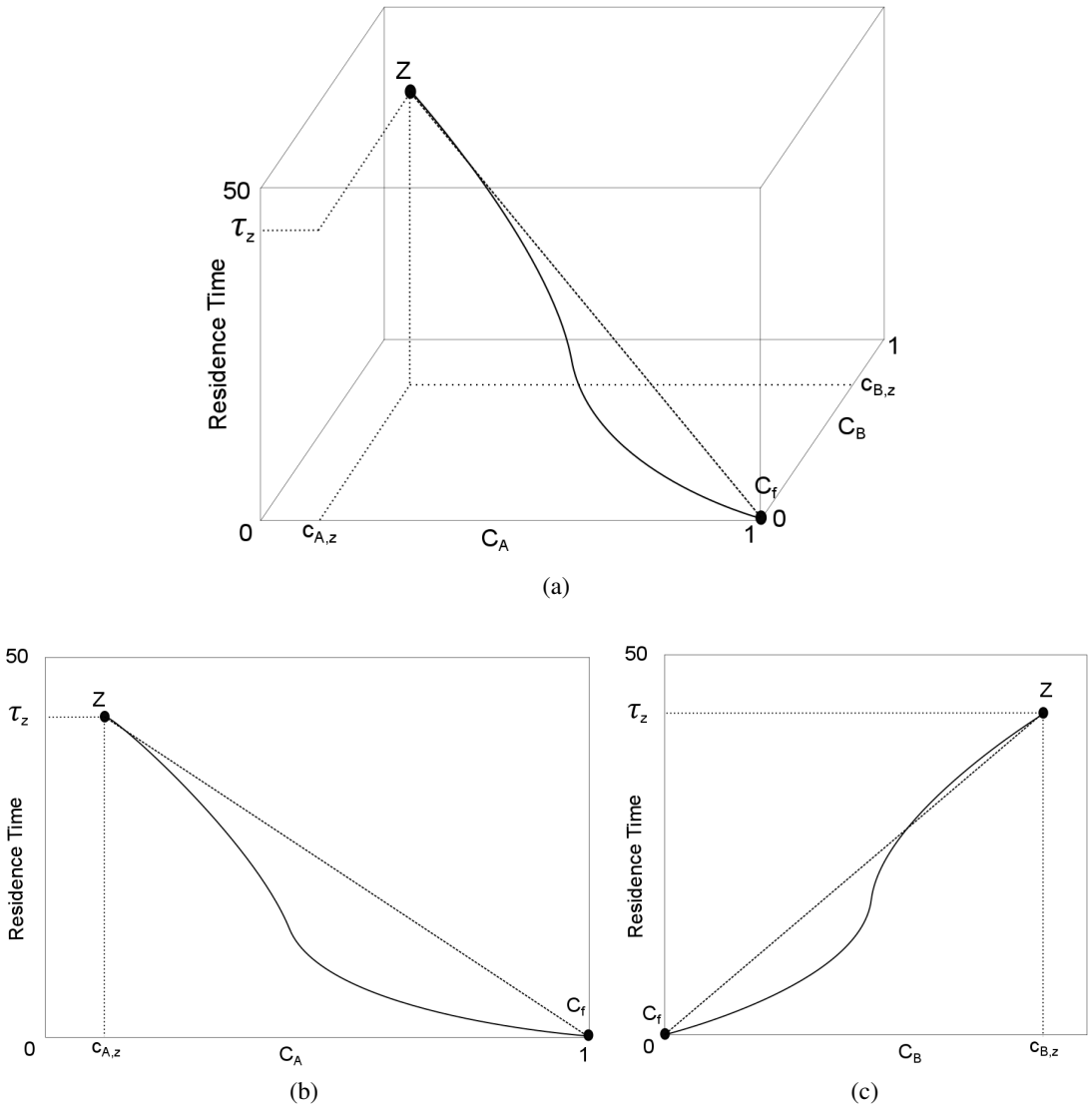

Figure 3.3.2: Arbitrary curve in 3D $C-\tau$ space (a) with the projections of this curve in $C_A-\tau$ (b) and $C_B-\tau$ (c) space.

Figure 3.3.2 provides an illustration of this. An arbitrary curve, $C_f - Z$, with an arbitrary effluent point, Z, exists in 3D $C-\tau$ space in Figure 3.3.2a. The production rate line is the straight line that joins C_f and Z but as two components are considered this line represents the production rate of both these components. The individual production rate lines are formed in 2D projections of Figure 3.3.2a in Figures 3.3.2b and 3.3.2c for components A and B respectively. It is clear that by combining the two 2D projections one may arrive at the 3D plot and hence the production rate vector in fact represents the production rate line in multiple dimensions. The individual production rates for each component are always represented and calculated in a 2D projection of the multiple dimension plot however.

For instance, the production rate of component A is

$$P_A = \frac{V(c_{A,z} - c_{A,f})}{\tau_z}$$

which represents the line in joining C_f and Z in Figure 3.3.2b. Likewise the production rate of component B is

$$P_B = \frac{V(c_{B,z} - c_{B,f})}{\tau_z}$$

which represents the line joining C_f and Z in Figure 3.3.2c. By combining these two projections the production rate line in Figure 3.3.2a can be obtained which is represented by the production rate vector:

$$\mathbf{P}(\mathbf{C}) = \left[\frac{V(c_{A,z} - c_{A,f})}{\tau_z}, \frac{V(c_{B,z} - c_{B,f})}{\tau_z}, \frac{V\left(c_{\tau,z} - c_{\tau,f}\right)}{\tau_z} \right]$$

Production rate can also be evaluated between any two points in $C - \tau$ space meaning the feed does not have to be included by default. The feed point should generally be included as the overall production rate will most likely be the target of the assessment. However the designer may choose to determine the best production rate between any two points in the space. Physically this translates to determining the production rate for a *portion* of the reactor network. This situation may arise when a specific point in the space is currently being achieved and will be used as a feed for further expansion of the reactor network.

This concept is illustrated in Figure 3.3.3. The production rate between points A and C is given by

$$P_{A-C} = \frac{V(c_1 - c_f)}{\tau_1}$$

while between points D and E it would be expressed as

$$P_{D-E} = \frac{V(c_3 - c_2)}{\tau_3 - \tau_2}$$

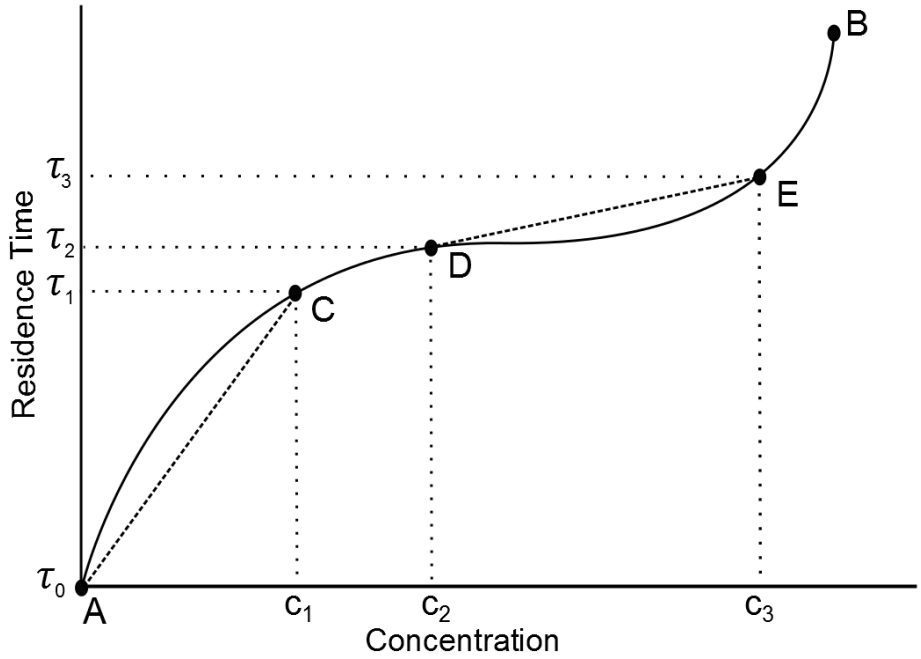

Figure 3.3.3: Production rate may be calculated between any two points in $C - \tau$ space such as between points D and E. Including the feed point merely provides the overall production rate of the entire reactor network.

As the production rate expression does not represent the mixing operation and simply evaluates production rate between two points in $C-\tau$ space, the production rates for a batch system would be represented in the exact same manner. The production rate between points A and C is given by

$$P_{A-C} = \frac{V(c_1 - c_f)}{t_1}$$

while between points D and E it would be expressed as

$$P_{D-E} = \frac{V(c_3 - c_2)}{t_3 - t_2}$$

From this it may be concluded that the production rate expression and application is equivalent in $C-\tau$ and $C-t$ spaces for continuous and batch systems respectively.

Expressing the production rate for continuous systems in terms of volume and residence time was done to show the similarity to the production rate in batch systems. Above it was shown that production rates are equivalent in application in $C-\tau$ and $C-t$ spaces. The expression was then developed into a vector in terms of volume and the gradients of each line connecting the feed and effluent points for each component. In this form it could be applied to both continuous and batch systems. However in Sections 3.2.1 and 3.2.3 it was found that the effluent point in $C-\tau/t$ space for equivalent reactor structures was different between the two system types. While time cannot be mixed in batch systems and therefore a different effluent point in $C-t$ space is achieved, the reactor structures for the systems remained equivalent. That is, the reactor structure for the batch system could be obtained by substituting the batch reactors that are equivalent mathematically to the continuous reactors in the continuous reactor structure. The translation between the reactor types was presented in Ming et al. (2013) and was discussed in Section 2.1.6.

Using this fact it is proposed that this method be used to obtain the batch reactor structure from $C-\tau$ plots which negates the need to plot in $C-t$ space. The algorithm for the use of production rates and obtaining the relevant reactor structures is given as follows:

1. Follow the standard AR construction algorithm presented in Section 3.1.2.1 to obtain the AR for the system under study in $C-\tau$ space. This plot is then used to determine the most desired effluent point both in targeted concentration and in production rate. Ideally the production rate should be maximised at this stage. It must be kept in mind from Sections 3.2.1 and 3.2.3 that production rate is heavily dependent on the throughput of the system which will most likely be specified or developed at a subsequent stage. Hence the production rate per unit volume is maximised at this stage. The production rate per unit volume would differ between continuous and batch systems if the mixing operation is involved due to the different effluent points obtained. As $C-\tau$ plots are being used, the interpretation of the plot at this stage is in terms of a continuous system only. Production rates may be congruous between the system types once volume and throughput are considered for both.

2. Using AR theory identify the continuous reactor structure for the system. Several options may be available all of which can achieve the desired point. Financial constraint or currently available reactors to the designer may be used at this stage to identify the most suitable structure.

3. Substitute the batch reactor equivalents of the continuous reactors to obtain the batch reactor structure. The obtained reactor structure will be the batch reactor equivalent of the most productive (per unit volume) continuous structure and hence be the most productive batch structure for that desired output.

4. This step is *optional* for a more detailed design solution. Once the reactor structures of each system are available, the throughputs of the systems must be assessed so as to actually achieve the highest production rate. The alternative would be to reduce the necessary reactor volume and this is not desired unless this is the aim of the solution. A simple rule may be followed in this instance to ensure the production rate is maximised for the given system. The rule is to always react the full reactor volume available to the designer within financial constraints. This ensures that the total throughput after reaction and mixing is applied is maximised and hence so is the production rate. If necessary various production rates and their associated capital and operating costs must be assessed to ascertain which is the most profitable option in the short or long term. This step would apply to both continuous and batch reactor systems.

This algorithm helps determine the most productive reactor structures and throughputs for both continuous and batch reactor systems. As can be seen, if the designer is looking to obtain the continuous reactor structure then steps 1, 2 and 4 are followed with 3 being skipped. Likewise for a batch reactor structure a designer would follow all the steps while only considering the batch structure in step 4. Step 4 is an optional step to obtain a more detailed design including the flow rates through and volumes of the reactors.

This algorithm and the concepts that led to it will be applied to two examples in Section 4 so as to demonstrate their usage and application to batch systems.

Key result: Production rates may be represented by Equation 3.3.1 and the production rate line or plane may be plotted in $C-\tau$ space for both continuous and batch systems. ARs in $C-\tau$ space are used to obtain the continuous reactor network after which the equivalent batch structure may be obtained. Hence plots in $C-\tau$ space are used in the context of both continuous and batch systems.

Chapter 4

Applications

The aim of this work was to further the application of AR theory to batch reactors by assessing the use of $C-\tau$ for batch systems. Thus far it has been concluded that due to differences between τ and t, plots in $C-\tau$ and $C-t$ spaces differed slightly. By using the batch equivalents of continuous reactors as defined in Ming et al. (2013), it was determined that $C-\tau$ may be used for both system types. These type of plots also provide a graphical method of assessing the most productive points of the AR and therefore can be extremely useful to designers of reactor systems. Using the concepts discussed thus far, two examples were performed. One example considers a simple 2D system while the second example considers a more complex 3D system. The method followed for both examples corresponded to the algorithm in Section 3.3 and is briefly summarised in Figure 4.0.1.

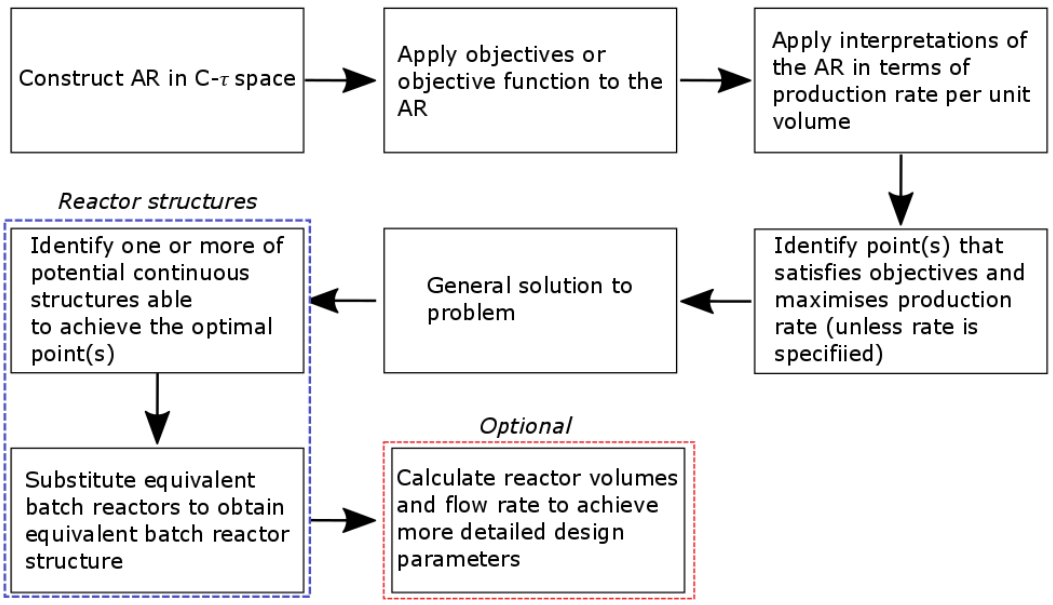

Figure 4.0.1: Summary of method applied in the application examples in Sections 4.1 and 4.2.

Note: In both examples presented, "Time" is used as the y or z axis label so as to indicate that the plots are applied to obtain the continuous *and* batch reactor structures. The plots are in $C-\tau$ space however as determined previously. Isothermal conditions, constant density and constant phase are assumed for the purpose of both examples.

4.1 Example 1 - Simple 2D System

4.1.1 Example 1 System and Brief

The first example selected seeks to apply the concepts and algorithm developed in Section 3.2 to a simple 2D system. Consider the system presented in Section A.1 namely for the single auto catalytic reaction

$$A + B \rightarrow 2B$$

The kinetics, with rate constants equal to unity, and feed point for the system were given as follows:

$$\mathbf{r}(\mathbf{C}) = \begin{bmatrix} r_A \\ r_B \\ r_t \end{bmatrix} = \begin{bmatrix} -c_A c_B \\ c_A c_B \\ 1 \end{bmatrix}, \quad C_f = \begin{bmatrix} 1 \\ 0.001 \\ 0 \end{bmatrix} mol/L$$

Assume that the unit of time for the system is minutes. In order to obtain the most productive reactor structure a goal of the structure needs to be defined. This goal need not be defined yet so as to highlight the benefits of the approach being undertaken. At this point in time the volume of the reactors or the throughput of the system will not be constrained or specified either as this will be discussed at a later point in the problem. These restrictions may be a result of space or financial constraints. In reality a designer may already know of constraints applied to the system but the initial steps do not require them to be known.

4.1.2 Simple Single Reactor System

First consider the simple solution of a single reactor type such as a PFR or standard batch reactor being used as the reactor structure. This may be the case if the AR technique is not utilised and the simplest system or what is merely available is used. The PFR would be operated to produce the required conversion through manipulation of the flow rate with respect to the volume of the reactor. This would determine the residence time of reactants and hence the conversion of reactants to products. Similarly, the batch reactor would be operated for a given length of time, the length of which would determine the conversion. This simple approach to the problem at hand is shown graphically in Figure 4.1.1.

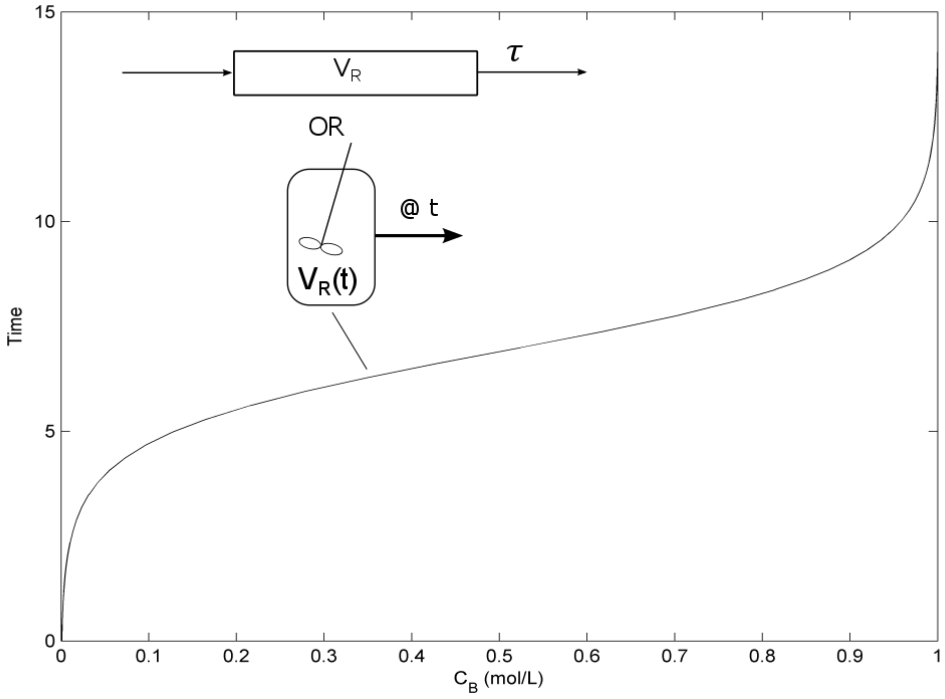

(a) Geometric representation of a single PFR or standard batch reactor.

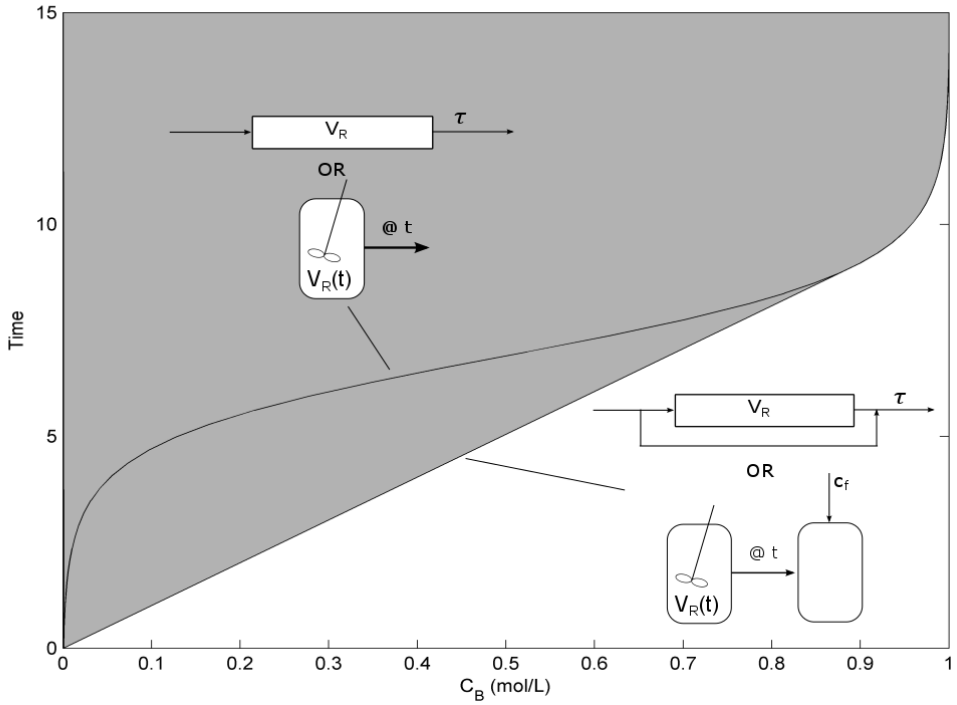

(b) Attainable region of the kinetics with a single PFR or batch reactor.

Figure 4.1.1: Example 1 - Single PFR or standard batch reactor for the system under consideration.

Figure 4.1.1a represents the trajectory in concentration-time space for both reactor types if only a single reactor is used. For any desired concentration of B, the corresponding residence time or reaction time can easily be obtained from the trajectory. This trajectory can be used to form an

AR for the reactor structure as shown in Figure 4.1.1b. As annotated in the figure, two reactor structures are possible namely the use of the reactor alone and then mixing the effluent of the reactor with the feed. The shaded region was obtained by determining the convex hull of the trajectory and filling in the region it defined. Doing so simulates the process of mixing between all achievable points through reaction. An elevated feed point was included in the convex hull as the region is unbounded with respect to residence time hence the shaded region above the trajectory.

From the AR in Figure 4.1.1b it is apparent that more structures would be possible if more than one reactor were considered. For example, a point on the trajectory that is >0.9 mol/L B can be mixed with the point that is equal to 0.3 mol/L B. However this would require the use of two PFRs/standard batch reactors. Furthermore, the AR could in fact be extended if the effluent of the reactor mixed with the feed is fed into another PFR. PFR trajectories initiated at these points could potentially extend the region below the current AR boundary. However as only a single reactor is utilised here this possibility of extension will not be considered.

If one were to ignore the benefits of mixing for the time being, from a production rate point of view the lower convex portion of the curve would be the ideal operation point of the reactor. This can be shown graphically and the exact point found using a production rate vector from the feed point. Both the vector and this point (A) are shown in Figure 4.1.2. Note that the production rate vector in this case overlaps the mixing line between the feed and Point A. Hence any point between the feed and Point A that lies on this line has the highest productivity per unit volume. If one were to discover this and explore the option of mixing, the range of effluent concentrations at the highest productivity rate increases significantly.

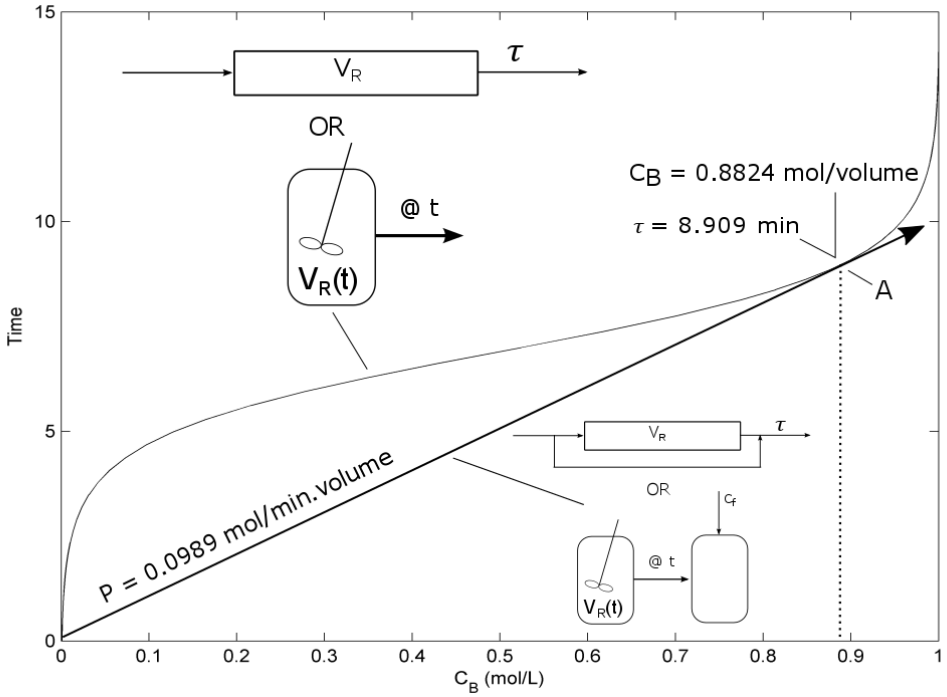

Figure 4.1.2: Example 1 - Single PFR/batch reactor trajectory for the system with production rate vector. The vector coincides with the mixing line between the feed point and Point A.

From Figure 4.1.2 and the previous paragraph, Point A would be the most productive if a single PFR or standard batch reactor were used without mixing being considered. This was determined

through the use of the production rate vector; the nearer the vector is to the x axis, the higher the production rate per unit volume. The lowest point that the vector intersects with the trajectory is Point A. If the concentration and residence time of Point A is used to determine the production rate then:

$$\hat{P_{B,A}} = \frac{c_B - c_f}{\tau - \tau_f} = \frac{0.8824 - 0.001\,mol/L}{8.909\,min} = 0.0989\,mol/min.L$$

Each point that lies on this vector has this production rate. As stated before, the vector overlaps the mixing line between Point A and the feed point that would be found if the convex hull of the trajectory were determined. It is therefore easy to see that 0.8824 mol/L is not the only concentration one is restricted to when seeking the most productive system but the full range between 0.001 and 0.8824 mol/L is also available. Hence, if the designer were targeting a specific concentration of B (or A for that matter), it would be easy to determine the most productive structure from Figure 4.1.2 i.e. those that lie on the vector. It is also apparent that concentrations on the trajectory >0.8824 mol/L may have high concentrations of B but they do exhibit lower production rates the higher the concentrations progress.

These results or interpretations highlight the benefit of this approach. No objective of the problem has been defined and yet multiple solutions have been determined for any objective that is put forward for this system. In fact, the same graphical solution can be used for multiple proposed objectives without having to recreate the solution in Figures 4.1.2 and 4.1.1b.

Now that the problem at hand has been considered from the use of a single reactor the full AR for the system may now be developed in order to consider the use of multiple reactors and reactor types. The algorithm in Section 3.3 will be followed from Section 4.1.3.

4.1.3 Full AR Construction and Selection of Desired Effluent Point

The first step of the algorithm presented in Section 3.3 requires construction of the AR in $C-\tau$ space. Fortunately this was already done in Section A.1 and this construction is found in Figure A.1.2. No desired target or specification was given in Section 4.1.2 and this allowed for the benefits of the AR approach to be realised. Now however it may be prudent to assign a target for the purposes of the example which can be changed at a later stage. For now, assume the process requires an output that has a concentration of B between 0.5 and 0.9 mol/L. This target range is completely arbitrary and it is assumed that any concentration in the range is a sufficient output of the process.

If lines are drawn to indicate at which concentrations the product is at the correct specification then Figure 4.1.3 is obtained. Note that the lines and crosses representing the reactors types were plotted over the AR to make discerning the reactor structure easier. Lines represent PFRs or batch reactors while crosses indicate CSTRs or fed-batch reactors.

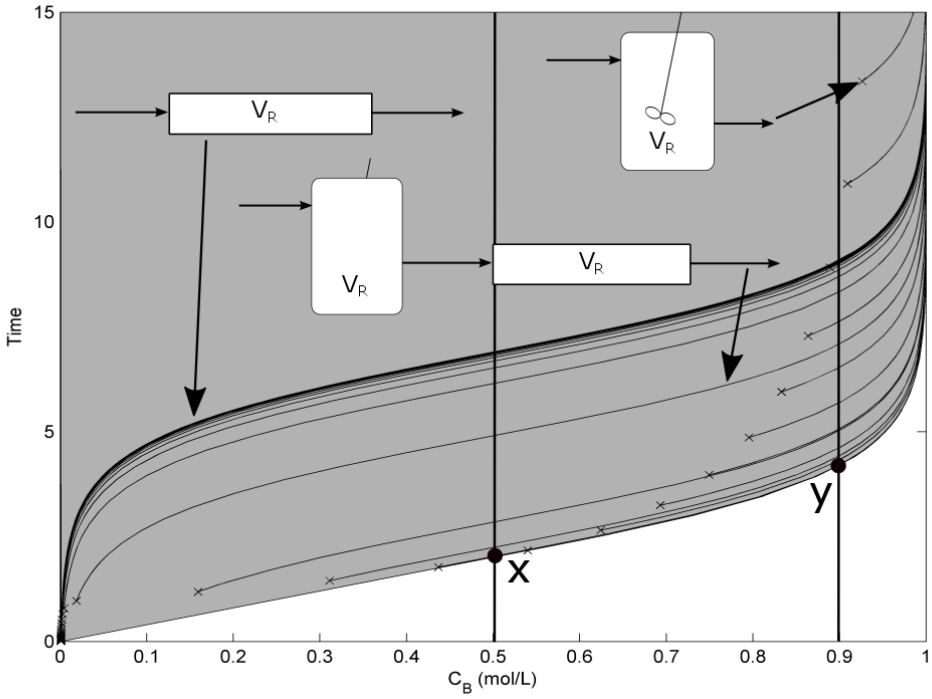

Figure 4.1.3: Example 1 - 2D AR in $C-\tau$ space for the single auto-catalytic reaction $A+B \rightarrow 2B$. The construction lines representing the different reactor types are shown in order to discern the reactor structures. Bold vertical lines have been drawn to indicate the concentration range at which the product is at the correct specification.

Based on the AR and specifics of the system the desired effluent point can now be sought. This point will be defined as the most productive point that is within the desired range of concentrations for B. As no flow rate has been specified as of yet, Equation 3.3.1 can be divided through by the volume in order to obtain the production rate per unit volume:

$$\hat{P}_B = \frac{\left(c_B - c_{B,f}\right)}{\tau}$$

From this it is clear that the desired effluent point will have the lowest residence time while being within the concentration range of 0.5-0.9 mol/L. The obvious points to consider are the two extreme concentrations in this range at the lowest boundary of the AR namely points x and y in Figure 4.1.3. These points satisfy the concentration requirements and also have the lowest residence time at the respective concentrations.

At point x the residence time was found to be $\tau = 2.022\,min$ and therefore:

$$\hat{P}_{B,x} = \frac{(0.5-0.001)\;mol/L}{2.022\,min} = 0.247\,mol/L.min$$

At point y the residence time was found to be $\tau = 4.212\,min$ and therefore:

$$\hat{P}_{B,y} = \frac{(0.9-0.001)\;mol/L}{4.212\,min} = 0.213\,mol/L.min$$

Even though point x has the lower concentration it has the higher production rate due to the lower residence time required to reach it. This shall therefore be selected as the desired effluent point going forward in the example.

4.1.4 Identifying the Continuous Reactor Structure

From zoomed in views of Figure 4.1.3 the reactor structures to achieve points x and y were found. Point x can be achieved by mixing the feed point with the effluent of a CSTR that has the residence time of 2.165 min as is shown in Figure 4.1.4.

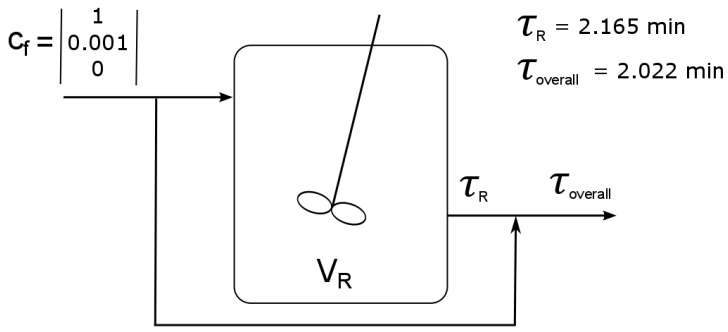

Figure 4.1.4: Example 1 - Continuous reactor structure required to achieve point x.

Likewise the reactor structure required to achieve point y was a CSTR with a residence time of 2.165 min followed by a PFR with a residence time of 2.047 min. This structure is shown in Figure 4.1.5. Note that the same CSTR residence time is achieved for both points x and y. This is expected as the CSTR would have to reside on the boundary of the AR in order to mix with the feed to produce point x but also feed the PFR that would form the AR boundary producing point y.

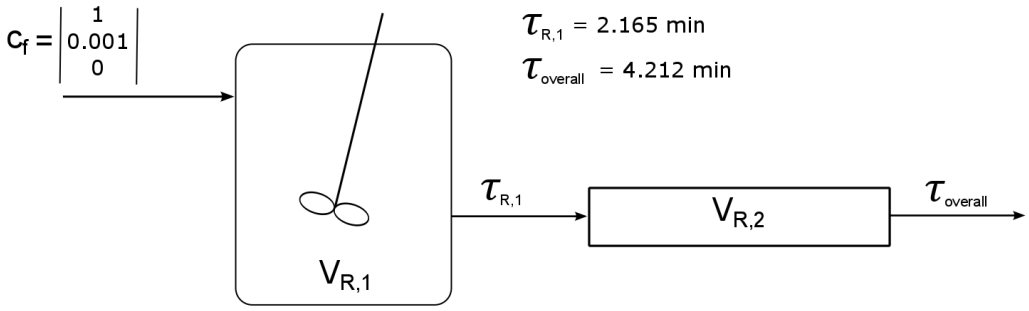

Figure 4.1.5: Example 1 - Continuous reactor structure required to achieve point y.

As point x was selected as the desired effluent point due to having the higher production rate per unit volume, Figure 4.1.4 represents the continuous reactor structure for the system. The fact that both reactor structures could be determined from the same AR construction and its accompanying theory is a strength of the method. The AR represents the general solution to the problem through which the reactor structure for any point in the AR can be determined. By

applying restrictions specific to the problem at hand the reactor structure suitable to solve the problem can be found. If another problem were to present itself concerning the same system, then the same AR could be used to solve it without having to re-construct the AR. In this regard AR theory is fairly robust.

4.1.5 Identifying the Equivalent Batch Reactor Structure

From the continuous reactor structure for point x the equivalent batch reactor structure may be obtained by substituting the batch reactor equivalents. Figure 4.1.6 is the resultant structure.

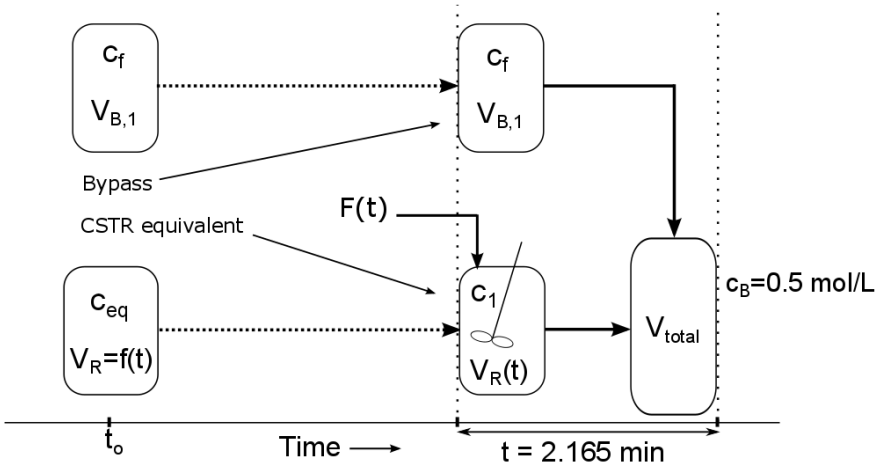

Figure 4.1.6: Example 1 - Equivalent batch reactor structure for the most productive point of the AR that meets the production requirements.

For later comparison the batch reactor structure to achieve point y of the AR was also obtained from the continuous reactor structure and is given in Figure 4.1.7.

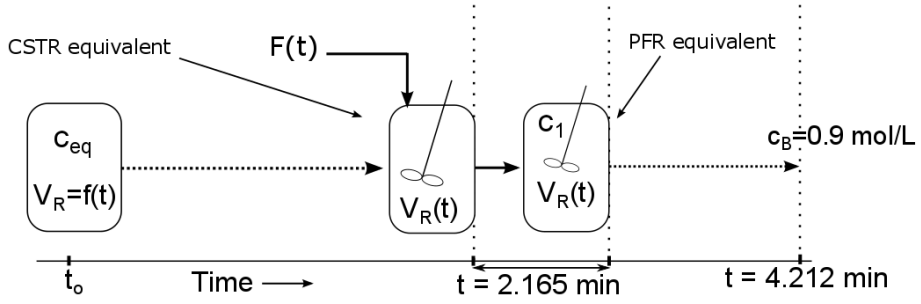

Figure 4.1.7: Example 1 - Batch reactor structure to achieve point y.

From Equation 2.1.17 the expression for the feed rate and the volume as they change with time can be determined. These expression will be useful when the next step of the algorithm is reached: examining the throughputs and volumes of the system. This fed batch reactor is the batch equivalent of a CSTR and hence the α value is constant. From Equation 2.1.17:

$$\frac{F(t)}{V(t)} = \alpha = \frac{1}{2.165\,min} = 0.462\,min^{-1}$$

The change in volume of the reactor is equal to the feed rate into the reactor. As both change with time and from the expression above:

$$\frac{dV}{dt} = F(t) = \alpha V$$

Rearranging:

$$\int_{V_o}^{V} \frac{dV}{V} = \int_{t_o}^{t} \alpha dt$$

Following integration expressions for the volume and feed rate at time t are found:

$$V(t) = V_o e^{\alpha t} \tag{4.1.1}$$

$$F(t) = \alpha V_o e^{\alpha t} \tag{4.1.2}$$

These are the expressions for the volume of the reactor and feed rate to the reactor as they vary with time, t. V_o is dependent on the total time of the system as well as the total volume of the reactor. This would be determined when evaluating the throughputs and volumes.

Fed batch reactors are initiated at a concentration and allowed to reach equilibrium. The concentration in the reactor would then remain the same even with the addition of new material. This is the property of the reactor that is equivalent to a CSTR which has an exiting concentration equal to the reactor contents and the contents remain at a single concentration throughout. Not all of the reactor contents would be removed at the end of the batch cycle as this would allow for the next batch to be initiated without re-establishing an equilibrium. For the purposes of the example it can be assumed that the entire reactor contents are removed and mixed which would be the case if there was no batch cycle to follow.

4.1.6 Assessing the Throughputs and Volumes of the Structures

The most desirable point on the AR in terms of production rate was selected earlier in the example using production rate per unit volume. Actual production rates are determined using the throughputs of the system. As discovered in Section 3.2, production rate is heavily influenced by throughput. As such, production rates are maximised for a particular case after considering the throughput and reactor volume.

4.1.6.1 Continuous System

Obtaining the product at $C_B = 0.5\,mol/L$ at a time of 2.022 min was determined to be the most productive and from the AR, Figure 4.1.4 was the arrangement required to reach this point. The residence time of the reactor was found to be 2.165 min and the ratio of V/Q must equal this value. V and Q have not yet been specified and could potentially be any two values that satisfy the given residence time. For example $V = 20L$ and $Q = 9.238\,L/min$ satisfies the ratio of 2.165 but so does $V = 100\,m^3$ and $Q = 46.189\,m^3/min$. This means that specifics of the process need to be taken in to account to fully determine the ideal volumes and flow rate of the system. If a general solution was sought then the residence time and AR would be this solution. This could then be applied at a later point to calculate the other relevant values. The AR would remain

the same and could be used to evaluate alternate points if other objective functions or desired outputs are identified. For example if the concentration of B were required to be <0.1 mol/L or >0/9 mol/L, the finalised reactor structures may differ but the attainable region for the system would be the same to determine those reactor structures. This is the distinct advantage of the AR method as its output is a "universal" solution to the system. For the problem at hand the residence time would remain the same and the volume and volumetric flow rate would be able to be changed to suit the residence time and constraints of the system.

For the problem at hand suppose the constraint is that the the maximum reactor size available is $1\,m^3$. Any volume up to this can be used. As $P \propto V$, reacting the full volume will yield the maximum production rate. If the volume of the reactor is $1\,m^3$, then the corresponding flow rate to achieve the residence time of 2.165 min is $0.462\,m^3/min$ or $7.698\,L/s$. This is just the flow rate through the reactor however. The total flow rate that exits the system is determined using the exiting residence time. Using both residence times a mixing fraction can be determined and from this the exiting flow rate. As the bypass has a zero residence time:

$$\tau_{total} = \lambda\,\tau_R$$

$$\lambda = \frac{\tau_{total}}{\tau_R} = \frac{2.022}{2.165} = 0.934$$

The mixing fraction is defined as being the ratio of one of the contributing flow rates to the total flow rate:

$$\lambda = \frac{Q_R}{Q_{total}}$$

$$Q_{total} = \frac{Q_R}{\lambda} = \frac{7.698\,L/s}{0.934} = 8.242\,L/s$$

These are then the design values for the system that meet the solution requirements and maximise the production rate of the product B. Note that they were determined in the final step without the production rate expression (aside from using the expression to state that the maximum volume should be reacted). This is because the production rate per unit volume was maximised in the earlier steps. By maximising the possible volume of the system, the flow rate would be maximised and hence the highest possible production rate would be obtained.

4.1.6.2 Batch System

For the batch system equivalent, the same residence time (actually *reaction time* in batch systems) applies to the reactor. Assume the maximum reactor volume restrictions also apply to the batch case. This means that a fed-batch reactor with a final volume of $1\,m^3$ reacts for 2.165 minutes. Using the equations for the feed rate and the volume derived in Section 4.1.5 the required feed rate to the reactor fed-batch reactor may be found.

α was found to be $0.462\,min^{-1}$ and with the final volume and Equation 4.1.1:

$$1\,m^3 = V_o exp(0.462\,min^{-1} \times 2.165\,min)$$

$$V_o = 0.368\,m^3 = 368\,L$$

This is the volume of initial material required in the reactor for the parameters stated. It is this volume that will be initiated at equilibrium before the feed to the reactor is commenced. Assuming there is another batch to follow the current one, this would also be the amount retained to initiate the next batch. The volume as it changes with time may be determined from Equation 4.1.1 by varying the time from 0 to 2.165 min and evaluating the volume throughout. As the feed rate is simply the volume at a given point in time multiplied by α (Equation 4.1.2), the same may be done for the feed rate and hence the volume and feed rate profiles were determined and are shown in Figure 4.1.8.

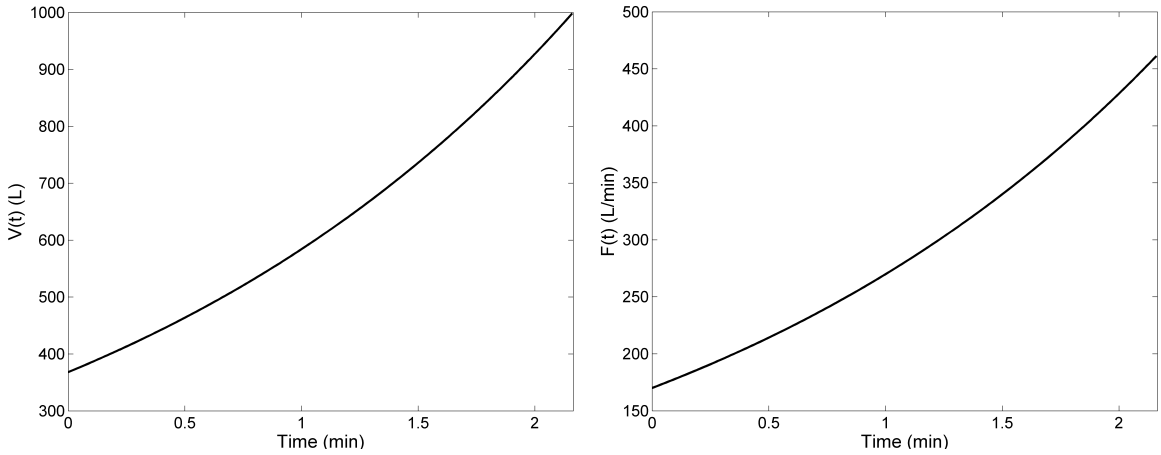

(a) (b)

Figure 4.1.8: Example 1 - Volume (a) and feed rate (b) profiles of the fed-batch reactor as they vary throughout the reaction time period.

After 2.165 minutes the contents are mixed with a portion of feed material to arrive at the final concentration of $C_B = 0.5\,mol/L$. The mixing fraction can be used once more to find the total final volume after mixing and assuming the entire contents of the reactor is mixed:

$$V_{total} = \frac{V_R}{\lambda} = \frac{1\,m^3}{0.934} = 1.071\,m^3$$

This concludes the first example as the continuous and batch reactor structures have been found given the constraints of the problem. It is reiterated that the same method and AR may be applied given alternate constraints.

Key result: Production rates were able to be maximised for given constraints for batch and continuous systems using a 2D AR in $C-\tau$ space. The equivalent batch structure was derived from the continuous reactor structure.

4.2 Example 2 - 3D System for Two Stages of Anaerobic Digestion

In Example 1 (Section 4.1), a simple 2D auto-catalytic system was considered. In order to explore the concepts in a more complex framework, a 3D system will be used in the second example. As time is considered to be a component of the attainable region, a 3D example would require a system with two independent reactions.

4.2.1 Example 2 System and Brief

The system selected for the example was that of anaerobic digestion which is the biological degradation of organic material in the absence of oxygen (Mata-Alvarez et al., 2000). Methane is the main targeted product of the process which can be utilised as a fuel for heating or cooking purposes (Olsson and Fallde, 2014). As the product gas contains roughly 50% methane and 50% carbon dioxide, the gas is often purified and upgraded so that the resultant methane may be used in processes or as a fuel in cars (Olsson and Fallde, 2014). This process is of general interest because it provides an energy source utilising waste or plant organic matter hence potentially being a carbon neutral or negative energy source.

Anaerobic digestion occurs in four distinct stages namely hydrolysis, acidogenesis, acetogenesis and methanogenesis (Mata-Alvarez et al., 2000; Sötemann et al., 2006). Each of these stages have reactions that occur which use the product of the previous stage to form the reactant of the following stage. If only a single reaction occurred in each stage it is clear that there would be four reactions, two greater than required for the current example. Therefore, only acetogenesis and methanogenesis will be considered with time as the third component/dimension. Reactions representing the two stages as well as kinetics for the reactions were obtained from Sötemann et al. (2006). The full model given in Sötemann et al. (2006) was not considered due to the two reaction limit and hence death rates of the acetogens and methanogens were also excluded from the example.

The reaction and reaction rate for acetogenesis are given as Equations 4.2.1 and 4.2.2 respectively.

$$2.5CH_3CH_2COOH + NH_4^+ \rightarrow CH_3COOH + C_5H_7O_2N + 0.5CO_2 + 3.5H_2 + H^+ \tag{4.2.1}$$

$$r_{aceto} = \frac{\mu_{max,aceto} c_{CH_3CH_2COOH}}{K_{s,aceto} + c_{CH_3CH_2COOH}} \left(1 - \frac{c_{H_2}}{k_{hyd} + c_{H_2}}\right) c_{acetogens} \tag{4.2.2}$$

The reaction and reaction rate for methanogenesis are given below in Equations 4.2.3 and 4.2.4. Note that the reaction for methanogenesis was modified from the one in Sötemann et al. (2006) in order to ensure the equation balanced.

$$3.5CH_3COOH + NH_4^+ \rightarrow CO_2 + CH_4 + C_5H_7O_2N + H^+ + 3H_2O \tag{4.2.3}$$

$$r_{meth} = \frac{\mu_{max,meth} c_{CH_3COOH}}{K_{s,meth} + c_{CH_3COOH}} c_{methanogens} \tag{4.2.4}$$

Equations 4.2.1 and 4.2.3 both contain H^+ as a product. As pH is a function of the concentration of H^+ ions, the pH of the system would be able to be determined at any point in the constructed AR. Section 4.3 investigates this possibility further and its integration with AR constructions.

The constants for Equations 4.2.2 and 4.2.4 were set (Equation 4.2.5) such that the propanoic acid was mostly reacted in ~3 days. Otherwise they were considered to be arbitrary as it is not the intention to mirror the model completely but assess the AR construction and application of the concepts in this work.

$$\begin{gathered}\mu_{max,aceto} = 1\ hr^{-1} \\ \mu_{max,meth} = 1\ hr^{-1} \\ K_{s,aceto} = 0.9\ mol/L \\ K_{s,meth} = 0.5\ mol/L \\ k_{hyd} = 0.2\ mol/L\end{gathered} \tag{4.2.5}$$

Based on these two stages of anaerobic digestion, the concentration vector and reaction rate vectors are formulated (Equation 4.2.6). In both Equations 4.2.1 and 4.2.3 the chemical formula for acetogens and methanogens is $C_5H_7O_2N$ as specified in Sötemann et al. (2006). Typically components with the same chemical formula would be considered the same chemical species and hence form a single entry in the concentration vector. In the current case, while the acetogens and methanogens have the same chemical formula, they are still separate bacterium species and hence shall be considered as such with separate entries in the concentration vector. A supporting reason is that the reaction rates for acetogenesis and methanogenesis are functions of the appropriate bacterium species and using the same entry in the concentration vector to represent both would alter the behaviours of the kinetics.

$$\mathbf{C} = \begin{bmatrix} c_{CH_3CH_2COOH} \\ c_{NH_4^+} \\ c_{CH_3COOH} \\ c_{C_5H_7O_2N}\,(acetogens) \\ c_{CO_2} \\ c_{H_2} \\ c_{H^+} \\ c_{CH_4} \\ c_{C_5H_7O_2N}\,(methanogens) \\ c_{H_2O} \\ \tau \end{bmatrix} \quad \mathbf{r} = \begin{bmatrix} -2.5r_{aceto} \\ -r_{aceto} - r_{meth} \\ r_{aceto} - 3.5r_{meth} \\ r_{aceto} \\ 0.5r_{aceto} + r_{meth} \\ 3.5r_{aceto} \\ r_{aceto} + r_{meth} \\ r_{meth} \\ r_{meth} \\ 3r_{meth} \\ 1 \end{bmatrix} \tag{4.2.6}$$

As propanoic acid and ammonium are the main feed components of the two stages, these two components have non-zero entries in the feed vector, C_f (Equation 4.2.7). Apparent in Equations 4.2.2 and 4.2.4 is that the initial concentration for the acetogens and methanogens cannot be zero. Similar to component B in Example 1 (Section 4.1), the reactions are auto-catalytic with respect to acetogens and methanogens and should have non-zero entries in the feed vector for these components. These entries are chosen to be slightly above zero as in Example 1.

$$\mathbf{C_f} = \begin{bmatrix} 1 \\ 1 \\ 0 \\ 0.001 \\ 0 \\ 0 \\ 0 \\ 0 \\ 0.001 \\ 0 \\ 0 \end{bmatrix} \tag{4.2.7}$$

In Example 2, no targeted result will be specified yet. A larger focus will be placed on determining the AR for the system in order to gain insight into the AR construction of a system

in $C-\tau$ space. Once a candidate AR is constructed then a potential objective for the system will be specified. Emphasis is placed on the fact that the AR constructed will be a *candidate* attainable region. This implies that the AR is not guaranteed to be the full complete AR but instead a potential or partial attainable region for the system.

4.2.2 Candidate Attainable Region Construction in $C-\tau$ Space

The standard theoretical method of constructing the candidate AR will be followed as outlined in Section 3.1.2.1. Each stage of the construction is shown with annotations on the plot for each reactor type in Figure 4.2.1. Figure 4.2.1 follows the construction from the initial PFR/batch reactor from the feed to the construction of the DSR from the feed. Equations 2.1.9 and 2.1.7 were used to determine the points for the PFR (or batch reactor) trajectories and CSTR (or fed-batch reactor) locus respectively.

The DSR trajectory was determined using Equation 2.1.10. A DSR was necessary because the AR has three dimensions (one being τ), regardless if only two reactions are taking place. In order to ensure the DSR traversed the AR boundary, the critical alpha policy needed to be found using Equation 2.1.12. Note that Equation 2.1.12 can only be used to determine the critical alpha policy for three dimensional problems.

Following the use of Equation 2.1.12, the α for the system at hand was determined to be Equation 4.2.8 with the components represented by letters in Equation 4.2.9. No issue arose in the use of τ as a component when determining α as it is defined in the concentration and rate vectors. A more detailed description with each step of how Equations 4.2.8 and 4.2.9 were determined can be found in Appendix B.

$$\alpha(\mathbf{C}) = \frac{s.u}{v.(w+x+y.z)} \tag{4.2.8}$$

$$\begin{aligned}
s &= 0.5c_{CH_3CH_2COOH}.c_{C_5H_7O_2N\,(aceto)}.(0.45c_{CH_3CH_2COOH}-1.305)\\
u &= \left(c_{CH_3COOH}.c_{C_5H_7O_2N\,(meth)}.\tau - c_{CH_4}.(c_{CH_3COOH}+0.5)\right)\\
v &= (c_{H_2}+0.2)(c_{CH_3CH_2COOH}-1)(c_{CH_3CH_2COOH}+0.9)\\
w &= -0.45c_{CH_3COOH}.c_{C_5H_7O_2N\,(meth)}.\tau\,(c_{CH_3CH_2COOH}+0.9)\\
x &= 0.45c_{CH_4}(c_{CH_3COOH}+0.5)(c_{CH_3CH_2COOH}+0.9)\\
y &= (0.45c_{CH_3CH_2COOH}-1.305)\\
z &= \left(c_{CH_3COOH}.c_{C_5H_7O_2N\,(meth)}.\tau - c_{CH_4}(c_{CH_3COOH}+0.5)\right)
\end{aligned} \tag{4.2.9}$$

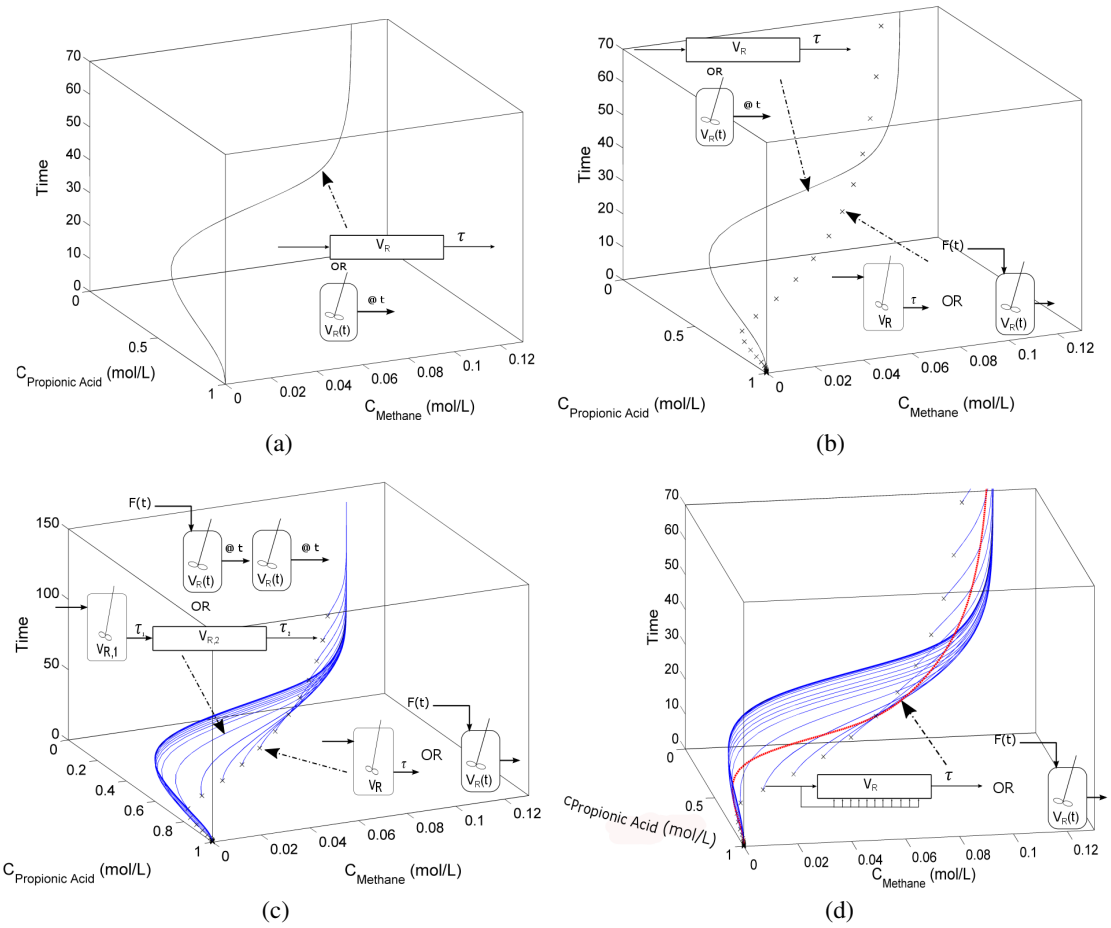

Figure 4.2.1: Example 2 - Initial stages of AR construction where the standard reactors are plotted. PFR or standard batch reactor is plotted (a) after which the CSTR or fed-batch reactor locus is added (b). PFRs or standard batch reactors are initiated at each CSTR/fed-batch reactor (c). The first critical reactor, the DSR or fed-batch reactor, is initiated at the feed point with the appropriate alpha policy (d).

Note that in Figure 4.2.1d the DSR seems to tend toward the initial PFR trajectory. By extending the integration period of both trajectories it was found that this is indeed the case as can be seen in Figure 4.2.2. As the time is escalated, the DSR tends closer towards the PFR trajectory. At a time of 300 hours the concentration vector of the DSR does not yet match the PFR but at a time of ~576 hours the DSR vector matches the PFR to 4 decimal places. This follows directly from Equation 2.1.10 (DSR expression) and the discussion in Section 2.1.6.2 regarding the use of the DSR expression for fed-batch reactors. In Section 2.1.6.2 it was stated that when $\frac{dC}{d\tau} = 0$ and $\alpha = 1/\tau$, the DSR expression reduces to the expression for a CSTR.

It is clear that $\frac{dC}{d\tau}$ cannot in this case reach 0 as τ is a component of the concentration vector. As the integration progresses for an ever-increasing time period, the time component of the concentration vector continually changes and hence $\frac{dC}{d\tau}$ will not reach 0. If α is considered to be $1/\tau$ then Equation 2.1.10 becomes

$$\frac{d\mathbf{C}}{d\tau} = \mathbf{r}(\mathbf{C}) + \frac{1}{\tau}(\mathbf{C}_o - \mathbf{C})$$

Extending the time of integration causes α to tend to 0 and hence the DSR expression reduces to the that of a PFR. This is corroborated by assessing Equation 4.2.8 which tends towards zero

as propanoic acid and acetic acid are consumed and reach zero concentration at higher time periods.

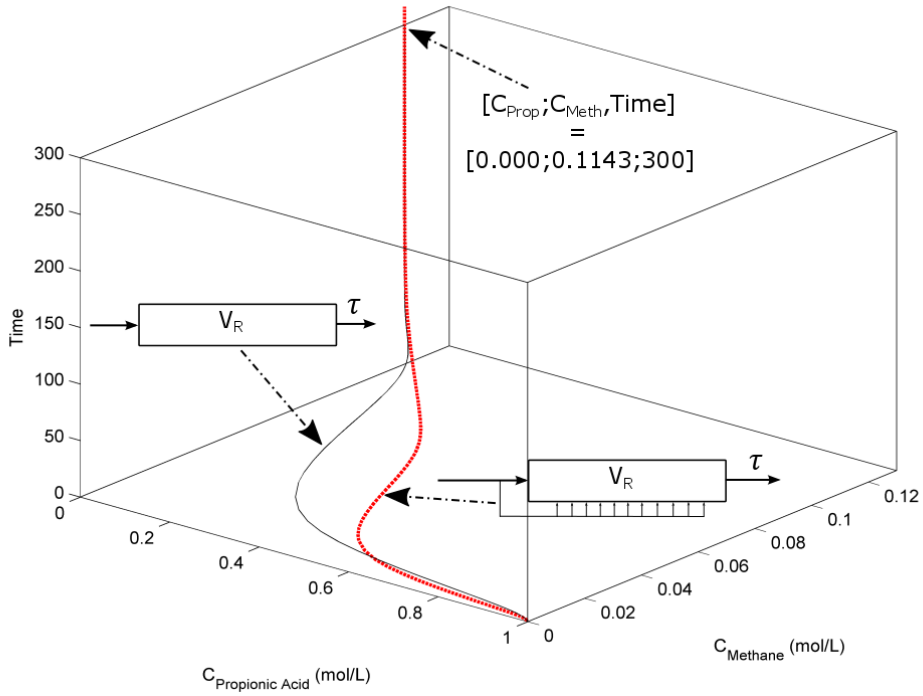

Figure 4.2.2: Example 2 - PFR/batch reactor and DSR trajectories are extended over a longer time period. The DSR traverses the AR boundary along a different path to that of the PFR but then tends towards the PFR trajectory.

Being a 3D attainable region, the critical CSTRs are also generally found for the system. A critical CSTR is a CSTR that lies on the boundary of the AR and hence often take the role of a connector on the AR boundary, as does the DSR (Feinberg, 2000a). Feinberg (2000a) have proven that for a CSTR to lie on the boundary of the AR, the following condition must be satisfied:

$$Det\left[\left(\mathbf{C}-\mathbf{C}_f\right), dr(\mathbf{C})\left(\mathbf{C}-\mathbf{C}f\right), \left(dr(\mathbf{C})\right)^2\left(\mathbf{C}-\mathbf{C}_f\right), ..., \left(dr(\mathbf{C})\right)^{d-1}\left(\mathbf{C}-\mathbf{C}_f\right), Null\right] = 0 \tag{4.2.10}$$

The matrix formed in Equation 4.2.10 has to be square in order for the determinant of the matrix to be calculated and has size $n \times n$. *Null* is the null space of A^T (Equation 4.2.11) where A is the stoichiometric matrix of the system. The stoichiometric matrix (Equation 4.2.12) consists of the stoichiometric coefficients in the reactions of the system and has size $n \times d$, n being the number of components and d the number of independent reactions. This results in *Null* having a size of $n \times n - d$.

$$Null = null(A^T) \tag{4.2.11}$$

$$A = \begin{bmatrix} A_{1,1} & \dots & A_{1,d} \\ \vdots & \ddots & \vdots \\ A_{n,1} & \cdots & A_{n,d} \end{bmatrix} \tag{4.2.12}$$

In the example thus far, τ has been considered as a component of the AR and is defined in the concentration and rate vectors as τ and 1 respectively. Consequently, residence time is able to be included as a component in the integration of the PFR and DSR equations as well as the solving of the CSTR equation. Residence time is also included in the determination of the α policy for the DSR due to its inclusion in the rate and concentration vectors. The first 3 columns of Equation 4.2.10 would therefore have 11 rows each with the 11th component being τ in the concentration and feed vectors. *Null* however may be a different case due to the stoichiometric matrix, A. A cannot contain τ as residence time does not participate in the reactions in a stoichiometric manner. It may be argued that the entries for τ in A would be zero for both reactions. A simple mass balance, shown below, would counter this notion as time does not behave in the same way as mass. A cannot contain τ as a result.

$$\mathbf{C} = \mathbf{C_f} + A.\varepsilon$$

$$\begin{bmatrix} c_{CH_3CH_2COOH} \\ c_{NH_4^+} \\ c_{CH_3COOH} \\ c_{C_5H_7O_2N}\,(acetogens) \\ c_{CO_2} \\ c_{H_2} \\ c_{H^+} \\ c_{CH_4} \\ c_{C_5H_7O_2N}\,(methanogens) \\ c_{H_2O} \\ \tau \end{bmatrix} = \begin{bmatrix} 1 \\ 1 \\ 0 \\ 0.001 \\ 0 \\ 0 \\ 0 \\ 0 \\ 0.001 \\ 0 \\ 0 \end{bmatrix} + \begin{bmatrix} -2.5 & 0 \\ -1 & -1 \\ 1 & -3.5 \\ 1 & 0 \\ 0.5 & 1 \\ 3.5 & 0 \\ 1 & 1 \\ 0 & 1 \\ 0 & 1 \\ 0 & 3 \\ 0 & 0 \end{bmatrix} . \begin{bmatrix} \varepsilon_1 & \varepsilon_2 \end{bmatrix}$$

$$\tau \neq 0 + \begin{bmatrix} 0 & 0 \end{bmatrix} . \begin{bmatrix} \varepsilon_1 & \varepsilon_2 \end{bmatrix}$$

Null would therefore not have 11 rows and Equation 4.2.10 could not be constructed for the system. For the current example determination of the critical CSTR points is therefore not possible using the standard AR theory discussed in Feinberg (2000a). It is not necessary for the AR construction however as the critical CSTRs would simply form part of the currently constructed AR. Hence for the purposes of the example it is not crucial that these points are determined. The fact that Equation 4.2.10 cannot be used for the system does however extend to all multiple-dimensional ARs in $C-\tau$ space. Different methods will have to be determined for such constructions.

In order to ensure the attainable region constructed from theory was as complete as possible, the AR was also constructed using a numerical AR construction method. Another purpose of using a different construction method was to confirm or deny existence of multiple steady states for the CSTRs in the system. Multiple steady states were expected due to the non-linear nature of the reaction rate expressions. Several methods were employed during the theoretical construction to check for the presence of multiple steady states (MSS). None of the following revealed the presence of MSS:

- Solving of the general CSTR equation (Equation 2.1.7) using a single guess for multiple times within a given time interval. This is the standard way of solving for the CSTR locus and is not expected to reveal MSS.

- Generation of a large number of random points within the $C-\tau$ space and assessment of each point against the condition for satisfying the CSTR equation. If MSS exist this method would allow for multiple loci to be found. However, in the current case it did not yield the desired results within a reasonable tolerance.

- Solving of the general CSTR equation using multiple guesses for multiple times within a given time interval. Essentially this involved repeating the first method for multiple different random guesses within the $C-\tau$ space and plotting all solution points. If multiple loci exist then this method would hint at their existence by finding either a separate additional locus or at least identify other CSTR points separate from the main locus. For Example 2 only the original locus was revealed.

As no MSS were found during the theoretical construction, the numerical construction method would aid in the confirmation of the theoretically constructed AR as well as confirm that no MSS exist in the *candidate* attainable region. It will not be stated however that the region is not indeed larger and that MSS absolutely do not exist although effort was placed in ascertaining this for the purposes of Example 2.

Use of the alternate numerical AR construction method resulted in the same candidate attainable region as that constructed using the theoretical method. Figure 4.2.3 is the candidate attainable region formed after the convex hull of the reactor trajectories and loci was found. It is this candidate region that will be used in the example going forward. Remember that this region represents all the possible effluent concentrations for the given kinetics. Any objective or objective function may be applied to this region in order to obtain the desired reactor structure or identify the portion of the region in which the target lies.

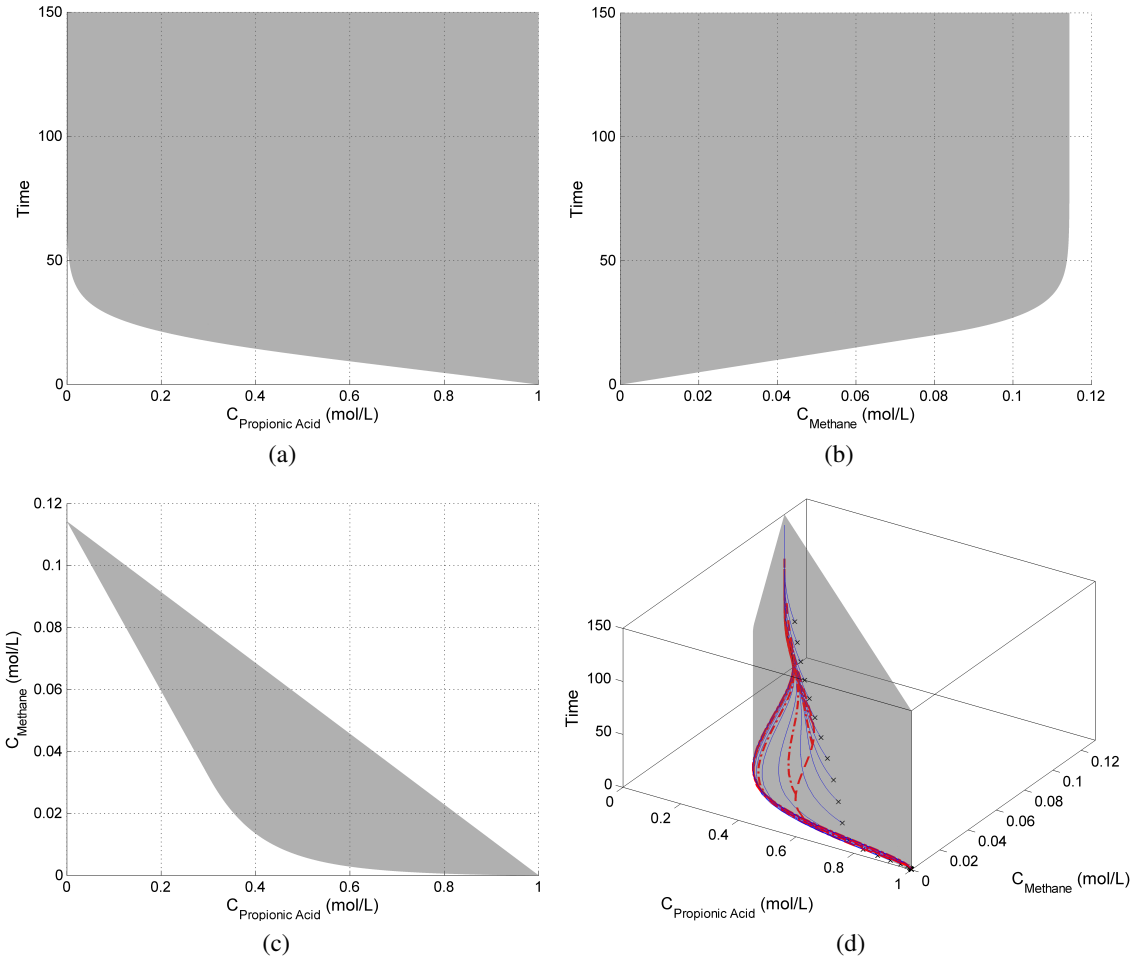

Figure 4.2.3: Example 2 - Candidate attainable region for the acetogenesis and methanogenesis reactions that make up the system under consideration in Example 2. Multiple views are shown here: $C_{Propanoic\,Acid} - \tau$ view (a), $C_{Methane} - \tau$ view (b), $C_{Propanoic\,Acid} - C_{Methane}$ view (c) as well as the 3D view of the region with the reactor trajectories and loci included (d).

4.2.3 Selection of Desired Effluent with Arbitrary Objective

Typically an attainable region allows one to identify all the concentrations that are possible given the system kinetics. Based on the construction of the AR, the minimum required reactor structures to acquire all points of the AR can also be identified. Feinberg (2000b) states that the maximum number of reactor structures needed to acquire any point within the AR is equal to the number of independent reactions (d). It is mixing between and combining these structures that any desired point within the constraints of the AR is able to be achieved. If a point on the boundary of the AR is sought, then the maximum number of parallel reactor structures required to achieve any point on the boundary is $d-1$ (Feinberg, 2000b). This was the approach of Ming et al. (2013), namely to determine the parallel reactor structures required to achieve all boundary points and convert these to batch reactor structures. Such an approach provides a more general solution to a problem.

This will not be the approach of the current work, as with the production rate being applied it is more desirable to obtain one of the possible reactor structures required to obtain the point. Production rates per unit volume are independent of the structure utilised in reaching points

within the space. However when evaluating the point and potential reactor structure with regards to production rate, a specified structure is preferred so as to calculate the associated volumes, flow rate and production rates. The fact that multiple different structures, often an infinite number, are potential structures for each point in the AR is highlighted here. This is why the specification of the parallel reactor structures required to achieve all points in the AR makes sense as a general solution. Only a single reactor structure that is able to achieve the desired point will be discussed here though as a more specific solution is targeted.

In Example 1 (Section 4.1), a range of concentrations was given as the desired effluent concentration. Any point which satisfied the range was applicable as a desired effluent point. Production rates of two possible points were calculated so that the point with the higher rate may be selected. The concentration range given may be thought of as the objective function but it is also true that the production rate could be considered as an objective function. In the second example the production rate equation will be treated as a secondary objective function with the production rate being specified beforehand. Both the production rate objective as well as the actual objective function will therefore need to be satisfied. We may also choose to use either only the production rate objective or only the objective function; it is not mandated that we use both functions but we shall here.

The production rate per unit volume target for the example is arbitrarily set to be

$$\hat{P}_{Methane} = 0.003\, mol/L.hr$$

which can be substituted in Equation 3.2.7 with reference to methane resulting in

$$\tau = \frac{1}{0.003\, mol/L.hr} C_{methane} - \frac{1}{0.003\, mol/L.hr} C_{f,methane}$$

As no methane is present in the feed, this reduces to

$$\tau = \frac{1}{333.33} C_{methane}$$

which is simply a straight line equation in $C_{methane} - \tau$ space. By applying this equation at every propanoic acid concentration a plane may be formed in the $C - \tau$ space of the AR construction. Where the plane intersects the candidate AR represents the points that satisfy the production rate objective. The addition of an objective function would potentially narrow down the desired points of the system.

Let us first consider the case if we only used the production rate plane as the objective for the design. Figure 4.2.4 provides a view of the candidate AR and the plotted production rate plane. As the view is $c_{Methane} - \tau$ the plane appears as a line due to the fact that the production rate objective is expressed in terms of in $c_{Methane}$ and τ only. If this line represented the only objective then the entire length of the line that intersects with the AR would represent solution points to the problem. Any option that fell within these points could be taken as a solution and the structure obtained for the selected point.

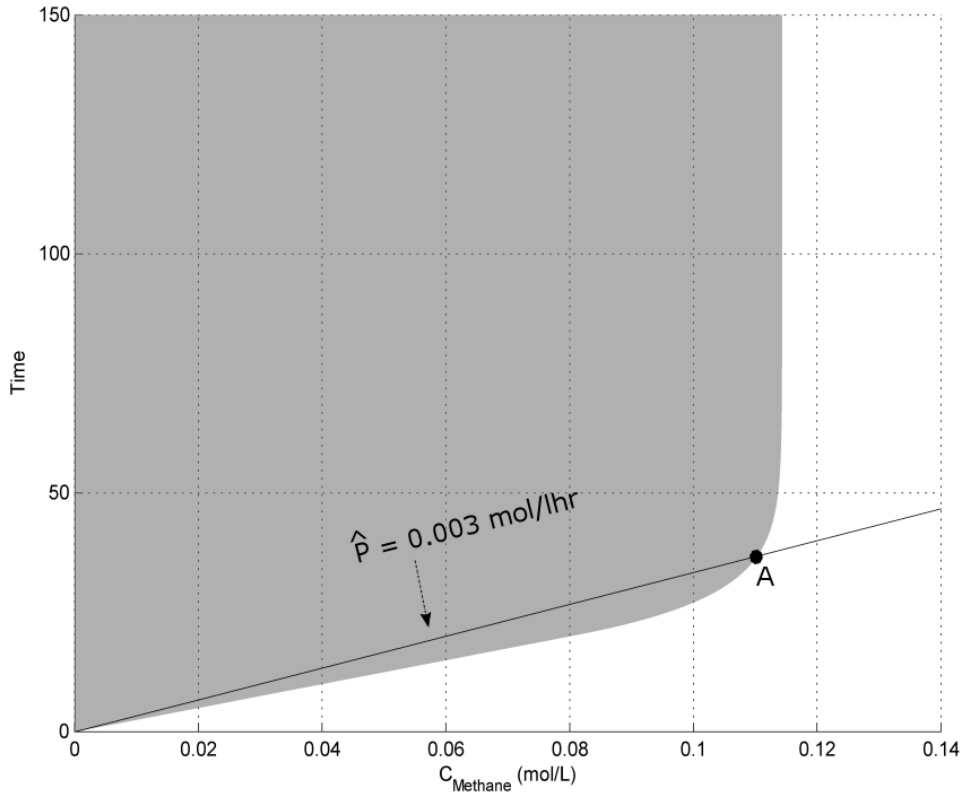

Figure 4.2.4: Example 2 - $c_{Methane} - \tau$ view of the candidate AR with the production rate line/plane intersecting the AR.

Say we then added another objective that stated the maximum methane concentration were sought. The added objective would narrow down the number of solutions that satisfied both objectives to Point A in Figure 4.2.4. This is not truly a single point as the AR is in three dimensions but the number of possible solutions to the problem has been reduced. We can see that the use of an objective in addition to that of the production rate objective is possible and provides a more focused solution to the problem. A function for the additional objective may also be utilised as will be done going forward in this example.

The objective function for the purpose of the example be arbitrarily set as done with the production rate. Similar to the production rate it will also be a function of methane only in order to simplify the solution path. An exponential function was selected and is shown in Equation 4.2.13.

$$\tau = e^{35.9722 * C_{Methane}} \tag{4.2.13}$$

It is clear that the intersection of the objective function, the production rate plane and the candidate attainable region will be the point(s) that satisfy all three and hence form the set of desired points. As the objective function and production rate equation are only functions of time and methane concentration, the point of intersection may be solved for by setting the equations equal to each other:

$$0 = e^{35.9722 * C_{Methane}} - \frac{1}{333.33} C_{Methane}$$

By finding the points at which the above is satisfied the point of intersection is determined. The intersection concentration of methane and time are found to be 0.0962 mol/L and 31.886

hours respectively. Figure 4.2.5 provides two views of the constructed candidate region with the objective function and production rate plane.

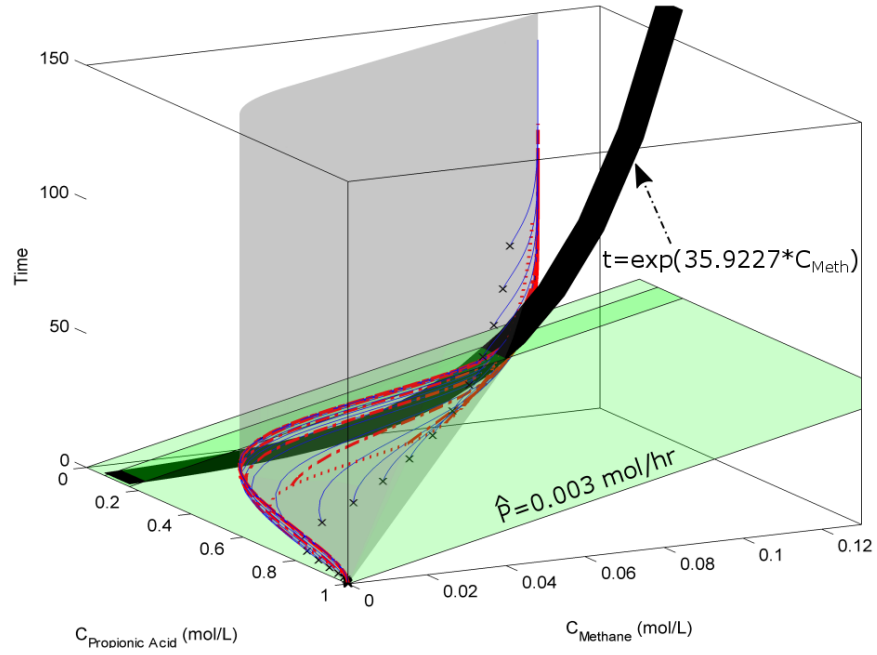

(a)

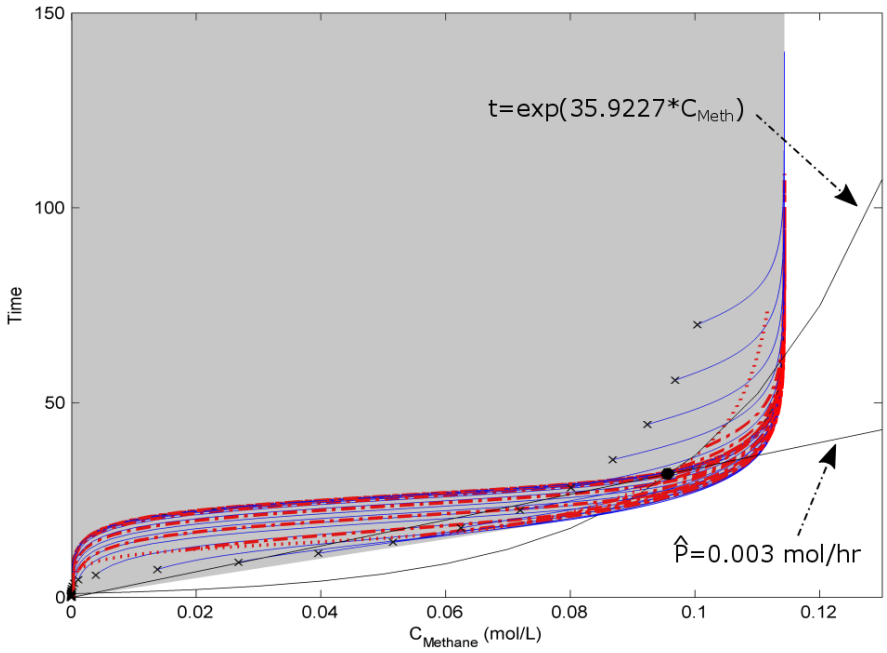

(b)

Figure 4.2.5: Example 2 - Constructed candidate attainable region with the objective function and production rate plane plotted on the same axes. A 3D view is provided in (a) with the $C_{Methane} - \tau$ view in (b). The points of intersection of all three define the desired effluent concentrations. This intersection is at a time of 31.886 hours, methane concentration of 0.0962 mol/L and a range of propanoic acid concentrations of ~0.07-0.165 mol/L.

4.2.4 Identifying the Continuous Reactor Structure

As mentioned previously, there are possibility an infinite number of reactor structures that will achieve a given point within the AR which is especially true if the point does not lie on the boundary. In this case there are a range of points as specified in Figure 4.2.5. Any reactor structure that achieves this range of concentrations is a solution structure to the problem at hand. We shall choose only one of the infinitely many possible structures in this example. One such structure that satisfies the two functions and is within the AR is shown in Figure 4.2.6. Figure 4.2.6 includes the geometric representation of the reactor network in $C-\tau$ space as well as the objective function and production rate plane within the same space.

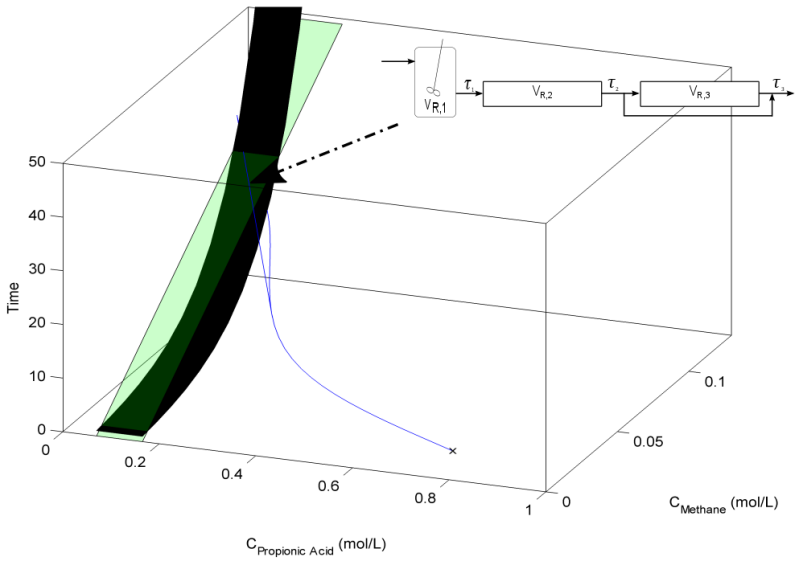

(a)

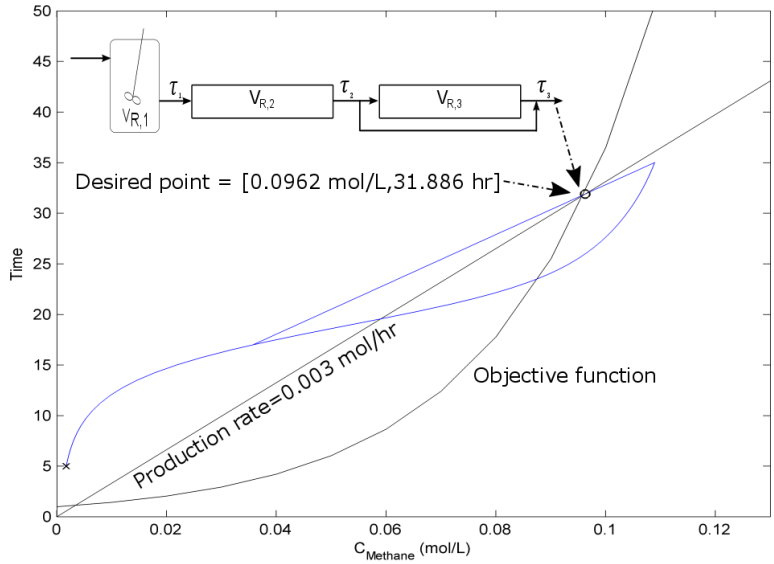

(b)

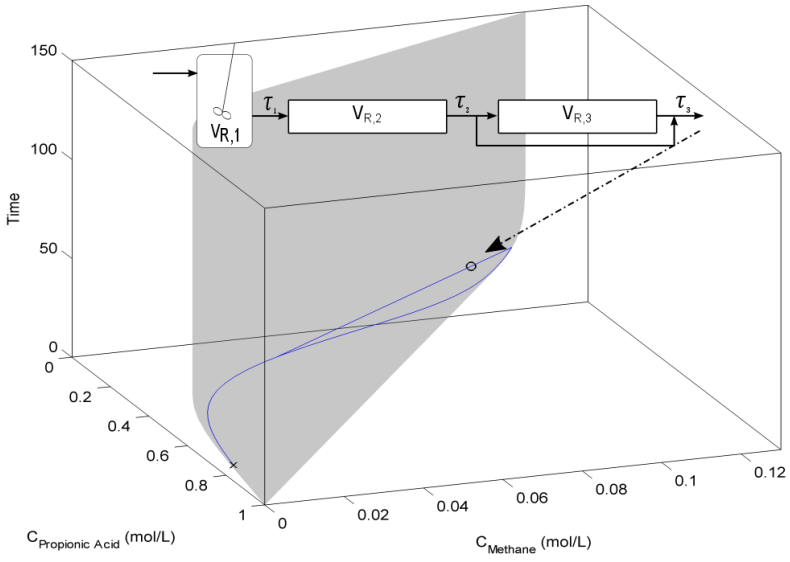

(c)

Figure 4.2.6: Example 2 - Continuous reactor network solution that satisfies the objective as well as the desired production rate. 3D view (a), 2D $C_{Methane} - \tau$ view (b). The structure exists as part of the AR and hence the point is attainable as shown in (c).

Figure 4.2.7 provides a more detailed graphic of the continuous reactor structure, including the effluent times of each point in the structure. As in Example 1, the flow rates and associated volumes to reach the specified residence time will be discussed later in the example. Concentration vectors corresponding with each of the points are provided in Equation 4.2.14.

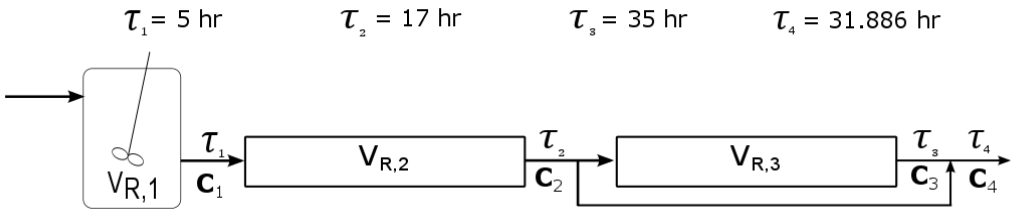

Figure 4.2.7: Example 2 - One of the possible reactor structures that satisfies the objective function and production rate plane and lies within the candidate attainable region. The concentration vector at each point is given in Equation 4.2.14.

$$c_1 = \begin{bmatrix} 0.8020 \\ 0.9191 \\ 0.0730 \\ 0.0802 \\ 0.0414 \\ 0.2772 \\ 0.0809 \\ 0.0018 \\ 0.0028 \\ 0.0062 \\ 5.0000 \end{bmatrix} \quad c_2 = \begin{bmatrix} 0.3281 \\ 0.6955 \\ 0.1436 \\ 0.2698 \\ 0.1702 \\ 0.9407 \\ 0.3045 \\ 0.0358 \\ 0.0368 \\ 0.1252 \\ 17.0000 \end{bmatrix} \quad c_3 = \begin{bmatrix} 0.0389 \\ 0.5067 \\ 0.0033 \\ 0.3854 \\ 0.3011 \\ 1.3455 \\ 0.4933 \\ 0.1089 \\ 0.1099 \\ 0.3811 \\ 35.0000 \end{bmatrix} \quad c_4 = \begin{bmatrix} 0.0889 \\ 0.5393 \\ 0.0276 \\ 0.3654 \\ 0.2785 \\ 1.2755 \\ 0.4607 \\ 0.0962 \\ 0.0972 \\ 0.3369 \\ 31.8860 \end{bmatrix} \tag{4.2.14}$$

From Equation 4.2.14 it is possible to discern the mixing fraction between the PFR effluent points by rearranging

$$\mathbf{c}_4 = \lambda \mathbf{c}_2 + (1-\lambda)\mathbf{c}_3$$

to solve for λ. The result of doing so is a mixing fraction, λ, of 0.173. This same mixing fraction will apply for the batch reactor but only in concentration space which in this case is two dimensional. The mixing fraction does not apply in time space for the batch case as reaction time cannot be mixed as it can be with residence time.

4.2.5 Identifying the Batch Reactor Structure

The batch reactor structure equivalent to the continuous structure in Figure 4.2.7 is found by substituting the corresponding batch reactors. As the bypass stream for mixing is not continuous, it is instead replaced with a non-reacting storage vessel in which the non-reacting portion of the first batch reactor's effluent is stored during the reacting time of the second reactor. The resulting structure is given in Figure 4.2.8a. Figure 4.2.8b provides a representation of the reactor structure in $C-t$ space. Note the mixing line is at the effluent reaction time of the structure which is in contrast to the continuous system in Figure 4.2.6. Batch process schedules may use

this view to identify the length of time a particular reactor structure needs to generate the desired output. We have not only identified the length of time but the structure itself. Therefore AR theory and its application to batch reactors may be an asset to identify and design the parameters for the reaction portion of a batch process schedule.

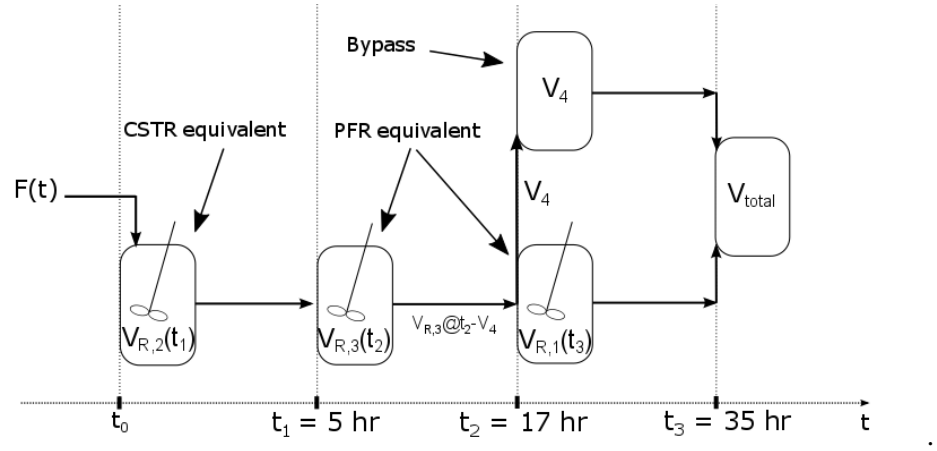

(a)

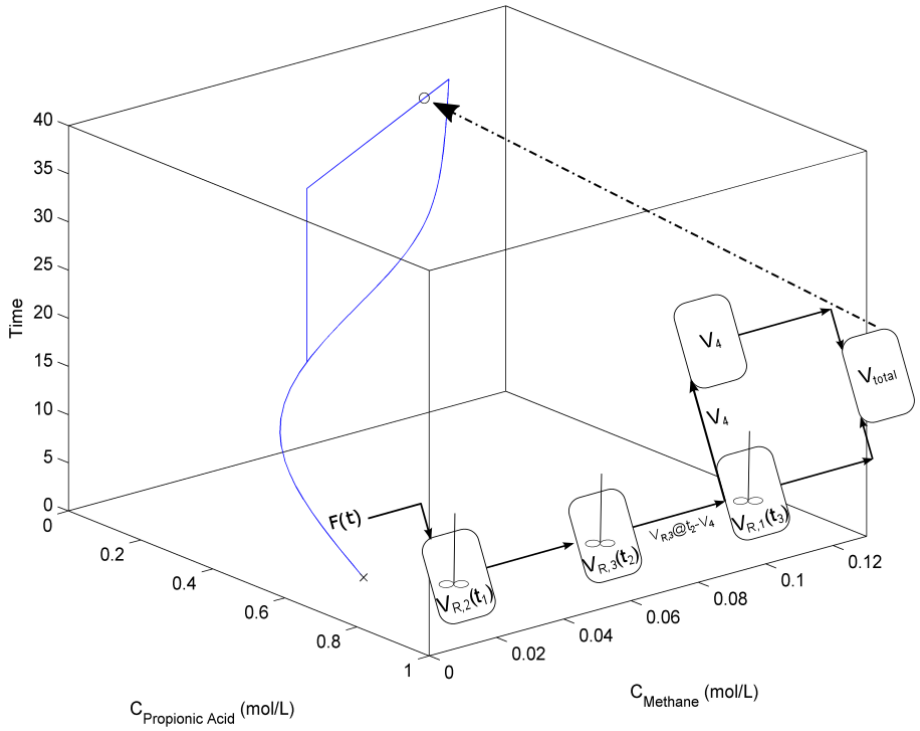

(b)

Figure 4.2.8: Example 2 - The batch reactor structure that corresponds to the continuous structure in Figure 4.2.7 (a). Most notable is the final concentration is reached at the maximum reaction time of the structure, unlike the continuous equivalent which has a reduced exit residence time due to mixing. (b) provides the true batch structure representation in $C-t$ space.

Equations 4.1.1 and 4.1.2 are again applicable to describe the fed-batch reactor's volume and feed rate due to the constant α nature of the CSTR-equivalent fed-batch reactor. The α value is the inverse of the reaction time of this particular reactor and is therefore 0.2 hr^{-1}.

4.2.6 Identifying Potential for Improved Production Rate

At this point a possible reactor structure has been identified to meet the output specified by the desired methane production rate and the objective function. This was made possible through the use of AR theory and the construction of a candidate attainable region for the system. Further specifics of the reactor networks, in continuous and batch form, such as flow rate and reactor volumes would be determined through further design or constraints. Setting either the reactor volumes or flow rates for the system would allow for the calculation of the other parameter. As with Example 1 these calculations will be performed on a basic level for Example 2 in Section 4.2.7.

It is possible to first assess the current structure and whether it indeed offers the most *productive* output. This should ideally be done while first obtaining the reactor network but was purposefully overlooked to display the potential advantage of using AR theory to solve such a design problem. Recall Figure 4.2.5b which provides a side view of the candidate region and objective functions in $C_{Methane} - \tau$ space. Such a view enables an easy assessment of the rate of methane production. From Equation 3.2.6 a lower time at a given methane concentration would indicate a higher rate of production per unit volume. Therefore, it is clear from Figure 4.2.5b that it is possible to achieve a higher production rate for the current system. The exact point this occurs is where the objective function intersects with the lower boundary of the AR. This is seen in Figure 4.2.9 in which both the previously specified production rate and new production rate vectors are shown. Point B is the initial point obtained at the lower production rate and Point C is obtained when the production rate plane is lowered to lie on the lower AR boundary to reach a higher production rate.

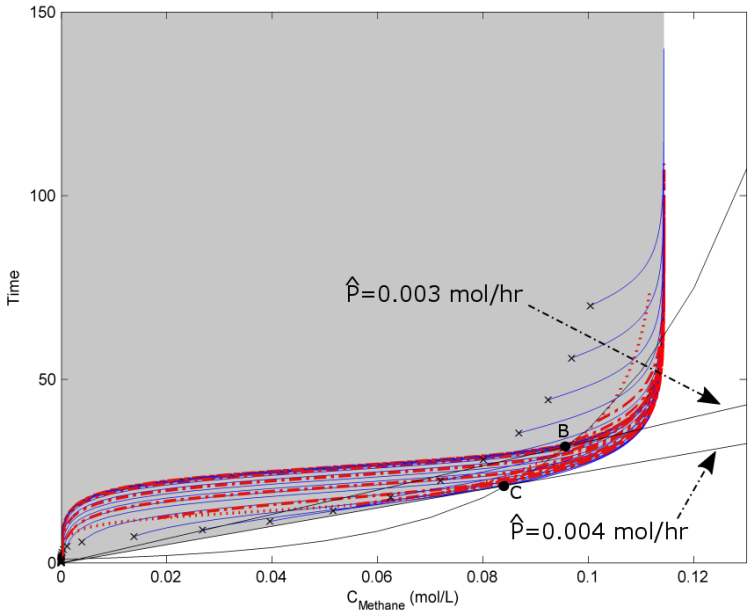

Figure 4.2.9: Example 2 - Construction of the candidate attainable region in $C - \tau$ space reveals that there is opportunity for further optimisation of the system in terms of production rate. The production rate plane is lowered until it intersects with the lower AR boundary and the objective function.

4.2.7 Evaluating Flow Rate and Volume Parameters of Selected System

As in the first example, the current known parameters for the selected reactor network are the concentrations of the components and the residence time or reaction time for continuous and batch systems respectively. The flow rate and reactor volumes can be determined from these values but the current solution to the problem may be seen as a general solution where the volumes or flow rates can be modified according to constraints. Once again a constraint will be applied to both the batch and continuous systems to develop the full set of parameters. It must be noted that this is an arbitrary constraint and would differ per application. As the volume was specified in Example 1, the entering flow rate will be specified in this example.

4.2.7.1 Continuous Reactor Network

Assume an entering flow rate of 20 L/hr for the continuous system and based on the structure in Figure 4.2.7 this flow rate therefore defines the total throughput of the system. Before performing further calculations the production rate of the continuous network may be found:

$$P_{Methane} = Q.C_{Methane,exit}$$

$$P_{Methane} = (20\,L/hr)(0.0962\,mol/L)$$

$$P_{Methane} = 1.924\,mol/hr$$

The bypass flow rate for the second PFR is evaluated using the mixing fraction and the total flow rate given above. Applying Equation 2.1.20:

$$\tau_4 = \lambda\,\tau_2 + (1-\lambda)\,\tau_3$$

With flow rate subscripts corresponding to the residence times in the above expression, λ represents

$$\lambda = \frac{Q_2}{Q_4}$$

and therefore

$$Q_2 = 0.173 \times 20\,L/hr = 3.46\,L/hr$$

By subtraction from the total flow rate, Q_3 is equal to 16.54 L/hr. Assessing the volume of each reactor in the network is as simple as applying Equation 2.1.8 with the corresponding residence time and flow rate the results of which are presented in Figure 4.2.10. This figure along with the concentration vectors in Equation 4.2.14 represent the full solution for the problem at hand given the constraints complied. Constraints may be varied at different levels of the problem but the solution path would be similar, if not identical to the one followed here. It is also worthy to note that the constructed AR candidate region would remain constant regardless of the constraints applied, be it a different objective function or limitations to the reactor volumes or feed flow rate available.

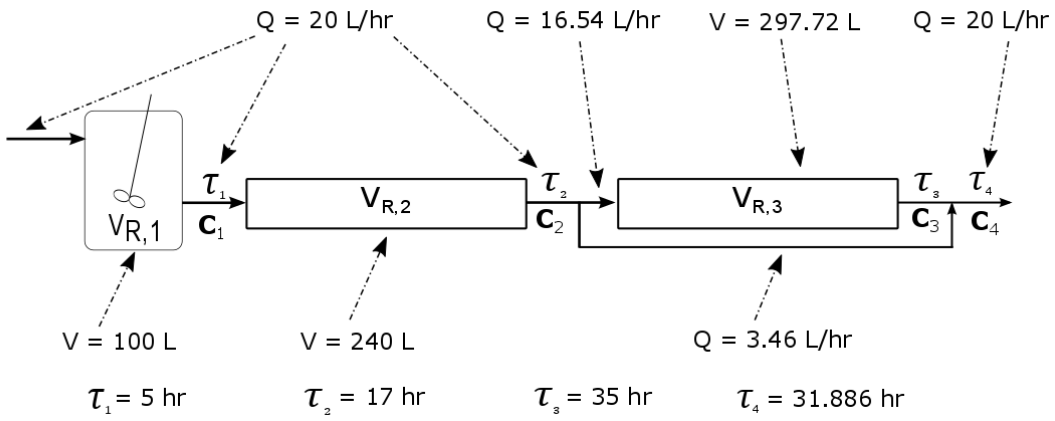

Figure 4.2.10: Example 2 - Full solution with flow rates and reactor volumes for the continuous reactor network if the entering flow rate is restricted at 20 L/hr.

4.2.7.2 Batch Reactor Network

The entering flow rate for the continuous reactor network was specified at 20 L/hr which does not have a direct equivalent in terms of a batch network. In order to convert it to terms of a batch system the continuous flow rate could be multiplied by the first reactor's reaction time which would result in a total volume of the first reactor. As with the continuous system doing so inherently decides the total output of the network although it is now volume and not flow rate. Another option would be to consider the overall reaction time of the network which as determined in Section 4.2.5 is equal to the exit time of the final batch reactor. The methane production rate of the batch network would clearly then be equal to the rate of production of the continuous reactor network. To obtain a comparable result in this example the latter path was selected. The total reactor network time is 35 hours and multiplied by the continuous flow rate it results in a total volume of 700 L.

One may then work back through the structure, obtaining the volumes of the reactors. The third batch reactor's volume is obtained by first determining the volume split between the reacting portion and the non-reacting "bypass". Using the same method as used for the continuous network,

$$\lambda = \frac{V_4}{V_{total}}$$

which results in

$$V_4 = 0.173 \times 700\,L = 121.1\,L$$

which is the volume from the second reactor that is left not to be reacted so as to be mixed with the effluent of the third reactor. A simple mass balance reveals that the second reactor volume is the sum of the bypass and third reactor volumes. Similarly the fed-batch reactor volume at a reaction time of 5 hours is also 700 L. Determining the initial volume of the fed-batch and feed rate to the fed-batch requires the use of Equations 4.1.1 and 4.1.2. With α being the inverse of the reaction time, and therefore having a value of 0.2 hr^{-1}, the initial volume, V_o, is

$$V_o = \frac{V(t)}{e^{\alpha t}} = \frac{700\,L}{e^{0.2\,hr^{-1} \times 5\,hr}} = 257.52\,L$$

The volume within the reactor as well as the feed-rate to the reactor vary with time and similarly to that done in Example 1, the volume and feed rate profiles are given in Figure 4.2.11.

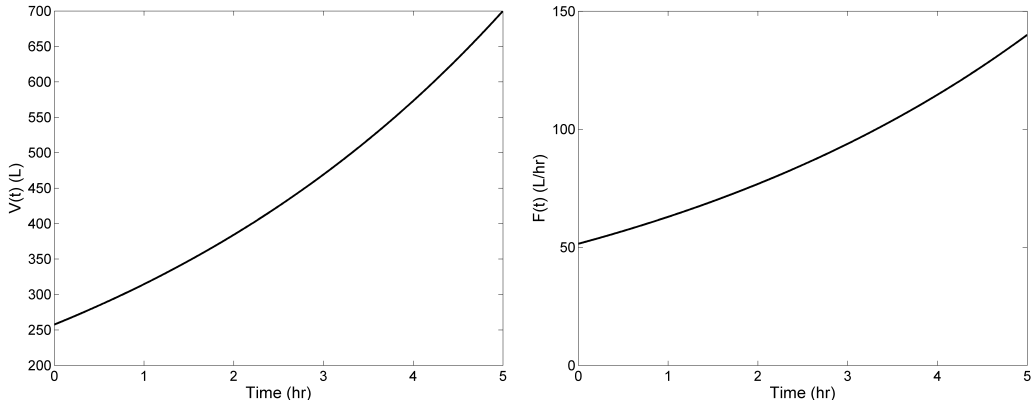

(a) (b)

Figure 4.2.11: Example 2 - Volume (a) and feed rate (b) profiles of the fed-batch reactor as they vary throughout the reaction time period.

A final batch reactor solution to the problem, given all the parameters and constraints discussed, is given in Figure 4.2.12.

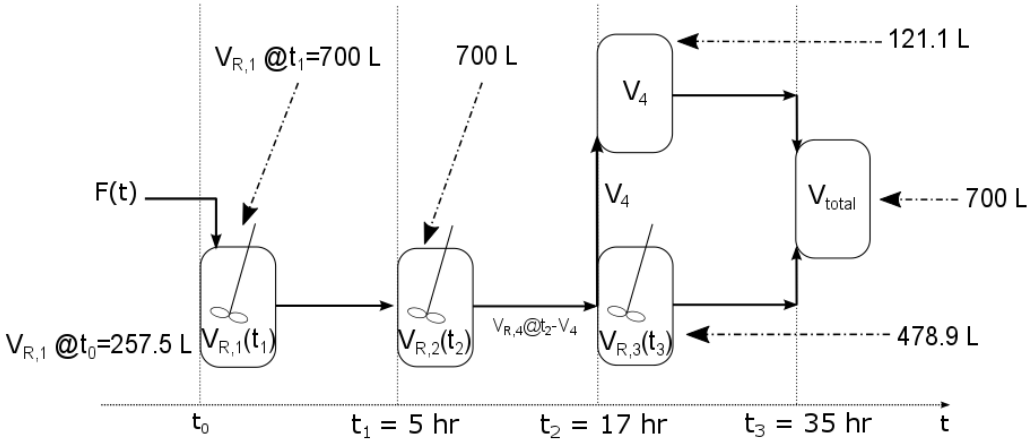

Figure 4.2.12: Example 2 - Solution batch reactor network for the problem including the specific constraints applied. All volumes and times are indicated while the feed rate profile for the fed-batch reactor is given in Figure 4.2.11.

Since the full solution to the problem has been obtained for both the continuous and batch systems, the example is complete. Batch reactor structures are able to be obtained from ARs constructed in $C-\tau$ space by directly substituting the continuous structure with the batch reactor equivalents.

Key result: In constructing a 3D AR in $C-\tau$ space, the critical CSTRs could not be identified using standard AR theory. A 3D AR plotted in $C-\tau$ space was used to obtain the batch reactor structure that met the given constraints and objectives.

4.3 Investigating Use of pH in Conjunction with ARs

So far in this work time as an additional variable to concentration in the AR has been discussed at length. Temperature has also been investigated as a variable or used in conjunction with AR theory ((Glasser et al., 1992b; Nicol et al., 2001) although a linear temperature model was used in both cases to satisfy the linear nature of mixing. A variable such as pH has not yet been investigated in conjunction with AR theory.

The second example covered in this work involved two stages of anaerobic digestion namely acetogenesis and methanogenesis. Both these associated reactions (Equations 4.2.1 and 4.2.3) contained H^+ ions as a product and hence the potential exists to investigate the use of pH as a variable within or with the AR. While deviating slightly from the focus on batch systems, this investigation should hopefully lay the foundations for future work and analysis of pH dependent systems with AR theory.

4.3.1 Definition of pH

pH is defined as the negative logarithm of the H^+ ions concentration in a solution as provided in Equation 4.3.1 (Brown et al., 2009). The pH scale typically ranges from 0 to 14 due as most solutions are likely to fit within this range . If one considers Equation 4.3.1, pH may extend beyond this range for H^+ concentrations $> 1\,mol/L$ and $< 10^{-14}\,mol/L$.

$$pH = -log_{10}[H^+] \tag{4.3.1}$$

The log scale is used to define pH due to the typically small concentrations of H^+ ions encountered in solutions.

4.3.2 pH and Attainable Regions

The linear mixing law has been shown to apply to concentration and residence time in Sections 2.1.2 and 2.1.7.1 respectively. Reaction time in batch systems was shown not to follow the linear mixing rule (Section 3.1) and hence typical convex ARs were not possible if reaction time was used as a variable. pH should be assessed in a similar manner in order to see how it may be applied with AR theory. If mixable in a linear fashion, then it could be used as an additional variable in an AR. If not then it will have to be used with accompanying plots, using the information obtained from the AR.

It is clear from inspection that pH will not follow the linear mixing law as it is a logarithm by definition (Equation 4.3.1). This can easily be shown through an example. Consider the concentrations

$$H_1^+ = 10^{-2} mol/L \;\; and \;\; H_2^+ = 10^{-3} mol/L$$

which when mixed using Equation 2.1.3 and a mixing fraction, λ, of 0.5 forms H_*^+:

$$H_*^+ = 10^{-2}(0.5) + (1-0.5)10^{-3} = 0.0055\,mol/L$$

The pH of H_*^+ is 2.26. It can be shown that pH does not follow the mixing law by using Equation 2.1.3 for pH and comparing the pH obtained to the pH of H_*^+:

$$pH_{mix} = -log(10^{-2})(0.5) + -log(10^{-3})(1-0.5) = 2.5 \neq pH_{*}^{+}$$

Therefore the pH obtained when the mixing law is applied to pH does not correspond to the actual H^+ concentration at that point. Hence pH cannot be used as a direct variable on an AR lest the convex property of the AR be lost in that dimension. Alternate methods of incorporating the pH will have to be sought.

As pH cannot be linearly mixed due to its definition it will have to be used in conjunction with AR theory and associated plots. One may actually consider similar plots to those done in Appendix A. These plots were constructed with the knowledge that reaction time could not be mixed linearly. Reaction time however was able to be included in the rate and concentration vectors while pH is not defined in either as it a function of one of the concentrations. pH would therefore be determined after the reaction processes have been completed. For example, once a PFR trajectory has been found through integration of the rate vector, the associated pH at each point may be calculated. Depending on the dimension of the AR, these may then be plotted as points above the trajectory to obtain a "map" of the pH progression throughout the applicable reaction processes. The resultant figure is *not* a *conventional* attainable region due to its concave nature. The pH variable is not present in the rate or concentration vectors and hence the geometrical properties of the reactors within the $C-pH$ space would not hold. These properties, such as the PFR trajectory being tangent to the rate vector at a point, would still apply within the C or τ dimensions.

This approach for a pH plot will be applied and investigated in Section 4.3.3 to Example 2 as H^+ ions were present in the system.

4.3.3 Use of pH in Conjunction with Example 2 (from Section 4.2)

Example 2 in Section 4.2 involved the 3D AR construction for the system consisting of two stages of anaerobic digestion, acetogenesis and methanogenesis. Using the AR and design constraints applied to the problem, continuous and batch reactor networks were proposed as solutions to the problem.

pH is often a crucial process variable to consider when analysing an anaerobic digester as the methane producing bacteria thrive in a pH range of 7-8 (Raposo et al., 2012). Anything outside of this range and the production of methane, the targeted product, may be inhibited (Raposo et al., 2012). Providing a view of the pH when constructing an AR for anaerobic digestion would therefore be informative. Such usefulness would extend to other processes that are sensitive to pH change. Before proceeding, it must be noted that as only two stages of anaerobic digestion were considered, the inlet concentration of H^+ was assumed to be zero which would not truly be the case for acetogenesis. Additionally, as only a partial model of the anaerobic process was used in the example, the pH is not expected to have resided within the ideal range of 7-8. The two previous statements indicate that it is not expected that the obtained pH values for the example conform to typical digestion pH levels. Use of the example will still provide insight towards the use of pH plots regardless if the pH conform to realistic digester levels or not.

In Section 4.3.2 it was suggested that pH be determined and plotted following the results of the reactor processes. This would form a "map" of the pH as reaction progresses. From Section 4.2.2 the AR for Example 2's system was given as Figure 4.3.1a. Figure 4.3.1b contains only the graphical representation of the reactors used to build the AR.

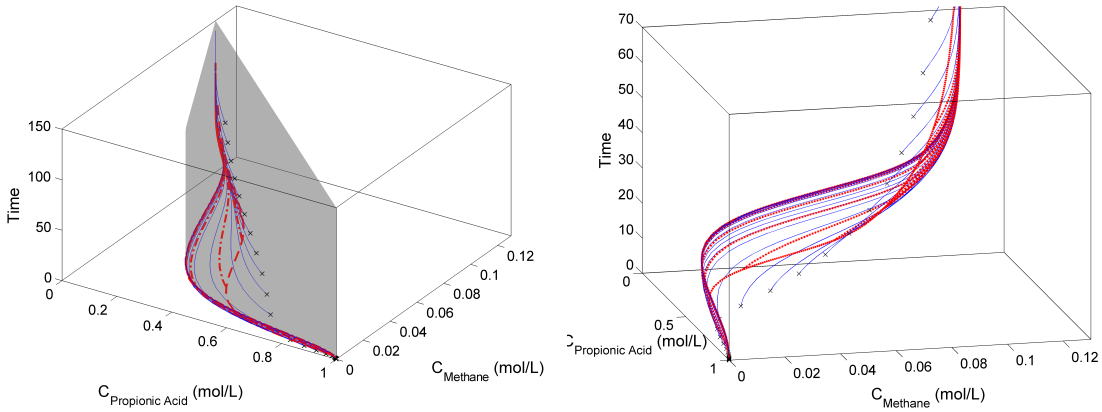

Figure 4.3.1: Attainable region (a) and associated reactor processes (b) from Example 2 in Section 4.2.2.

In order to visualise the pH value at each distinct point, one of the variables will have to be substituted with pH. In this case τ was replaced with pH as a dimension on the plot. A 2D projection of the reactors in $C_{meth} - C_{propanoic}$ space would remain with associated pH values plotted as a third variable or as values above the reactor points. Note that the AR itself remains in three dimensional space. In replacing τ a new AR is not being formed as pH cannot form a dimension on an AR. We are simply using the 2D projection of the AR and incorporating the pH values obtained at each point. The resultant plots are shown in Figure 4.3.2. The points that are plotted above the 2D reactor projection in Figures 4.3.2c and 4.3.2d are merely the points of the reactor trajectories and CSTR points in Figures 4.3.2a and 4.3.2b. Either type may be used to visualise the changing pH as reaction progresses. Note that the pH initiates at a high point. This is due to the pH at the feed point being undefined ($[H^+] = 0$). A similar shape of the graph would have been obtained however if the feed point was in the ideal pH range (7-8) for digestion as mentioned above.

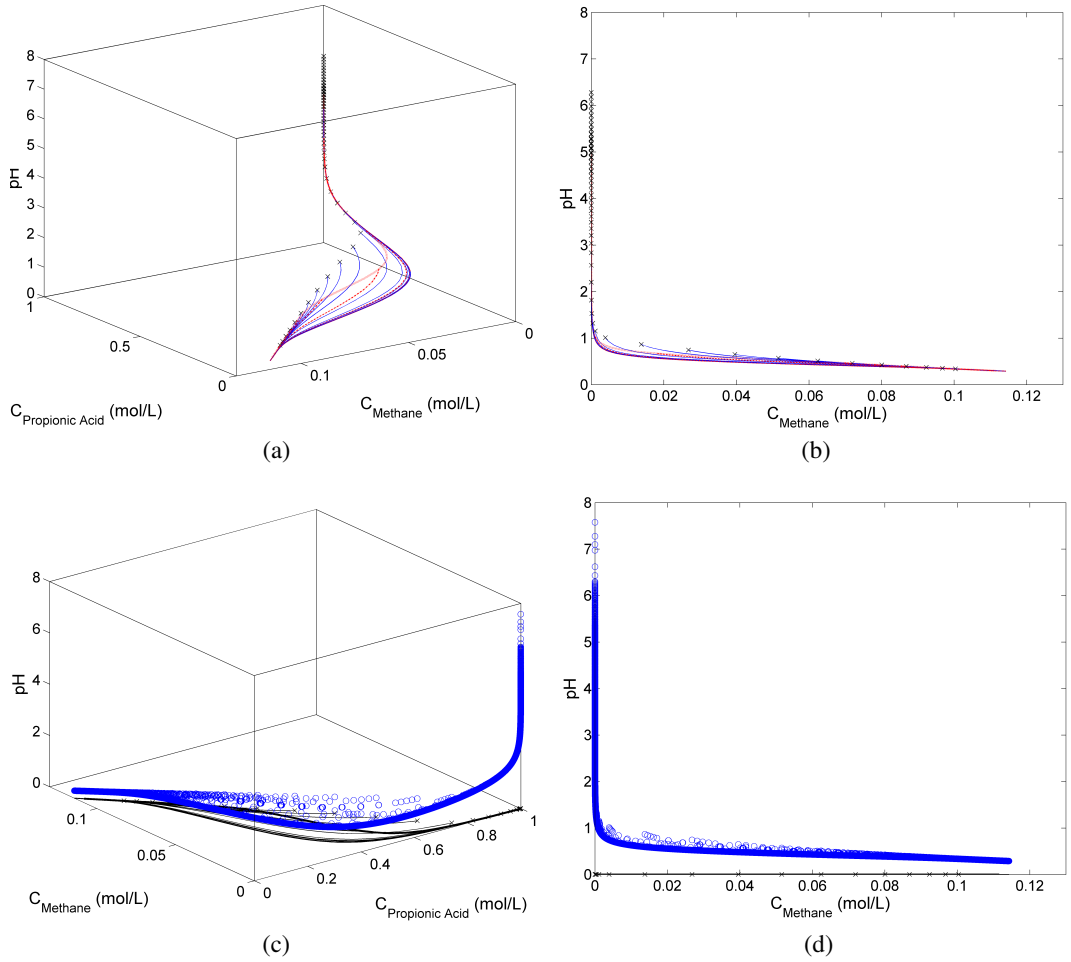

Figure 4.3.2: pH assessed at each of the reactor points from Example 2. In (a) and (b) pH is used as a third variable with a 3D and $C_{meth} - pH$ view respectively. (c) and (d) provide a 3D and $C_{meth} - pH$ view respectively of a 2D projection of the reactors from the AR with the pH points plotted above.

If one were to interpret the results in Figure 4.3.2, the pH does not remain in the ideal range of 7-8 and hence methane production would be inhibited. This is especially true in this case the more the reaction progresses. A corrective action, such as the addition of a buffer (Raposo et al., 2012), would need to be taken to ensure methane production remained unhindered. This is the benefit of such an analysis - the ability to visualise the full range of possible concentrations and pH levels.

Figure 4.3.2 considers only the points formed through reaction. Mixing may also be applied between these points as is done to form the full attainable region. Such an action would fill in the remaining points on the pH profile. Mixing between these points was done by first forming a matrix containing all the vectors formed through reactions as rows. Random vectors throughout the matrix were mixed using a random mixing fraction and repeating the process for a set number of points until the pH profile was formed. Figure 4.3.3 provides the full pH profile of the candidate attainable region constructed in Example 2. This $C - pH$ plot is far more useful than the ones obtained in Figure 4.3.2 as the full AR is considered. It is such a profile that should be used in conjunction with the AR to provide insight into systems that are sensitive to pH fluctuations.

It must be noted by the reader that Figure 4.3.3 still represents an AR even though it does not conform to the conventional AR property of being convex. This pH profile or AR is still providing information regarding which points are achievable and hence may be called an AR.

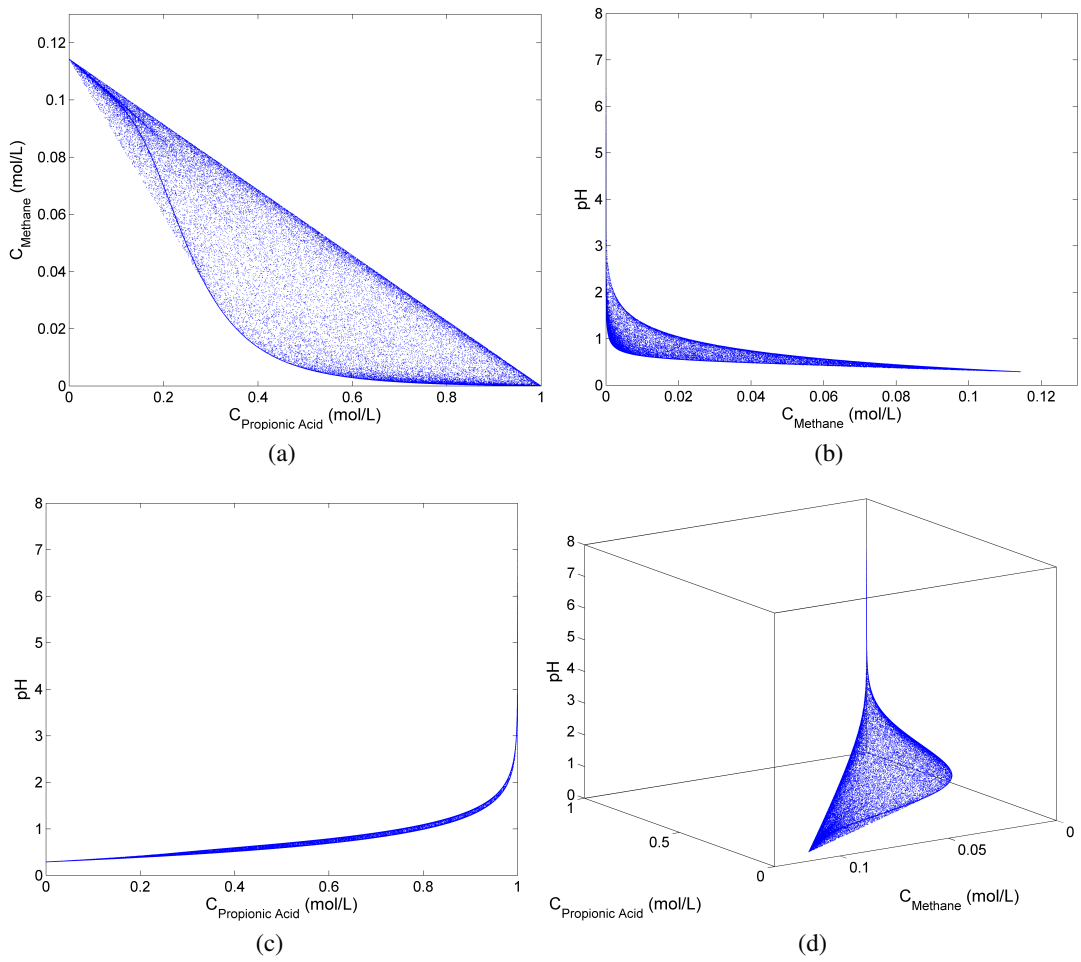

Figure 4.3.3: Full pH profile for the candidate attainable region from Example 2. (a) $C_{meth} - C_{prop}$ view, (b) $C_{meth} - pH$ view, (c) $C_{prop} - pH$ view and (d) 3D view.

4.3.4 Additional Example of pH Profile

In Section 4.3.3 the pH was plotted along with the 2D projection of the methane and propanoic acid concentrations. It was found that when the full 2D projection of the AR in concentration space was considered, a pH profile for that space was able to be formed. Such a profile would be invaluable in assessing an AR for systems that are sensitive to pH fluctuations. An additional example is now proposed to obtain a pH profile for another system.

Say the system in question consisted of a single auto-catalytic reaction as given in Equation 4.3.2. The concentration, feed and rate vectors are provided in Equation 4.3.3.

$$A + B \rightarrow 1.5B + H^{+} \tag{4.3.2}$$

$$C = \begin{bmatrix} C_A \\ C_B \\ C_{H^+} \\ \tau \end{bmatrix} \quad C_f = \begin{bmatrix} 1 \\ 0.01 \\ 0.001 \\ 0 \end{bmatrix} \quad r = \begin{bmatrix} -C_A C_B \\ 0.5 C_A C_B \\ C_A C_B \\ 1 \end{bmatrix} \tag{4.3.3}$$

Defined in concentration-time space, this system would form a two-dimensional AR with τ as the second variable. The constructed AR in 2D $C_B - \tau$ space is given in Figure 4.3.4. As it is only a 2D AR, only PFRs and CSTRs were required in its construction.

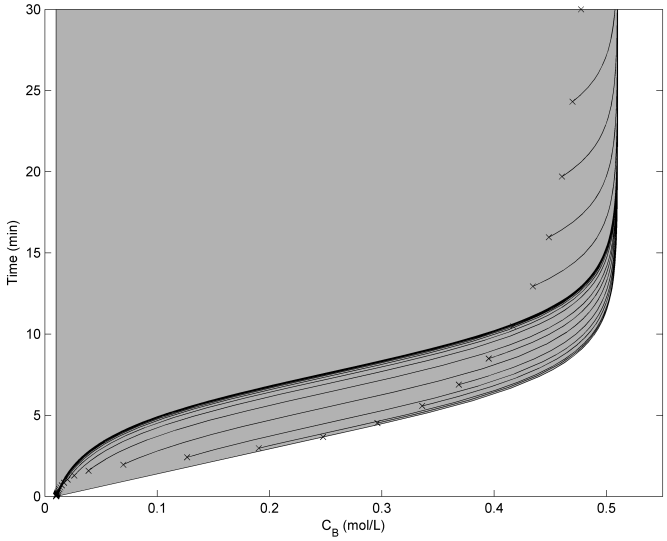

Figure 4.3.4: Two-dimensional candidate attainable region for the given auto-catalytic reaction in $C_B - \tau$ space.

Based on the constructed AR and the points achievable through reaction and mixing, a similar method to Section 4.3.3 was used to obtain the pH profile of the system. The resultant profile is given in Figure 4.3.5.

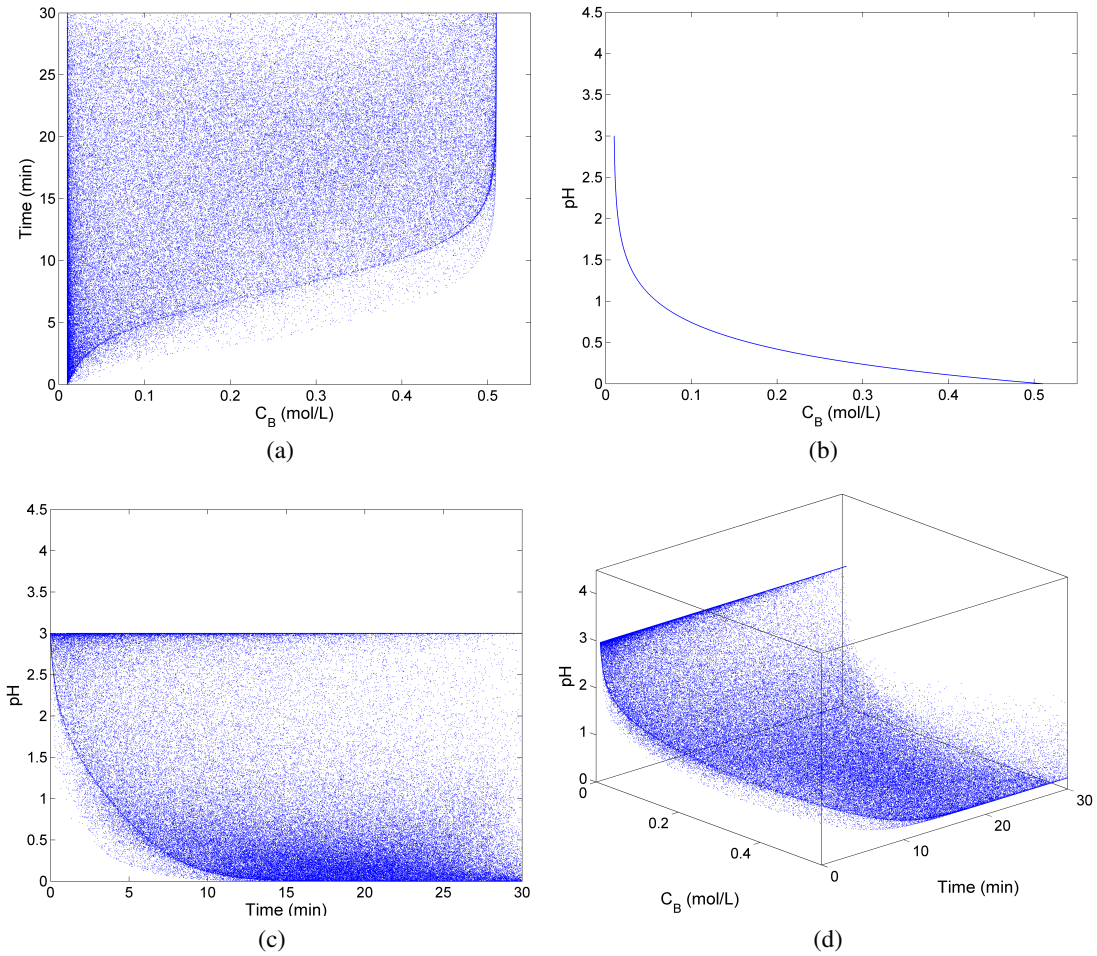

Figure 4.3.5: pH profile for the single auto-catalytic reaction provided. (a) $C_B - \tau$ view, (b) $C_B - pH$ view, (c) $\tau - pH$ view and (d) 3D view.

4.3.5 Conclusions on pH Profiles

This section aimed to investigate the potential use of pH as a variable with ARs. While not able to be used as a variable within an AR, it is able to be used in conjunction with a projection of an AR to form a pH profile for the system. This profile may then be assessed alongside the AR to determine the most suitable reactor structure for systems that are sensitive to fluctuations in pH. A result such as this opens the door for other variables to be considered in a similar manner. Variables that can be expressed as a function of one or more of the component concentrations may be incorporated in a similar manner to form a profile of that variable for a projection of the AR. The projection in question can be of any two independent components of the system under study. These profiles do not constitute conventional attainable regions themselves but may be incorporated into the design process as they provide more information about the system.

Key result: Another variable, such as pH, may be plotted in conjunction with a projection of the AR to form a non-conventional AR profile of that variable.
Our approach thus far in this work has been to work in a convenient space that provides us with the most information. Once the information is obtained we may convert to an alternate space or system that is most practical for the problem faced. This is evident in the approach used to obtain the optimal batch reactor structure for a system. We first plotted the AR in the convenient $C-\tau$ space from which we could assess the objective function, production rates and obtain the continuous reactor structure. We then converted the information to obtain the batch structure.
The ability to plot another variable along with a projection of an AR gives us the option of another space in which to obtain more information to solve the problem.

4.4 Discussion of AR Theory Positioning in Batch Landscape

Most of this work has been focused on attainable region theory and on furthering its application to batch reactors. In order to understand the results significance we must evaluate where the theory may be applied within the batch landscape of process scheduling and traditional optimisation. These were briefly introduced in Section 2.2 and the positioning of AR theory within these areas was suggested.

The results of the two examples considered (Section 4) revealed that an AR constructed in $C-\tau$ space may be used to determine the most productive point that met a given objective. To further refine the solution we may construct plots using a projection of the AR (in C or $C-\tau$ space) along with an alternate process variable that would not conventionally form part of an AR. Examples of such variables are pH, temperature and pressure and the execution is discussed in Section 4.3. These plots may be used to identify desirable points of the AR in term of the additional variable. Using this and the objective we may obtain a continuous reactor structure that corresponds to achieving a desirable point in $C-\tau$ space. At any point in time a different objective may be selected and the same AR would be used to solve the problem demonstrating the robustness of the technique. To obtain the batch reactor structure the continuous reactors are substituted for the batch reactor equivalents. Figure 4.0.1 provided a flow chart of this general method before the examples were carried out. Based on the addition of the new plots from Section 4.3, the revised general method may be represented as Figure 4.4.1.

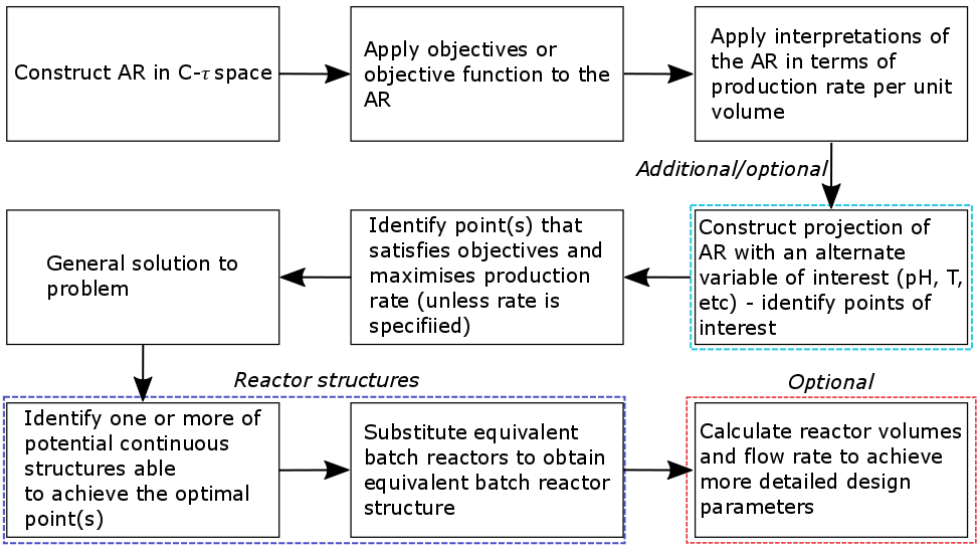

Figure 4.4.1: Revised method for application of AR theory to batch reactors.

This resultant structure may be used to further optimise the process variables and individual reactors and within the scheduling of a batch process. Scheduling may utilise the reactor structure itself as part of the overall batch process or use the effluent time of the structure as the reaction time for the reaction portion. In Section 2.2.1 it was mentioned that the output of scheduling was in the form of a Gantt chart. Note the similarities of the representation of the batch structures (Figures 4.1.6 and 4.2.12) to Gantt charts. Furthermore the traversal of the batch structure in $C-t$ space (Figure 4.2.8b) may also be considered similar to a Gantt chart. Such outputs may be utilised by those pursuing the schedule of a batch process to identify both the structure and total required time for the reactor structure. Note that mixing was considered not to take up time in the current work or within Figure 4.2.8b. This does not present an issue as the minimisation of the reaction time alone would provide a reduction in time across the entire process. In other words the overall time would be reduced even when considering the practical aspects of the time to mix and transfer products.

Taking these points into consideration attainable region theory provides a unique contribution towards the optimisation of batch processes including reaction. The above and the relationship between the different aspects of AR theory, batch process optimisation and scheduling is summarised in Figure 4.4.2.

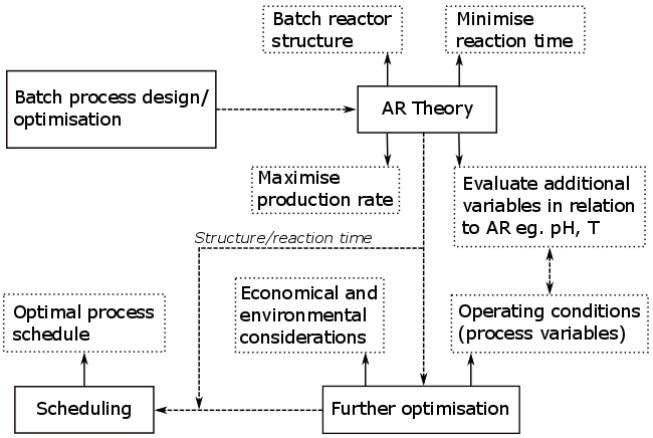

Figure 4.4.2: General proposed method for design and optimisation of batch processes. Includes inter-relationships between attainable region theory, batch optimisation and batch process scheduling.

Chapter 5

Conclusions and Recommendations

Ming et al. (2013) showed that attainable region theory could be applied not only to continuous reactor systems but to batch reactor systems as well. While mathematical equivalents between the continuous and batch reactor types facilitated this application, these equivalents do not all apply when considering time as a component of the attainable region. Most notable is the operation of mixing. Concentration follows the linear mixing rule for both cases but the difference in the nature of time results in the time of batch systems not following this same rule. Residence time of continuous reactors is defined in terms of volume and flow rate thus enabling linear mixing whereas the time for batch reactors is reaction time which cannot be mixed.

When plotting with time as a component the difference in nature of time means a different interpretation would be used when plotting the attainable region and considering the mixing operation. For a point in concentration-reaction time space to be mixed with another, the one of lower time must be escalated in time such that the two may be mixed. This means that the effluent time of a batch system will always be equal to the effluent time of the final batch reactor and time cannot be reduced through mixing as it can with residence time. Ming et al. (2013) showed that one may obtain the batch reactor network/structure by replacing the reactors in the continuous network with their batch equivalent and this same principle may be used in the case of using time as a component of the AR. Therefore construction of the AR would always be done in $C-\tau$ space and the continuous structure would first be determined followed by determination of the batch equivalent.

This is fortunate as AR plots in $C-\tau$ space offer additional insight into the system. The obvious advantage is the ability to visualise the time as reaction and mixing progress. Those who wish to optimise a particular system in terms of time or volume in the case of residence time may find this advantage particularly helpful. Scheduling of batch processes with a reacting portion may also include such a method during design of a suitable reactor network. The second advantage is the easy visualisation of points that offer higher production rates. Production rates were defined as the mols/mass produced over the time taken to produce the product. This means for a given concentration the lowest time taken to produce that concentration represents the most productive point on the AR in terms of production rate per unit volume. Plots in $C-\tau$ space enable these points to be viewed graphically hence opportunity for greater production rates are readily identifiable. Production rate by definition may be used as an additional objective function in $C-\tau$ space when time is made the subject of the production rate expression. Hence it can be used in any system constructed in $C-\tau$ space, even if a two-dimensional projection of the targeted component and time is used for more complex, higher dimension systems. As both continuous and batch systems derive from the same plot in $C-\tau$ space, the concept of production rates may be applied to both although care must be taken to assess the effluent time in a batch system.

While most AR construction using standard theory are identical for plots in C and $C-\tau$ space, determination of the CSTRs that lie on the AR boundary could not be done using the standard AR theory given in Feinberg (2000a). This is specific to $C-\tau$ plots in three dimensions and higher and is due to the use of the stoichiometric matrix in the calculations. Time, be it residence or reaction time, cannot be entered into the stoichiometric matrix as it does not behave in a stoichiometric manner within the reaction. Likewise it would not take part in a mass balance expression of the system. Note that this is applicable to both continuous and batch systems as both result from interpretation of the plot in $C-\tau$ space.

Due to the presence of H^+ ions in one of the examples performed, it was thought that pH may be able to be incorporated into an attainable region. The definition of pH led to its exclusion as a variable of the AR itself but pH profiles were plotted for projections of two different ARs. These profiles aid in providing additional information and can be used in conjunction with the AR in systems sensitive to large fluctuations in pH. This result leads to the possibility that other variables may be used in a similar manner.

The above conclusions let to the ability of attainable region theory to form a part of the traditional batch landscape of scheduling and optimisation. Prior to these actions taking place, the batch reactor structure may be determined such that the reaction time of the structure is minimised and the production rate for a given objective is maximised. This provides the scheduling task with a reactor structure and a total time for completion of the reaction portion. Furthermore, plots similar to those for pH mentioned above may be used to optimise the system in terms of a particular variable and used in conjunction with standard optimisation.

The conclusions above address all the research questions posed in Section 1.2.2 and hence the objectives of this work were met. Several additional questions arose while working through the theory and examples put forward that did not fall within this work's scope. These include further needs within the field that are required to fully benefit from the advantages of attainable region theory. This would aid the application of attainable region to more complex systems and incorporate it further within batch optimisation and scheduling. Recommendations for further investigation in the field are given below.

1. One aspect that could not utilise standard AR theory was the determination of the critical CSTRs of an AR in $C-\tau$ space. This was the result of the nature of time compared to that of mass or concentration in the stoichiometric matrix. A method to determine the critical CSTRs when in $C-\tau$ space or whether one can be found should be the subject of further investigation.

2. In the examples put forward, the continuous and batch structures were determined through inspection of the AR and the geometric representation of the reactor types. This is possible in lower dimensions but becomes a challenge in attainable regions greater than three dimensions. Further study should be focused on identifying structures in higher dimensions which would make AR theory and its applications more accessible. As theoretical AR construction increases in complexity as the number of independent participating reactions increases, this should also apply to ARs constructed numerically. Hence such a method may be numerical in nature itself. Furthering AR theory in this manner would make it more applicable as a solution over a larger variety of complex problems.

References

Abraham, T. K., Feinberg, M., 2004. Kinetic bounds on attainability in the reactor synthesis problem. Industrial & Engineering Chemistry Research 43 (2), 449–457.

Aziz, N., Mujtaba, I., 2002. Optimal operation policies in batch reactors. Chemical Engineering Journal 85 (2), 313–325.

Brown, T. L., LeMay, H. E., Murphy, C. J., Bursten, B. E., 2009. Chemistry The Central Science, eleventh Edition. Pearson.

Cheong, D.-Y., Hansen, C. L., Stevens, D. K., 2007. Production of bio-hydrogen by mesophilic anaerobic fermentation in an acid-phase sequencing batch reactor. Biotechnology and Bioengineering 96 (3), 421–432.

Davis, B. J., Taylor, L. A., Manousiouthakis, V. I., 2008. Identification of the attainable region for batch reactor networks. Industrial & Engineering Chemistry Research 47 (10), 3388–3400.

Dietz, A., Azzaro-Pantel, C., Pibouleau, L., Domenech, S., 2006. Multiobjective optimization for multiproduct batch plant design under economic and environmental considerations. Computers & Chemical Engineering 30 (4), 599–613.

Feinberg, M., 1999. Recent results in optimal reactor synthesis via attainable region theory. Chemical Engineering Science 54 (13), 2535–2543.

Feinberg, M., 2000a. Optimal reactor design from a geometric viewpoint - iii. critical cfstrs. Chemical Engineering Science 55 (17), 3553–3565.

Feinberg, M., 2000b. Optimal reactor design from a geometric viewpoint. part ii. critical sidestream reactors. Chemical Engineering Science 55 (13), 2455–2479.

Feinberg, M., Hildebrandt, D., 1997. Optimal reactor design from a geometric viewpoint - i. universal properties of the attainable region. Chemical Engineering Science 52 (10), 1637–1665.

Ferrer-Nadal, S., Mendez, C. A., Graells, M., Puigjaner, L., 2007. A novel continuous-time milp approach for short-term scheduling of multipurpose pipeless batch plants. Computer Aided Chemical Engineering 24, 595.

Fogler, H. S., 2010. Elements of chemical reaction engineering, 4th Edition. Prentice-Hall International London.

Glasser, B., Hildebrandt, D., Glasser, D., 1992a. Optimal mixing for exothermic reversible reactions. Industrial & Engineering Chemistry Research 31 (6), 1541–1549.

Glasser, B., Hildebrandt, D., Glasser, D., 1992b. Optimal mixing for exothermic reversible reactions. Industrial & Engineering Chemistry Research 31 (6), 1541–1549.

Glasser, D., Crowe, C., Hildebrandt, D., 1987. A geometric approach to steady flow reactors: the attainable region and optimization in concentration space. Industrial & Engineering Chemistry Research 26 (9), 1803–1810.

Glasser, D., Hildebrandt, D., 1997. Reactor and process synthesis. Computers & Chemical Engineering 21, S775–S783.

Hildebrandt, D., Glasser, D., Crowe, C. M., 1990. Geometry of the attainable region generated by reaction and mixing: with and without constraints. Industrial & Engineering Chemistry Research 29 (1), 49–58.

Horn, F. M., 1964. Attainable and non-attainable regions in chemical reaction technique. In: Chemical Reaction Engineering (Proceedings of the 3rd European Symposium). Pergamon Press, London U.K.

Liu, Y., Karimi, I., 2007. Novel continuous-time formulations for scheduling multi-stage batch plants with identical parallel units. Computers & Chemical Engineering 31 (12), 1671–1693.

Macku, L., Novosad, D., 2015. Enhancement of a semi-batch chemical reactor efficiency through its dimensions optimization. Procedia Engineering 100, 360–369.

Manousiouthakis, V. I., Justanieah, A. M., Taylor, L. A., 2004. The shrink–wrap algorithm for the construction of the attainable region: an application of the ideas framework. Computers & Chemical Engineering 28 (9), 1563–1575.

Mata-Alvarez, J., Mace, S., Llabres, P., 2000. Anaerobic digestion of organic solid wastes. an overview of research achievements and perspectives. Bioresource Technology 74 (1), 3–16.

McGregor, C., 1998. Choosing the optimal system structure using the attainable region approach for systems involving reaction and separation. Ph.D. thesis, University of the Witwatersrand Republic of South Africa.

Méndez, C. A., Cerdá, J., Grossmann, I. E., Harjunkoski, I., Fahl, M., 2006. State-of-the-art review of optimization methods for short-term scheduling of batch processes. Computers & Chemical Engineering 30 (6), 913–946.

Ming, D., Glasser, D., Hildebrandt, D., 2013. Application of attainable region theory to batch reactors. Chemical Engineering Science 99, 203–214.

Moniz, S., Barbosa-Póvoa, A. P., de Sousa, J. P., 2014. Simultaneous regular and non-regular production scheduling of multipurpose batch plants: A real chemical–pharmaceutical case study. Computers & Chemical Engineering 67, 83–102.

Nicol, W., Hernier, M., Hildebrant, D., Glasser, D., 2001. The attainable region and process synthesis: reaction systems with external cooling and heating: The effect of relative cost of reactor volume to heat exchange area on the optimal process layout. Chemical Engineering Science 56 (1), 173–191.

Oktem, Y. A., Ince, O., Sallis, P., Donnelly, T., Ince, B. K., 2008. Anaerobic treatment of a chemical synthesis-based pharmaceutical wastewater in a hybrid upflow anaerobic sludge blanket reactor. Bioresource Technology 99 (5), 1089–1096.

Olsson, L., Fallde, M., 2014. Waste (d) potential: a socio-technical analysis of biogas production and use in Sweden. Journal of Cleaner Production, 1–9.

Pan, M., Li, X., Qian, Y., 2009. Continuous-time approaches for short-term scheduling of network batch processes: Small-scale and medium-scale problems. Chemical Engineering Research and Design 87 (8), 1037–1058.

Raposo, F., De la Rubia, M., Fernández-Cegrí, V., Borja, R., 2012. Anaerobic digestion of solid organic substrates in batch mode: an overview relating to methane yields and experimental procedures. Renewable and Sustainable Energy Reviews 16 (1), 861–877.

Rooney, W. C., Hausberger, B. P., Biegler, L. T., Glasser, D., 2000. Convex attainable region projections for reactor network synthesis. Computers & Chemical Engineering 24 (2), 225–229.

Seid, R., Majozi, T., 2012. A novel technique for prediction of time points for scheduling of multipurpose batch plants. Chemical Engineering Science 68 (1), 54–71.

Seodigeng, T., Hausberger, B., Hildebrandt, D., Glasser, D., 2009. Recursive constant control policy algorithm for attainable regions analysis. Computers & Chemical Engineering 33 (1), 309–320.

Sötemann, S., Van Rensburg, P., Ristow, N., Wentzel, M., Loewenthal, R., Ekama, G., 2006. Integrated chemical/physical and biological processes modeling part 2-anaerobic digestion of sewage sludges. Water SA 31 (4), 545–568.

Appendix A

Example Constructions in $C-t$ Space

This Appendix contains example construction in $C-t$ space using the alternative to determining the convex hull of the points found by reaction as detailed in Section 3.1.2.2. Since these example were purely focused on demonstrating the application of this method in $C-t$ space, Steps 5-7 of the standard AR construction algorithm (Section 3.1.2.1) for the 3D examples were not considered. These steps would not add to the purposes of the demonstration although it is recognised when constructing in 3D space they do need to be performed. Assessment and discussion of these steps for $C-\tau$ space is carried out in Section 4.2.

A.1 Example AR Construction in 2D Concentration-time Space

An example AR construction in 2D $C-t$ space was performed for the auto catalytic reaction $A+B \rightarrow 2B$. The kinetics, with rate constants equal to unity, and feed point for the system are given as follows:

$$\mathbf{r}(\mathbf{C}) = \begin{bmatrix} r_A \\ r_B \\ r_t \end{bmatrix} = \begin{bmatrix} -c_A c_B \\ c_A c_B \\ 1 \end{bmatrix}, \quad C_f = \begin{bmatrix} 1 \\ 0.001 \\ 0 \end{bmatrix}$$

Time and the concentration of component B were selected as the variables for this AR. Component A could be calculated through mass balance if necessary. Construction followed steps 1-4 of the algorithm presented in Section 3.1.2.1. These steps were followed to solve for the batch reactor trajectory initiated at the feed and the fed-batch reactor points. Batch reactor trajectories were then initiated at each of the fed-batch reactor points and all the reactors were then plotted in 2D space. The result is shown in Figure A.1.1a.

For a continuous system the convex hull would be found at this point and the region filled. This option was not available for this batch system and hence the proposed algorithm from Section 3.1.2.2 was then followed. A maximum of 25 units of time was set for the system. These units could be seconds, minutes or hours. Assume for the purposes of this example that the units were seconds. Using loops in the code, the feed point's time component was increased to that of each fed-batch reactor point and select points along the batch reactor trajectory and these points were stored. Mixing lines were plotted between the time-elevated feed points and each of the reactor points. The batch trajectory initiated from the topmost fed-batch reactor was also utilised to aid in adding mixing lines to the the topmost area. Figure A.1.1b displays the resultant mixing lines.

Vertical lines were then plotted from each of the fed-batch reactor points and select points along the batch reactor trajectory up until the set maximum time of 25 seconds. This represents the time component of these concentration increasing while no reaction occurs. The result is given in Figure A.1.1c.

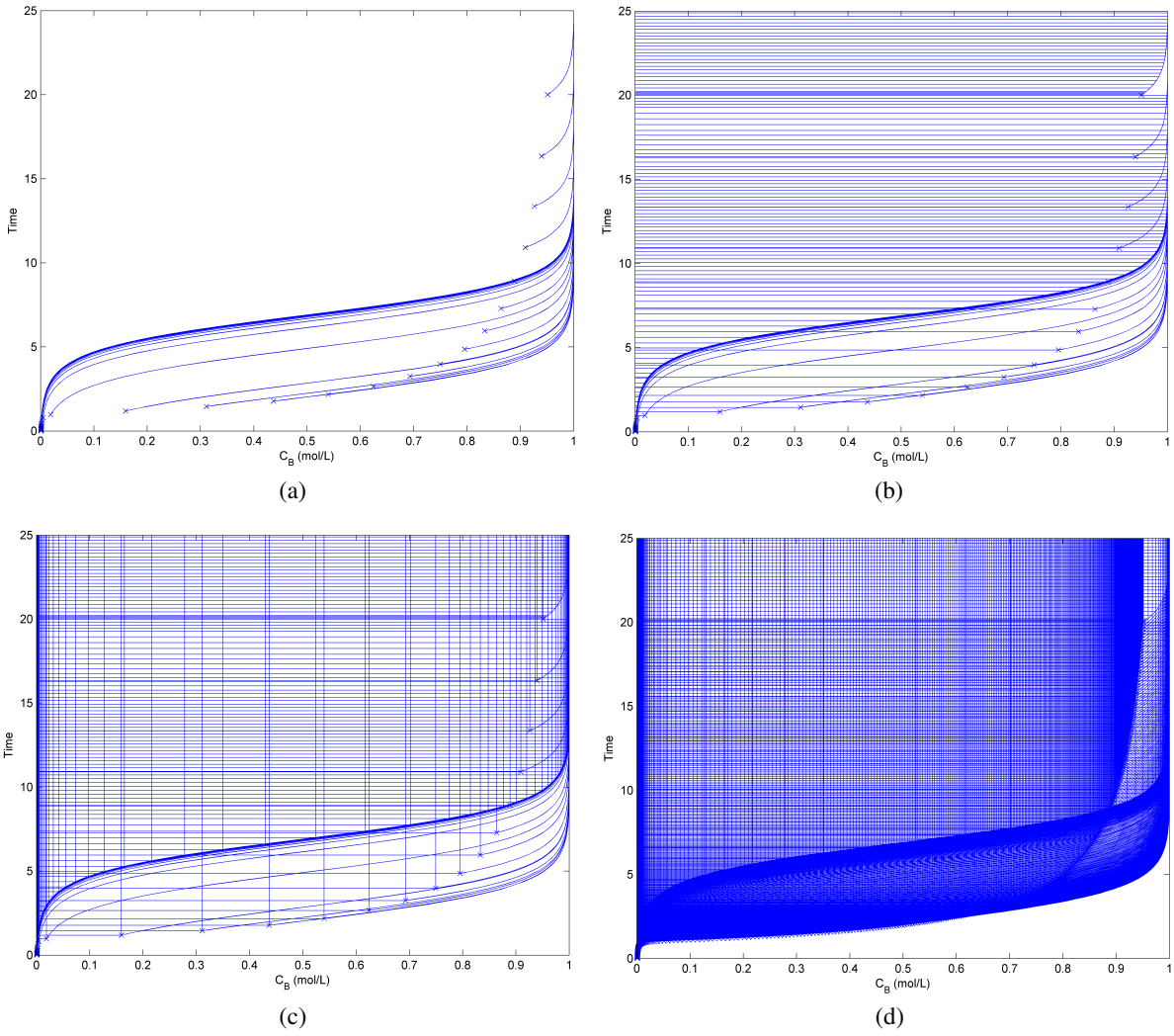

Figure A.1.1: Graphical results of the 2D example of AR construction in $C-t$ space. (a) - Plotting the batch and fed-batch reactors for the system. (b) - Mixing reactor points in concentration space with time-elevated feed. (c) - Elevating the time of the reactor concentrations. (d) - Batch attainable region when a greater number of fed-batch reactors are plotted and used in the construction.

Figure A.1.1c depicts what is essentially the attainable region for the system at hand when carried out in a batch reactor structure. However the term "region" is used loosely here as clear space is still present. More fed-batch reactors may be plotted to define the region more clearly. The result of plotting 1000 fed-batch reactors, compared to the 50 used in the above figures, is shown in Figure A.1.1d. Figure A.1.1d is a clearer depiction of the region. Any designer would recognise that any point within the region defined by the reactors, vertical lines and horizontal lines is attainable.

In Figure A.1.1d it can be noted that a concavity exists between the feed point and the fed-batch reactors on the lower boundary of the region. This concavity is not made convex through mixing

when focused on a batch system. Figure A.1.2 provides the equivalent AR for the continuous system using the same kinetics and feed point. The only difference between the two ARs is the presence of the aforementioned concavity in the batch system AR. Due to this difference, the AR for the continuous system has a larger area than that of the batch system AR.

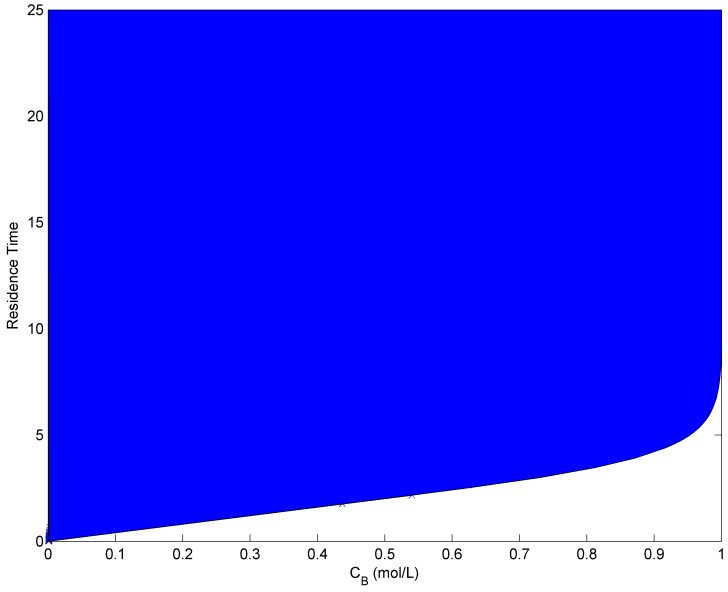

Figure A.1.2: 2D example of AR construction - AR constructed for continuous reactor system for comparison.

A.2 Example AR Construction in 3D Concentration-time Space - Example 1

Constructions in 3D $C-t$ space are more complex than those in 2D. Mixing of concentrations now takes part in 2D concentration space and as a result a volume is formed when combined with time as a variable. The obtained region is also more difficult to fill using only vertical or horizontal lines. Doing so would require more computational power than defining the boundary of the AR. Hence the constructing procedure presented for this example and that in Section A.3 aimed to define the boundary. Two examples were performed to show how each construction may differ according to the system under study.

This example used the two reactions $A \rightarrow B$ and $B \rightarrow C$. The associated kinetics, with rate constants equal to unity, and feed point for the system were:

$$\mathbf{r}(\mathbf{C}) = \begin{bmatrix} r_A \\ r_B \\ r_C \\ r_t \end{bmatrix} = \begin{bmatrix} -c_A \\ c_A - c_B \\ c_B \\ 1 \end{bmatrix}, \quad C_f = \begin{bmatrix} 1 \\ 0 \\ 0 \\ 0 \end{bmatrix}$$

Time and the concentrations of components A and B were selected as the variables for this AR. The concentration of component C could be calculated through a mass balance over the system. As with the 2D example, the reactors were solved for and plotted first as shown in Figure A.2.1a.

As can be seen the batch trajectory forms the outer boundary and the fed-batch reactor points lie within this boundary. This indicates that construction of the AR may be possible using the batch trajectory alone.

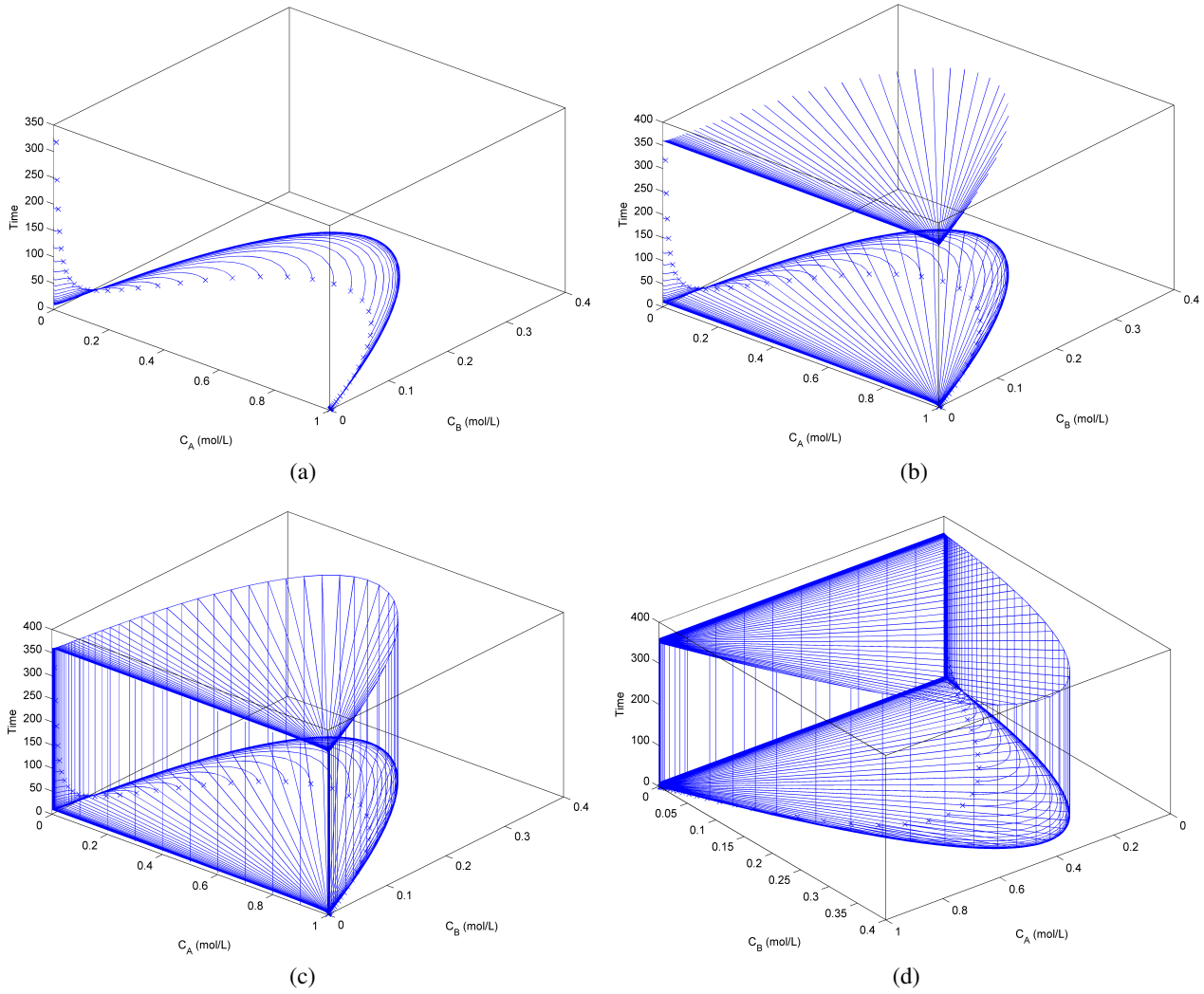

Figure A.2.1: Graphical results of the first example of AR construction in 3D $C-t$ space. (a) - Plotting the batch and fed-batch reactors for the system. (b) - Inserting horizontal mixing lines to form top and bottom boundaries of AR. This is achieved by elevating the time component of the feed point as well as the batch reactor trajectory and mixing the concentrations of the two. (c) - Adding the visual representation of time elevation to form the side boundary of the AR. (d) - Alternate viewpoint of the AR.

In the next step of AR construction the feed point had its time component elevated to match that of select points along the batch reactor trajectory. Each elevated point was then connected with the corresponding trajectory point with a horizontal mixing line. All these points were then elevated to a time of 350 time units (assume the units are seconds) and mixing lines were drawn to construct the upper boundary of the AR. These constructions are shown in Figure A.2.1b. It was recognised that the time could progress beyond the set maximum of 350 seconds. This maximum was selected as it encompassed all the fed-batch reactor points.

The time elevation performed was then shown graphically using vertical lines. These lines formed the side boundaries of the AR as shown in Figure A.2.1c. The boundaries of the AR

were defined and therefore the AR for the batch reactor system was completed. The entire region within the boundaries represented by the lines represents the AR for the batch system. An alternate view of the AR is provided in Figure A.2.1d with the continuous reactor AR shown in Figure A.2.2.

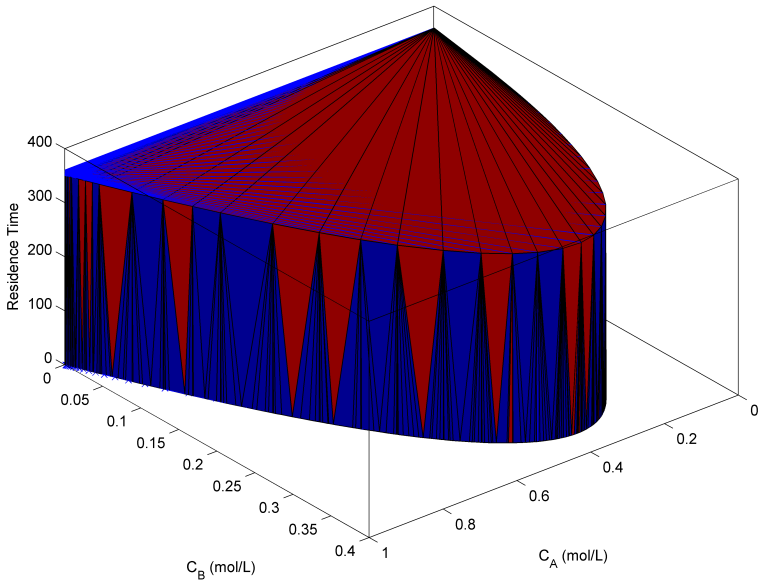

Figure A.2.2: 3D Example 1 of AR construction - AR for continuous system for comparison.

When comparing Figures A.2.1d and A.2.2 it is difficult to determine any noticeable difference between them. This is a result of the system having a convex nature. However concavities are present in the batch AR due to the time component. This is most noticeable between the feed point and the end of the batch reactor trajectory. Since the feed point was elevated to equal the time of the last point on the batch trajectory and a straight line used to join these points, a concavity forms below this mixing line. Figure A.2.3a provides an angle of the batch AR at which this is noticeable. This is contrasted to the continuous AR provided in Figure A.2.3b which does not contain this concavity. As with the 2D example, except now volume is considered, the continuous system AR has a larger volume than the AR constructed for the batch system.

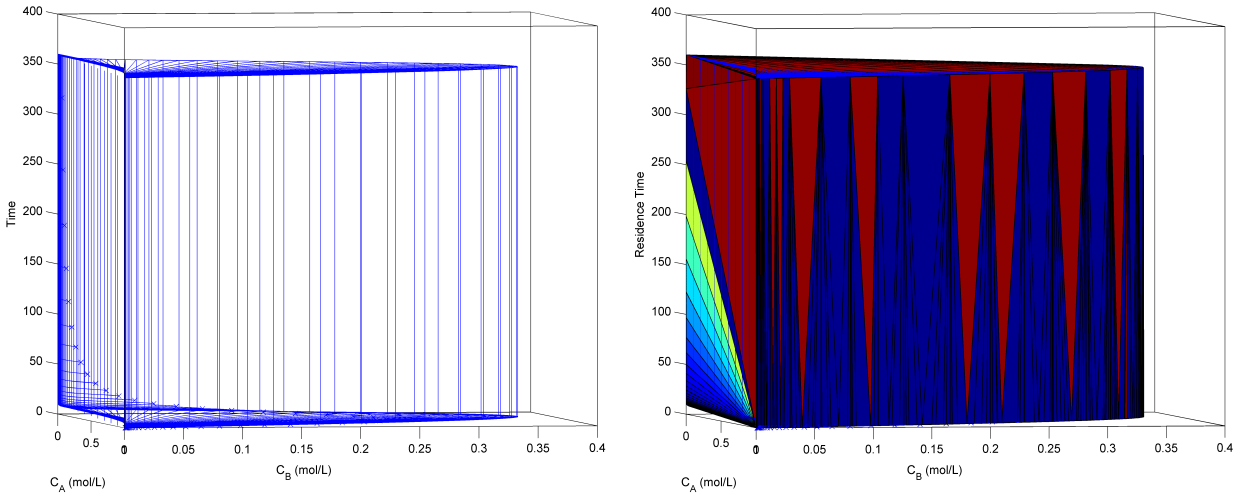

(a) (b)

Figure A.2.3: Comparison of the batch and continuous ARs highlighting the concavity present in the batch system. (a) - View of the batch reactor AR showing the concavity between the feed point and the batch reactor trajectory. (b) - Same view of the equivalent continuous reactor AR with filled-in concavity.

A.3 Example AR Construction in 3D Concentration-time Space - Example 2

A second example construction was performed in 3D $C-t$ space to highlight the fact that constructions performed in this manner may differ in their execution based on the system being studied. This example used the same reaction from the 2D example construction ($A+B \rightarrow 2B$) with the second reaction being $A \rightarrow C$. The kinetics with rate constants equal to unity and feed point for the system were:

$$\mathbf{r}(\mathbf{C}) = \begin{bmatrix} r_A \\ r_B \\ r_C \\ r_t \end{bmatrix} = \begin{bmatrix} -c_A c_B - c_A \\ c_A c_B \\ c_A \\ 1 \end{bmatrix}, \quad C_f = \begin{bmatrix} 1 \\ 0.001 \\ 0 \\ 0 \end{bmatrix}$$

Again, time and the concentrations of components A and B were selected as the variables for this AR construction. Component C could be calculated if needed by performing a mass balance over the system. It was expected that the shape of this AR differed greatly from that of the first 3D construction example (Section A.2) and hence a slightly different method would be utilised. As before, the batch reactor trajectories and fed-batch reactor points were plotted first as shown in Figure A.3.1a. As can be seen the bottom boundary of the AR was formed by the batch reactor trajectories initiated at the fed-batch reactor points. Only the side and top boundaries thus had to be constructed with vertical and horizontal lines.

It was realised that the right side of the AR Figure A.3.1a formed a straight line in concentration space $C_A - C_B$ if viewed from the top. As a result, this side of the AR could be constructed using horizontal lines between elevated feed points and the fed-batch reactor points. Select points from the batch reactor trajectory initiated from the final fed-batch reactor were also joined with elevated feed points to ensure the maximum time was reached. In this case a maximum time of

40 time units was set. Assume for the purposes of this example that the time seconds used was seconds. The result of these constructions is shown in Figure A.3.1b.

The other side of Figure A.3.1a is curved in concentration space however and hence the boundary could not be formed through the use of horizontal lines. Time elevations of select points of the batch reactor trajectory were thus utilised to construct this side of the AR boundary. The far edge that resides on the axis where $c_A = 0$ was also constructed using time elevations. This side's boundary was formed by the batch trajectories initiated at the fed-batch reactor points. The final points of these trajectories were simply elevated to the maximum time in order to construct the boundary on this side. Figure A.3.1c depicts the results of these constructions.

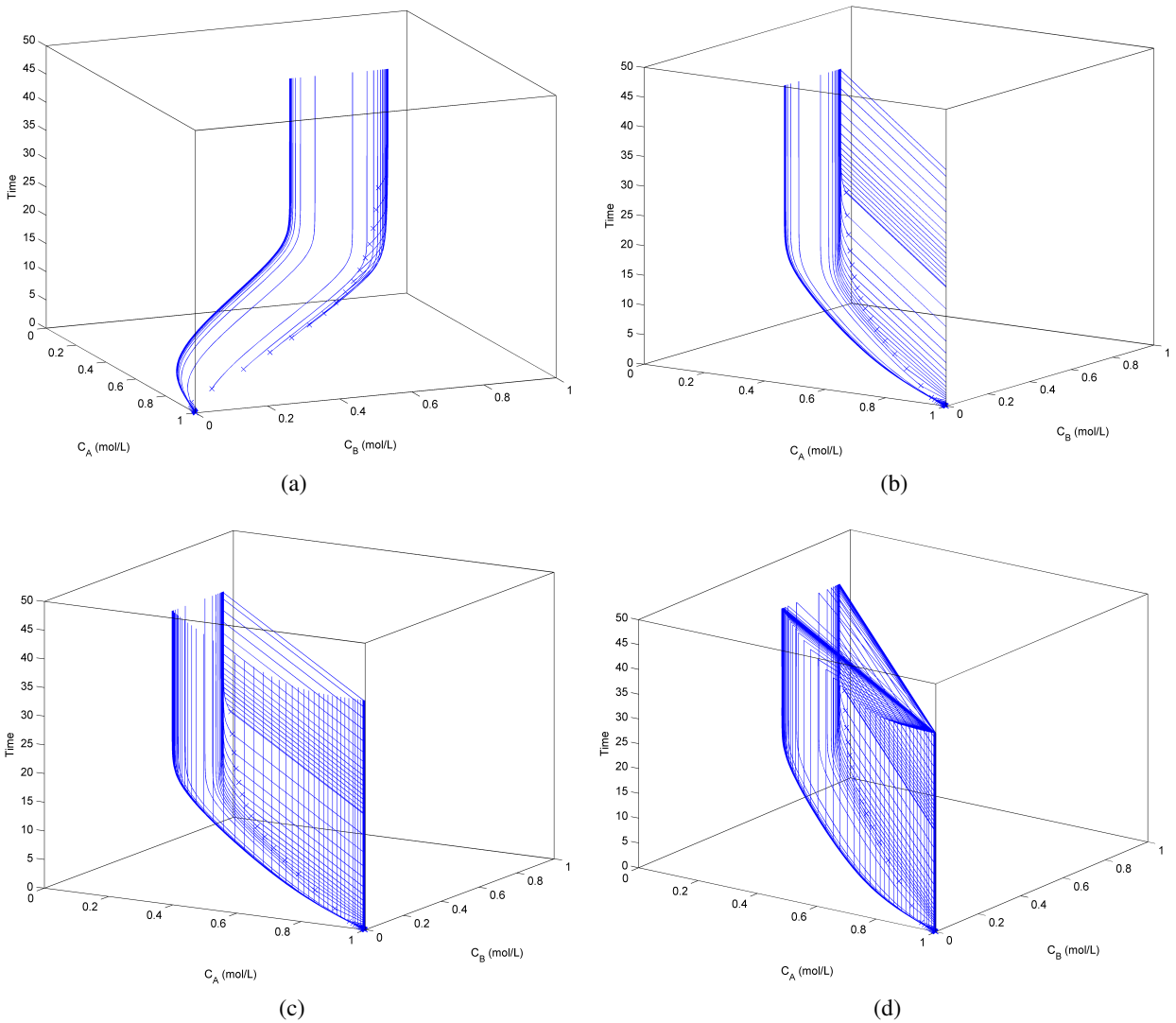

Figure A.3.1: Graphical results of the second example of AR construction in 3D $C-t$ space. (a) - Plotting the batch and fed-batch reactors for the system. (b) - Insertion of horizontal mixing lines between an elevated feed point and fed-batch reactors. The batch reactor trajectory that initiates from the last fed-batch reactor was also joined with elevated feed points. (c) - Use of vertical lines to construct the remaining side boundaries of the AR. (d) - Use of horizontal mixing lines to create the top boundary of the AR.

Finally the top boundary that exists at the maximum time of the AR had to be constructed. This was performed using horizontal mixing lines between the maximum time elevated feed point

and the vertical time elevations obtained in Figure A.3.1c. The finished batch reactor AR for the current system is shown in Figure A.3.1d. An alternative view of the AR is provided in Figure A.3.2a with the equivalent continuous AR shown in Figure A.3.2b.

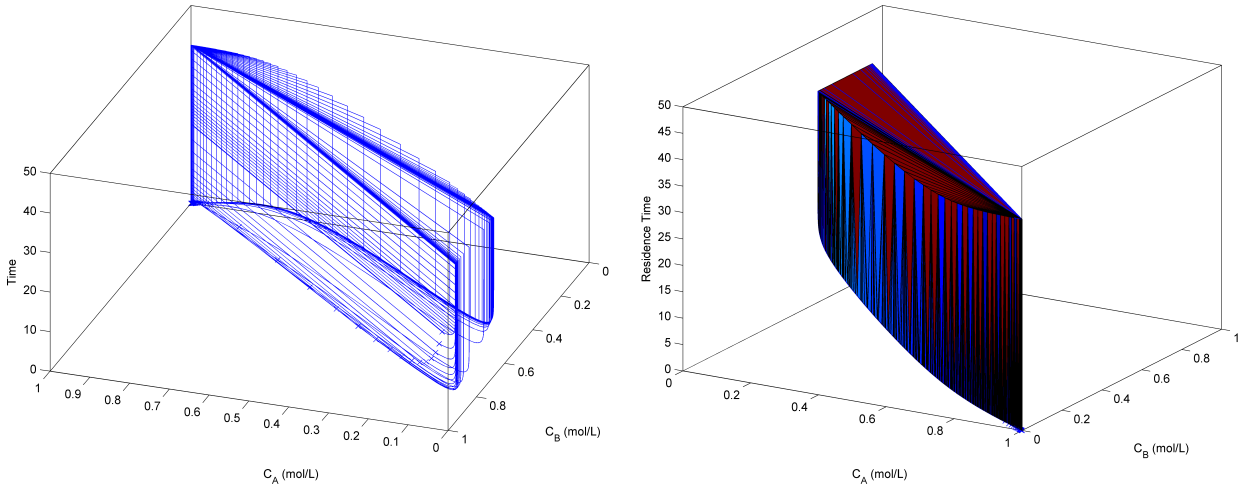

(a) (b)

Figure A.3.2: Second 3D example of AR construction in $C-t$ space. Alternative view point of the batch reactor AR (a) with the continuous system version of the AR (b).

Again, when comparing Figures A.3.1d and A.3.2b it is difficult to discern any difference between them from this view point. If one looks at a side view including the feed point, as shown in Figure A.3.3a, a concavity is clearly present between the feed point and the batch reactor trajectories. The equivalent view of the continuous AR in Figure A.3.3b shows that this concavity is filled in through the use of mixing. Once again, the AR constructed for the continuous system has a slightly larger volume than that of the batch system AR.

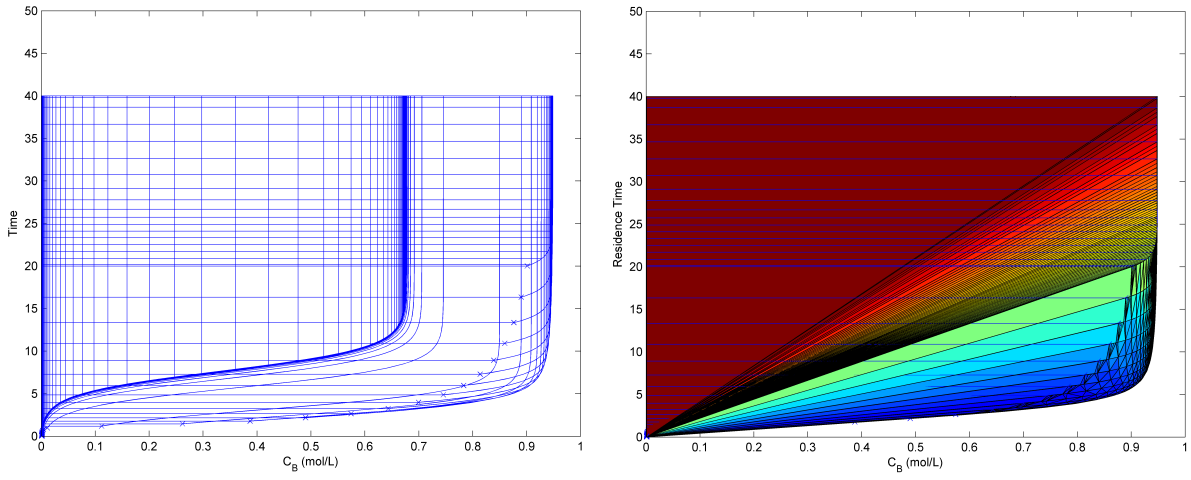

(a) (b)

Figure A.3.3: Second 3D example of AR construction in $C-t$ space. (a) - View of the batch reactor AR showing the concavity between the feed point and the batch reactor trajectories initiated at fed-batch reactor points. (b) - Equivalent view of the continuous reactor AR with filled-in concavity.

Appendix B

Determination of $\alpha(\mathbf{C})$ in Example 2

In Example 2 the critical α policy for the DSR/Fed-batch reactors had to be found. This was done using Equations 2.1.11 and 2.1.12 and performed in Python Notebook. The results of each step are shown in this section allowing the reader to see the steps followed.

In this Appendix the following nomenclature is used for the component concentrations:

c_{Pr} Concentration of propionic/propanoic acid (mol/L)

c_{Meth} Concentration of methane (mol/L)

c_{Ace} Concentration of acetic acid (mol/L)

c_{Zmeth} Concentration of methanogens (mol/L)

c_{Zaceto} Concentration of acetogens (mol/L)

c_{H2} Concentration of hydrogen (mol/L)

t Residence time (hr)

First the mixing vector, $v(\mathbf{C})$, was defined as $\mathbf{C}-\mathbf{C}_f$. C and $\mathbf{C}_f$ here are only expressed using the components that form a dimension of the AR. As C_f remains constant $\mathbf{v}(\mathbf{C})$ is

$$\begin{bmatrix} c_{Pr}-1 \\ c_{Meth} \\ t \end{bmatrix}$$

A component of Equation 2.1.11 (equation for $\psi(\mathbf{C})$) is the normal vector, $n(\mathbf{C})$, which is defined as the cross product of the mixing and rate vectors ($\mathbf{v}(\mathbf{C})\times\mathbf{r}(\mathbf{C})$). The result of finding this cross product is

$$\begin{bmatrix} \frac{1}{c_{Ace}+0.5}\left(-c_{Ace}c_{Zmeth}t+c_{Meth}\left(c_{Ace}+0.5\right)\right) \\ \frac{1}{(c_{H2}+0.2)(c_{Pr}+0.9)}\left(-0.5c_{Pr}c_{Zaceto}t+\left(c_{H2}+0.2\right)\left(-c_{Pr}+1\right)\left(c_{Pr}+0.9\right)\right) \\ \frac{1}{(c_{Ace}+0.5)(c_{H2}+0.2)(c_{Pr}+0.9)}\left(c_{Ace}c_{Zmeth}\left(c_{H2}+0.2\right)\left(c_{Pr}-1\right)\left(c_{Pr}+0.9\right)+0.5c_{Meth}c_{Pr}c_{Zaceto}\left(c_{Ace}+0.5\right)\right) \end{bmatrix}$$

Another component of the $\psi(\mathbf{C})$ expression is the Jacobian of the rate vector, $d\mathbf{r}(\mathbf{C})$, defined as

$$\mathbf{dr}\left(\mathbf{C}\right)=\begin{bmatrix} \frac{\partial r_A(\mathbf{C})}{\partial c_A} & \cdots & \frac{\partial r_A(\mathbf{C})}{\partial c_n} \\ \vdots & \ddots & \vdots \\ \frac{\partial r_n(\mathbf{C})}{\partial c_A} & \cdots & \frac{\partial r_n(\mathbf{C})}{\partial c_n} \end{bmatrix}$$

Finding the Jacobian of the rate vector yields

$$\begin{bmatrix} \frac{2.5c_{Pr}c_{Zaceto}}{(c_{Pr}+0.9)^2}\left(-\frac{c_{H2}}{c_{H2}+0.2}+1\right)-\frac{2.5c_{Zaceto}}{c_{Pr}+0.9}\left(-\frac{c_{H2}}{c_{H2}+0.2}+1\right) & 0 & 0 \\ 0 & 0 & 0 \\ 0 & 0 & 0 \end{bmatrix}$$

Equation 2.1.11 is then used to obtain $\psi(\mathbf{C})$:

$$\frac{0.45c_{Zaceto}\left(c_{Pr}-1\right)\left(c_{Ace}c_{Zmeth}t-c_{Meth}\left(c_{Ace}+0.5\right)\right)}{\left(c_{Ace}+0.5\right)\left(c_{H2}+0.2\right)\left(c_{Pr}+0.9\right)^2}$$

$\nabla\psi(\mathbf{C})$, a component of the $\alpha(\mathbf{C})$ equation, is determined by finding the partial derivatives of $\psi(\mathbf{C})$ with respect to all components (c_{Pr}, c_{Meth} and t):

$$\begin{bmatrix} -\frac{1.0c_{Zaceto}(0.45c_{Pr}-1.305)(-1.0c_{Ace}c_{Meth}+1.0c_{Ace}c_{Zmeth}t-0.5c_{Meth})}{(1.0c_{Ace}+0.5)(1.0c_{H2}+0.2)(1.0c_{Pr}+0.9)^2} \\ -\frac{0.45c_{Zaceto}(c_{Pr}-1)}{(1.0c_{H2}+0.2)(1.0c_{Pr}+0.9)^2} \\ \frac{0.45c_{Ace}c_{Zaceto}c_{Zmeth}(c_{Pr}-1)}{(1.0c_{Ace}+0.5)(1.0c_{H2}+0.2)(1.0c_{Pr}+0.9)^2} \end{bmatrix}$$

Finally we may compute $\alpha(\mathbf{C})$ using Equation 2.1.12:

$$-\frac{0.5c_{Pr}c_{Zaceto}\left(0.45c_{Pr}-1.305\right)\left(c_{Ace}c_{Zmeth}t-c_{Meth}\left(c_{Ace}+0.5\right)\right)}{\left(c_{H2}+0.2\right)\left(c_{Pr}-1\right)\left(c_{Pr}+0.9\right)\left(-0.45c_{Ace}c_{Zmeth}t\left(c_{Pr}+0.9\right)+0.45c_{Meth}\left(c_{Ace}+0.5\right)\left(c_{Pr}+0.9\right)\right.}$$
$$\left.+\left(0.45c_{Pr}-1.305\right)\left(c_{Ace}c_{Zmeth}t-c_{Meth}\left(c_{Ace}+0.5\right)\right)\right)$$

Hence we have the critical alpha policy for the DSR and fed-batch reactor which was given as Equations 4.2.8 and 4.2.9 in Section 4.2.